DEVELOPMENT OF BIOCHAR-BASED MATERIALS FOR THE RECOVERY OF PHOSPHORUS FROM WASTEWATER

By

Patrick Matthew Melia

School of Life Sciences, Pharmacy and Chemistry

Kingston University London

2019

A thesis submitted for the degree of Doctor of Philosophy

at Kingston University London, Kingston-upon-Thames, United Kingdom

Abstract

Phosphorus (P) is an irreplaceable element essential for life. It is relied upon, as mineral-derived phosphate fertilisers, for maintaining global agricultural productivity. Excess P in surface water causes eutrophication, where hypoxic effects and algal toxins degrade the environment and are hazardous to health. Therefore, the removal of P from wastewater, before the discharge of effluents to the environment, is important. Additionally, due to the finite nature of geological sources of mineral P, it is now crucial that P is not only removed from wastewater but captured in forms suitable for its direct reuse as recovered fertiliser. There are various routes to achieving this, however, approaches developed can be limited to large wastewater treatment plants or have limited ability to remove P to the low concentrations (< 1 mg P/L) increasingly required by legislation. Biochars, as adsorbents for the recovery of P, are attractive due to their known native soil ameliorant and carbon sequestration properties. Biochar-based materials saturated with P could have further benefit as being a recovered P fertiliser.

This thesis has critically reviewed the feasibility and trends in the various technological approaches for the recovery of P from wastewater treatment plants and also the state-of-the-art in the development of biochar and biochar-based materials for the capture of P. Complimentary characterisation approaches suitable for biochar analysis related with its environmental uses were assessed before subsequent work investigated the forces driving the capture of P with biochar derived from various sources. This work found that the concentration of Ca and Mg within various unmodified biochars was the main driver of P adsorption, with CO_2 activation (carried out to increase biochar surface area and porosity) providing only a limited improvement. Building on this initial work, the thesis has culminated in the development of novel modified biochars with enhanced properties for the efficient recovery of P. Various biochar composites removed > 90% of P from an initial concentration of 10 mg P/L and presented moderate release of P after extraction at mildly

acidic and basic pH, which attempted to replicate soil solutions. Upon further study through isotherm and kinetics experiments the adsorption was found to occur at a rapid rate (reaching equilibrium within < 5 min); whilst maximum capacities were modest in most cases (10–15 mg P/g composite), the heat of adsorption was found to be higher than commonly reported in the literature.

This thesis has made a significant contribution to the analysis, use, and mechanisms involved in biochar-P interactions, and has furthered the development of biochar composites with improved properties for P recovery through novel routes.

Acknowledgements

Firstly, I would like to thank my supervisors (Dr. Peter Hooda, Professor Andrew Cundy and Dr. Saran Sohi) but most of all Dr. Rosa Busquets – I could not have found a better team and first supervisor. I would like to acknowledge the UK Biochar Research Centre and The University of Edinburgh for not only supplying the biochar samples for study throughout the thesis, but for welcoming me on several occasions whilst visiting facilities.

At Kingston University I would like to express my sincere appreciation to Drs Wendy Brosnan, Simon Crust, Tracey Davies, Simon DeMars, (Prof.) Peter Foot, Richard Giddens, Ian Gill, Rizwan Merali, Richard Singer, Siamak Soltani and Paul Stovell. This is for support and discussion relating to experimental work carried out throughout the PhD. I would like to add my additional appreciation for the Kingston University Doctoral School and specifically Professors Andy Augousti and Barbara Pierscionek (now at Nottingham Trent University), for the opportunity to carry out a PhD and for the studentship received, and Rosalind Percival for continued support.

Outside of Kingston University, Dr. Santanu Ray is acknowledged for carrying out XPS analysis at The University of Brighton and for taking time to explain the fundamentals of the analysis. I am extremely grateful to Peter Lyons at The University of Brighton for help with analysis (both XRD and ICP, in desperate moments when Kingston's were out of action). I must mention that without previous encouragement and guidance from Peter Lyons, Christopher English and Prof. Andrew Cundy at The University of Brighton, I may never have set out on a PhD or discovered how rewarding research can be – I am extremely grateful. Drs Yishan Zheng and Steve Tennison are thanked for their discussions relating to porosimetry analysis, Dr. Michael Chipps at Thames Water is thanked for providing wastewater samples.

I would like to thank all my fellow PhD students both inside and outside of the lab for their various discussions, distractions and experiences but especially Luke, Navid, Rav, Marco,

Mateo, Federico, Yousaf, Alex, Nihad, Cameron, James, Gabriel, and others (you know who you are). Finally (and most importantly), I would like to thank my family and friends for their support throughout but especially to Siobhan and my parents – without them I would not have completed this thesis.

Table of Contents

List of Figures

List of Tables

List of Acronyms

BET – Brunauer-Emmett-Teller

C_0 – initial concentration

C_{eq} – equilibrium concentration

EC – electrical conductivity

EDS – energy dispersive X-ray spectroscopy

EPA – Environmental Protection Agency

EU – European Union

FTIR – Fourier-transform infrared spectroscopy

GAC – granular activated carbon

ICP-AES – inductively-coupled plasma – atomic emission spectroscopy

ICP-MS – inductively-coupled plasma – atomic emission spectroscopy

LDH – layered double hydroxide

LOD – limit of detection

LOQ – limit of quantification

MSP – pelleted *Miscanthus* straw

OSR – pelleted oilseed rape straw

P – pressure at equilibrium

P_0 – saturated vapour pressure

q_{eq} – quantity adsorbed at equilibrium (mg/g)

q_{net} – net quantity adsorbed at equilibrium (mg/g)

RH – rice husk

S_{BET} – specific surface area (m^2/g)

SEM – scanning-electron microscopy

SS – pelleted sewage sludge

SWP – pelleted soft wood

TEM – transmission electron microscopy

V – volume (L)

V_p – pore volume (cm^3/g)

W – weight (g)

WSP – pelleted wheat straw

WWTPs – wastewater treatment plants

XPS – X-ray photoelectron spectroscopy

XRD – powdered X-ray diffraction

1 Introduction

Phosphorus (P) is a nutrient essential for life – the maintenance of agricultural productivity is globally dependent upon the application of P-rock derived fertilisers (Schoumans et al., 2015) – geological reserves of P are finite. Excess P, of just ~0.02 mg P/L (Correll, 1998) in aquatic environments, can lead to promoted algal growth, hypoxia, and negative effects from algal toxins (Stoddard et al., 2016). Both the depletion of geological reserves of P and the eutrophication of water bodies are clear signs that the use of P is unsustainable. Development of technologies enabling the capture and reuse of P from waste streams is one way to increase P sustainability – wastewater treatment plants (WWTPs) represent a significant opportunity to recover P for reuse in agriculture. Removal of P from wastewater is common practice (due to legislation in many countries aimed at protecting surface water from eutrophication), and is carried out through precipitation using salts of Fe or Al, and biological techniques (Morse et al., 1998). P removed through these processes, however, is not always suitable for direct reuse as fertiliser or soil amendment due to contamination concerns and/or the limited bioavailability/solubility of the P component. There are technologically proven P recovery approaches such as the precipitation of struvite ($NH_4MgPO_4 \cdot 6H_2O$) and the thermochemical treatment of sewage sludge (Egle et al., 2015), however both demand a high level of technical input in terms of infrastructure and operation, which can limit these routes of recovery to larger WWTPs. The need for more WWTPs to increasingly achieve lower P discharge limits (< 1 mg P/L), in line with commitments to the EU Water Framework Directive (European Commission, 2000) for example, and some requirements to start recovering P (European Sustainable Phosphorus Platform 2017) drive the development of new technological options (Melia et al., 2017). These new technological options must be both simple and effective in enabling recovery of P from small-scale treatment works and achieve low P concentrations in effluent. Proposed revisions to EU fertiliser regulations aim to enable the reuse of P from a wider variety of recovered forms such as biochars, ashes, and

struvite. This is a critical time for the development of capable technologies enabling reuse of P from wastewater.

Biochar is a "stable" form of carbon derived from the pyrolysis (heating in a low-oxygen atmosphere) of biomass, which is often abundant or considered a waste. It is produced for environmental applications – namely carbon sequestration efforts, soil amelioration (Crombie et al., 2015) and the removal or immobilisation of various contaminants from water or soil respectively (Ahmad et al., 2014; Rajapaksha et al., 2016) – or as a by-product of the production of bio-oil and syngas, or to produce energy. The use of biochar for the capture and reuse of P is attractive due to the known native ameliorant properties of biochar when applied to soil and the sequestration of carbon – P-enriched biochar (i.e. after adsorption of P from wastewater) would have an additional benefit as a recovered fertiliser. Modification of biochar (post-pyrolysis), and its use as a sorbent or filtration media is a novel approach to recover P from WWTPs.

1.1 The aim

The aim of this thesis is to understand and develop the use of biochar and biochar-based materials as adsorbents for the capture of P from wastewater and to consider the practicalities of using biochar-based composites for P recovery. This will be achieved through the following objectives.

1.2 Objectives and structure of the thesis

1. To define the technologies used and trends in the recovery of P from wastewater through a literature review.
2. To establish the challenges of biochar characterisation and develop approaches to overcome them when analysing biochar for environmental applications.
3. To understand the driving forces of P uptake using biochar by characterising and assessing P uptake with unmodified and washed biochar samples.

4. To enhance P recovery from wastewater with biochar by modifying biochar post-pyrolysis.
5. To assess P uptake and release with the modified biochars and propose modified biochars offering advantageous properties for the recovery of P.

Each objective has been addressed in a self-contained chapter, which includes a brief and focussed introduction, results, and discussion – an overall summary of the information obtained across chapters, and their implications are given in Chapter 8, followed by a view to further research.

2.2 Biochar

Biochar has received much attention due to its unique properties enabling a variety of beneficial environmental applications, namely its potential for carbon sequestration (Crombie et al., 2015), soil amelioration (Kätterer et al., 2019), and the removal or immobilisation of various contaminants from water or soil respectively (Ahmad et al., 2014; Gámiz et al., 2019; Rajapaksha et al., 2016). Biochar has only quite recently been considered an attractive adsorbent capable of recovering P – for example, it was proposed in works by Chen et al. (2011) and Yao et al. (2011). Aside from biochar, commonly tested materials investigated for capturing P have included natural and modified minerals including zeolites (Choi et al., 2012; Xinggang Wang et al., 2014), mining, metallurgical and industrial by-products (Xinjun Wang et al., 2014) and synthetic metal oxides/hydroxides (Long et al., 2011; Tu and You, 2014; Xie et al., 2014). However, these materials may often be unattractive for soil application after P saturation, having only sparingly soluble forms of P present (i.e. low P bioavailability), and/or presenting potential contamination concerns such as excessive leaching of heavy metals/metalloids, and/or being high in cost. In contrast, granular carbons such as biochar can be attractive adsorbent materials due to their relatively high surface area, porosity, surface functionality, tailorability, and are often of suitable particle size to be applied as filtration media in a column or through flow apparatus. For example, granular activated carbon (GAC) is widely applied commercially to remove organic contaminants and heavy metals/metalloids from industrial and municipal wastewaters. However, GACs and synthetic carbons are expensive to produce and thus would be unsuitable for application to soil if used to remove P from wastewater. Biochar, unlike GAC, has not been activated thus requiring less energy to produce (lower cost) and implying less CO_2 emission in its production, making it more suitable for use in larger quantities and for application to soil after P adsorption; the application proposed in this thesis.

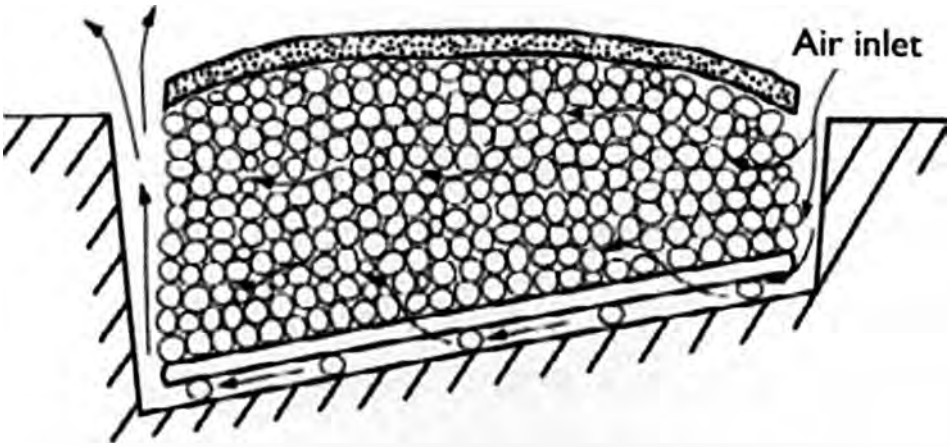

Figure 2.1 Large pit kiln. Taken from Lehman and Joseph (2009), originally adapted from FAO (1983).

Pyrolysis can be achieved within a variety of apparatus, but traditionally within a kiln (Figure 2.1). The low-oxygen atmosphere is achieved by covering the biomass, for example with earth, but more modern kiln designs and processes will involve purging/feeding the reactor with inert gases (most commonly N_2). Feedstocks used in the production of biochar can vary considerably, and include agricultural/food wastes and by-products (Klasson et al., 2014; Sun et al., 2014; Yao et al., 2011a), forestry wastes (Z. Wang et al., 2015), sewage sludge (Chen et al., 2015; Yuan et al., 2016), paper waste (Van Zwieten et al., 2009), marine macroalgae (Jung et al., 2016) and poultry litter (Cantrell et al., 2012; Y. Wang et al., 2015). The pyrolysis process is covered in great detail elsewhere (for example, Lehman and Joseph (2009)), however, it is important to highlight a few key points here. The variety of native biochar characteristics that can be prepared originate primarily through the choice of biochar feedstock, the pyrolysis temperature reached and the heating rate. Throughout the pyrolysis process, there are several changes and major developments that occur as volatile compounds of the feedstock are lost, and the structure of the biochar-carbon becomes more graphitic. For instance, some thermal decomposition occurs at temperatures > 100°C as biomass loses moisture content; < 400°C, cellulose and hemicellulose are known to break down; where

over a wider range of temperatures, up to 900°C, lignin breaks down (Yang et al., 2007), with depolymerisation taking place, accompanied by dehydration, leading to the condensation of the solid phase to produce the "stable" char (Shafizadeh, 1984; Sjöström, 1993). In essence, it is the varying amount and distribution of these constituents (cellulose, hemicellulose, and lignin) as well as the mineral content within the feedstock; the effect that the temperature reached during pyrolysis has on them; the heating kinetics (which determines the degree of reaction completion); and the structure (for example vascular tissue within some parts of the biomass formerly used for the uptake of nutrients and water) that ultimately determine the physical and chemical nature of the resulting biochar. In most cases, the physical structure of the feedstock material is retained with the pyrolysis treatment, and therefore the raw material has a large influence over the resulting structural characteristics of the biochar. The mineral content of the feedstock determines the resulting metal/ash content that can be retained on the surfaces and in the structure of the biochar even after washing.

2.4 Biochar characteristics

It is important to consider biochar characteristics generally and to consider what an ideal material may look like as an effective technology capable of recovering P. Ultimately, the environmental application of biochar is highly dependent upon its specific characteristics, for example: surface area, porosity, concentration of bioavailable nutrients, metal content and speciation, the degree and type of carbon functionality, pH and electrical conductivity (EC), and resulting surface charge all have a role. Figure 2.2 indicates some key characteristics and their interconnectivities with potential relevance for the recovery of P. These features and their interplays are exposed here. There are studies which have found concerns regarding the use of biochar in environmental applications – for example, polycyclic aromatic hydrocarbons are known to form during the pyrolysis process and can be present on the surface of biochars, but these were found to be bioavailable at very low levels only (Hale et al., 2012; Wang et al., 2017).

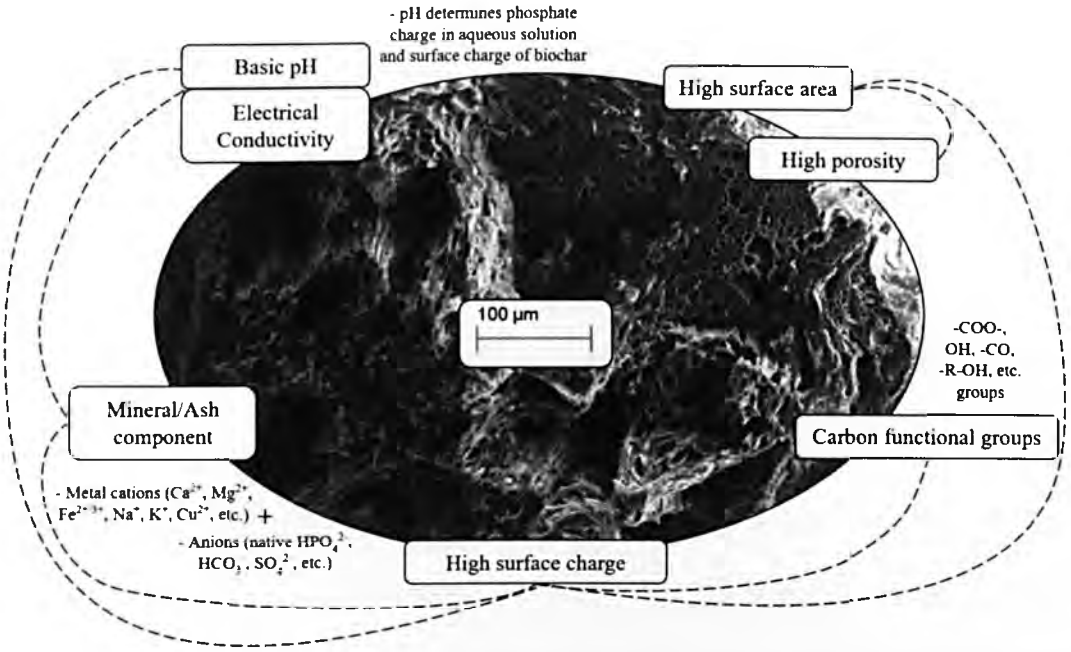

Figure 2.2 Diagram highlighting some key biochar properties and components that may have importance in the recovery of P from aqueous solution. The dashed lines represent their interconnectivities.

Surface area generally increases with increasing pyrolysis temperature, however at higher temperatures structures can begin to deteriorate and this can impact on the surface area. For example, biochars produced from mixed woods, maize, and meadow grass had the largest surface area when pyrolysed at 550°C opposed to the respective biochars pyrolysed at 450°C and 500°C (Břendová et al., 2012). Lua et al. (2004) showed that increasing the pyrolysis temperature from 250–500°C increased the surface area of activated carbon produced from pyrolysed pistachio nut shells, but temperatures above 500°C generally led to a decrease in both surface area and total pore volume. Likewise, Jung et al. (2016), found the highest surface area with biochar pyrolysed at 400°C as opposed to 600, 800 or 200°C. This decrease in surface area and porosity could be due to the collapse of structure at the higher pressures associated with the higher temperatures of pyrolysis, or the decomposition and softening of volatile fractions within the biochar structure (Lua et al., 2004) such as tar or melted ash (Lehman and Joseph, 2009). The temperature at which these deteriorations start to occur depend upon the feedstock, but it is generally around 600–800°C.

Some text on this page is under review as part of a book chapter to be published by Wiley in 2019

There are several approaches that can increase surface area and porosity other than changes to pyrolysis temperature – the most basic approach being physical processing such as grinding, either pre- or post-pyrolysis, but it will have limited impact on the overall surface area. Activation is the most common approach used to specifically increase surface area and porosity (such as in the production of GAC) and is achieved either thermally using high temperatures (800–900°C) and gases such as CO_2 or steam, or chemically with agents such as phosphoric acid or potassium hydroxide (Lozano-Castelló et al., 2007; Naushad et al., 2015). Surface areas of biochars tend to be < 500 m^2/g, most often found to be between 0–250 m^2/g (Ahmad et al., 2014; Břendová et al., 2012) – for instance, biochar produced from oak wood at 500°C and 800°C had surface areas of 107 m^2/g and 249 m^2/g respectively (Jung and Kim, 2014), a sewage sludge biochar pyrolysed at 900°C had a surface area of 68 m^2/g (Chen et al., 2015) – this is opposed to commercial GACs, from mined coal, that can have surface areas > 1000 m^2/g. Biochars tend to have macroporosity (pores > 50nm) and some large mesopores (pores 2–50nm) – these are mainly derived from the original structure of the biochar feedstock (phloem and xylem vessels). In the case of P capture, neither steam activation or changes to pyrolysis temperature (leading to higher surface area) were found to be effective in increasing P removal using pine sawdust biochar pyrolysed at 300 and 550°C (Lou et al., 2016). High surface area is usually desirable for adsorption processes; however, this study suggests that high surface areas (of up to 400 m^2/g), derived from higher pyrolysis temperatures and/or activation with steam, on their own are largely ineffective for enhancing the removal of P from solution, without an associated high content of cationic species. However, it is still unclear what the overall effect of higher surface area has on the uptake of P, using biochars with higher metal content especially.

The changes that occur during pyrolysis as the temperature is increased leads to an increased ordering of the carbon structures, becoming more structured and graphitic at higher temperatures. As functional groups within biochar-carbon are situated at the edges of carbon sheets (Boehm, 2002, 1994; Salame and Bandosz, 2001), the chemistry of the surface of

biochar is highly dependent upon this treatment temperature; with a decrease in carbon oxidised groups at higher pyrolysis temperatures. This change is indicated elementally, with an increase in C content and a decrease in O, H, N and S contents in biochar – biochars, however, are still known to have an abundance of carbon functionality on their surfaces. It is possible that P could interact with carboxylic or phenolic groups, for example, however, this is unlikely under the environmental conditions of the adsorption process, and at the pH values of most biochars in aqueous solution where most moieties will be found deprotonated and hence negatively charged. P exists as phosphate in the environment and in aqueous solution (mainly as HPO_4^{2-} or $H_2PO_4^-$, depending on pH), where basic pH results in a higher abundance of HPO_4^{2-}/PO_4^{3-} species. It is not clear from the literature the relationship biochar surface chemistry and P interaction has.

The feedstock mineral component determines the ash/metal content of biochar and is closely related to the pH and EC in solution. Biochar pH increases with pyrolysis temperature due to increased content of ash (such as carbonates and oxides) – common inorganic components of biochar are K, P, S, Ca, Na, Mg, Fe, and Zn, as well as a presence of organic groups that can be present as Bronsted-Lowry bases at environmental pH (such as amines, amides or phenoxy groups). It is known that at the same pyrolysis temperature, wood-derived biochars tend to have a much lower mineral/ash content than non-wood biochars – for example, Uchimiya et al. (2011) showed that for grass chars, ash content was almost 20% for pyrolysis temperatures of > 700°C, whereas wood and pine needle chars had ash contents of 2–4%. It has been shown that biochar produced at < 400°C had a low pH, low EC and surface area (Lehmann, 2007; Li et al., 2013) compared with biochar pyrolysed at higher temperatures which tend to possess higher alkalinity. The ash/metal component of biochar is often now considered to be the main factor that determines the effectiveness of biochar or biochar-based materials for the adsorption of P. The trade-offs and interplays that occur between biochar structural and chemical properties however are important and still not fully understood. Biochars are complex heterogeneous materials and there are often difficulties in

fully understanding, as well as any attempts to engineer, how biochar and P interact. The following sections focus on the use of biochar for P removal and recovery from water and set out the various approaches used.

2.5 P recovery with biochar

Ultimately, producing biochar to enable effective recovery of P through adsorption, necessitates the balancing of critical characteristics. Some works have found difficulties in removing P from water with unmodified biochar. Jung et al. (2015), evaluated the P removal ability of 5 unmodified biochars and found that 3 of the 5 biochars possessed negative capacities to remove P, i.e. more native-P release than uptake. Amongst the 5 samples, an oak wood derived biochar had a limited ability to remove P, and a peanut shell biochar removed 61.3% of P from an initial concentration of 5 mg P/L. This was attributed to the higher concentrations and ratios of Mg and Ca compared to native-P. Similarly, Takaya et al. (2016) found limited removal of P using a variety of unmodified biochars pyrolysed from wood, greenhouse waste, municipal waste, and anaerobic digestion presscake (< 10% removal from initial concentrations of 400 mg PO_4^{3-}/L).

Some biochar feedstocks are known to have high concentrations of cations and may be chosen specifically due to their higher mineral/ash content and the known affinity between those constituents (such as Ca, Mg, Fe, and Al) and P. For example, marine macroalgae has a high mineral content (specifically Mg and Ca) – Jung and Ahn (2015) found maximum adsorption of P (experimental data fitted to Langmuir-Freundlich adsorption model) to be 3.36 mg P/g of brown marine macroalgae-derived biochar. Jung et al. (2016) found that marine macroalgae biochar pyrolysed at 400°C had an adsorption capacity of 18.2 mg P/g from an initial concentration of 50 mg P/L. Other feedstock materials used to produce biochar for P adsorption purposes have included Mg-accumulated tomato tissues and anaerobically digested sugar beet tailings (Yao et al., 2013, 2011a) – the Mg-accumulated tomato tissue biochar, once saturated with P, showed potential for P reuse through extraction

studies and bioassays via grass seedling growth. Dai et al. (2017) investigated the P removal ability of crab shell derived biochar pyrolysed at various temperatures (300–900°C) and found an increase in P removal (up to almost 100% in aqueous solution and about 60% from biogas effluent) with increases to pyrolysis temperature. Although some of these materials possess efficient removal of P, the feedstock materials may be limited if considered for larger scale use (i.e. relatively unavailable or having inconsistent physical or chemical properties over time), and often have significantly lower abilities to remove P (in terms of their maximum adsorption capacity but also kinetic rate) compared with modified biochars in the literature. Marine macroalgae stands out as an effective biochar feedstock that may enable efficient removal of P, whilst being potentially practical for use at larger scales.

2.6 Gaps in knowledge

Analytical methodology for the study of biochar for their use in environmental applications, P recovery among them, is not generally established and hinders progress in the development of biochar as an environmental tool. To date, methodology for the characterisation of soils (or biochar amended soils) and activated carbons is adopted for the study of biochars, despite soils/activated carbons and biochars being very different systems. The lack of consensus on analytical methodology and the various approaches used leads to only approximate information with non-optimal approaches "borrowed" from other areas – this can lead to inaccuracies and make the comparison of results throughout the literature difficult.

When this study started, there was very limited understanding of how specific biochar characteristics impacted the interaction of biochar and P, and the interplay between various characteristics and P is still lacking. For example, it is not clear from the literature to what extent higher surface area and porosity of biochar increases the P adsorption capacity; how the content of some specific metals in biochars' structures can lead to higher P adsorption; or if the concentrations of certain functional groups, pH and EC have major influence over the uptake of P.

There are a wide variety of approaches for using and now modifying biochar for the aim of P recovery (the modification of biochar is introduced and discussed within Chapter 6). The specific choice of biochar feedstock and pre-pyrolysis modifications have been the most common approaches used in the literature to bring about an increased ability for biochar-based materials to capture P. Post-pyrolysis modification of biochar has not been explored to the same extent. Finally, although some papers have tested the availability of P from saturated biochar-P materials in desorption studies and bioassays, it is important that further research here is carried out because the factors leading to the effective or controlled release of P have not yet been defined.

In this thesis, the approach chosen has been to first assess and establish effective characterisation and analytical techniques for assessing biochar characteristics (Chapter 4), which will be later used in the rest of the thesis, before elucidating key biochar characteristics that influence the interaction of P within washed biochar matrices (Chapter 5). Chapters 6 and 7 aim to modify these biochar materials post-pyrolysis to achieve the aim of deriving an enhanced material with effective P recovery.

3 Materials and methods

This chapter introduces the materials, methods, and instrumentation used throughout the thesis – the more detailed and specific methodology used in individual experiments is introduced within their respective Chapters (4–7). Chemicals were of analytical grade, otherwise specified.

3.1 Standard biochar materials

Table 3.1 An overview of the standard biochar materials used throughout the thesis.

Sample	Feedstock	Highest pyrolysis treatment temperature (°C)
SS550	Sewage sludge	550
SS700	Sewage sludge	700
WSP550	Pelleted wheat straw	550
WSP700	Pelleted wheat straw	700
OSR550	Pelleted oilseed rape straw	550
OSR700	Pelleted oilseed rape straw	700
MSP550	Pelleted *Miscanthus* straw	550
MSP700	Pelleted *Miscanthus* straw	700
RH550	Rice husks	550
RH700	Rice husks	700
SWP550	Pelleted soft wood	550
SWP700	Pelleted soft wood	700

The sorbents investigated for the capture of P throughout this work are 12 standard biochar materials derived from 6 different feedstocks pyrolysed at 2 treatment temperatures. The biomass was pyrolysed at the UK Biochar Research Centre – Table 3.1 details the biochar materials used, their feedstocks, treatment temperatures, and sample names. These 12 biochars and treatment temperatures were chosen specifically because they offer a range of biochar characteristics and are derived from a variety of widely available biomass. This enables the study to encompass the range of potential driving and limiting factors in terms

of specific biochar interactions with P whilst maintaining potential practicality on larger scales. The materials were received in 1 L containers that were purged with N_2 after pyrolysis and kept sealed until used. Further details on the preparation process of biochars have been reported by the UK Biochar Research Centre (Mašek et al., 2018).

3.2 Biochar sample preparation

Biochar was crushed gently using a pestle and mortar and sieved, using sieves with mesh sizes of 1 mm and 500 microns, to 0.5–1 mm to ensure that fragments of biochar were within same size range and in agreement with works from the UK Biochar Research Centre and others (Jung et al., 2016; Shepherd et al., 2017). The crushed biochar materials were then washed through flow with ultrapure water (200 bed volumes) to remove residual ash. The experimental work completed in Chapter 5 aimed to understand the driving forces controlling P uptake with these unmodified and washed materials and to inform an approach to modify and enhance them through post-pyrolysis modification. Therefore, the washing step aimed to create a clean slate – i.e. a more homogenous biochar structure with residual ash and loose components removed – which would then be utilised in subsequent work to enhance and modify. The washing step was carried out prior to all experimental work, unless specified, including the characterisation of biochars, and was followed by drying in a vacuum oven at 60°C until dry (achieving constant weight).

3.3 Adsorption studies

Na_2HPO_4 was used as the source of P in all adsorption studies. For comparison of P adsorption ability between biochars, adsorption tests were carried out in batch mode under equilibrium conditions using an orbital shaker at 90 rpm, 25°C for 48h. Analysis of P concentrations at initial and equilibrium conditions were carried out using Inductively Coupled Plasma–Atomic Emission Spectroscopy (ICP-AES) (ULTIMA 2C, Jobin Yvon Horiba), after filtering using 0.22 μm syringe-driven PES filters (Merck Millipore, Ireland). To assess the performance of biochars that showed very low adsorptive capacity (i.e.

unmodified biochar in Chapter 5) it was necessary to use high initial P concentrations (when compared with concentrations of P in wastewater) and high adsorbent to adsorbate doses – an initial P concentration of 50 mg P/L and a biochar dose of 50 g/L was used. For assessment of P adsorption using chemically modified biochars (Chapters 6 and 7), wastewater-relevant initial P concentrations were used (i.e. < 10 mg P/L) and a lower adsorbent doses of 5 g/L due to the significant enhancement in P removal ability – the same analytical method and shaking conditions (in terms of intensity and time) were used.

The adsorptive capacity (q_{eq}, mg P/g biochar) was obtained from the mass of P removed from solution by the biochar per mass of biochar, as expressed in equation 1, where C_0 and C_{eq} are the initial and final P concentrations in solution respectively. V (L) is the volume of solution and w (g) is the weight of adsorbent used.

$$q_{eq} = (C_0 - C_{eq})\frac{V}{w} \qquad (1)$$

After the through flow washing step was undertaken, some biochar samples still presented water soluble P release (i.e. native P) and therefore it was necessary to quantify this using control samples (biochar incubated with ultrapure water). A net P removal capacity was also measured (q_{net}, mg P/g biochar). This was calculated as q_{eq} (equation 1) added to the P release assessed (i.e. mg P released/g biochar) using the control samples. This was assessed in Chapter 5 only, i.e. when working with unmodified biochar – the release of P was negligible when working with chemically modified biochar samples (Chapter 6 onwards).

3.4 Analysis of P, metals, and metalloids

The analysis of P and major elements (Na, Mg, Al, S, K, Ca, Mn, Fe, Cu, and Zn) was carried out using ICP-AES. Minor elements were analysed using Inductively Coupled Plasma–Mass Spectroscopy (ICP-MS) (7700 Series, Agilent Technologies). The concentration working

range used of the metal analysis via ICP-MS was generally 0.1 µg/L to 100 µg/L, and via ICP-AES was 0.1 mg/L to 100 mg/L. Standards were prepared from the dilution of a stock solution, 100 mg/L multi-element standard (VWR Chemicals) in 5% HNO_3 – a separate certified standard was used for P analysis, 992±6 mg/L (Alfa Aesar). Analysis was carried out where the calibration of individual metals presented r^2 value > 0.995.

Quality parameters (limit of detection, repeatability, reproducibility, and accuracy) were assessed for the quantification of P, metals, and metalloids reported. The limits of detection and quantification (LOD and LOQ, respectively) were calculated based on the standard deviation of the response, and the slope of the calibration curve.

$$LOD \text{ or } LOQ = \frac{F\,SD}{b} \qquad (2)$$

where b is the slope of the calibration curve and SD is the standard deviation of the response of the blank run > 10 times, and F a factor as either 3.3 (for LOD) or 10 (for LOQ) (Shrivastava and Gupta, 2011) – a general convention used in order to determine at what levels the signal of a concentration can be differentiated from that of a blank. Repeatability was determined in all runs by repeating measurements in triplicate, the average value was taken in all cases and where the relative standard deviation was deemed to be high (i.e. > ~5%, dependent upon concentration), the sample was reanalysed. Accuracy was checked against the reference in every analytical run – the reference was P (or a multi-elemental standard) in water, diluted from the certified reference to be within the intermediate concentration range in terms of the calibration and expected sample concentrations. The reference also allowed for correction of any instrumental drift in the signal, which can occur with ICP analysis (more prevalent when using ICP-MS) – this helped check that the in-run reproducibility was acceptable. Reproducibility was checked by analysing samples on

different days, however, it was ensured that each set of samples analysed for each individual study throughout the thesis were included within the same analytical run – this eliminated the potential for any issues relating to sample reproducibility.

3.5 Biochar characterisation

3.5.1 Surface area and porosity measurements

The structures of the biochars and activated carbons were determined via N_2 adsorption-desorption isotherms at 77 K. All isotherms were carried out with a BELSORP-miniII porosimeter (MicrotracBEL, Japan). Prior to the gas adsorption isotherm measurement, the samples were degassed for 24h at 150°C. The specific surface area (S_{BET}) was calculated using the standard BET (Brunauer-Emmett-Teller) model (Brunauer et al., 1938), the BJH (Barrett-Joyner-Halenda) model (Barrett et al., 1951) was used to determine pore size distribution. Total pore volume, V_p, was estimated at $P/P_0 \sim 0.99$, which is a relative pressure at which all of the pores of the sample can be considered to be filled with N_2, where P and P_0 denote equilibrium pressure and the saturated vapour pressure of N_2 at 77 K, respectively.

3.5.2 Scanning electron microscopy (SEM) and SEM – Energy-dispersive X-ray spectroscopy

Scanning electron microscopy (SEM) was used to study the morphology and macroporosity of the samples. Biochar was mounted on specimen stubs fitted with adhesive carbon pads, sputter coated with gold-palladium and examined using a Zeiss Evo50 (Oxford Instruments, Cambridge, UK) SEM – micrographs were obtained at an accelerating voltage of 20 kV, unless specified. SEM – Energy Dispersive X-ray Spectroscopy (EDS) (Oxford Instruments, Cambridge, UK) was carried out where the qualitative determination of abundant elements at the surface of the sample was needed and for mapping the distribution of metals.

3.5.3 Light microscopy

Light microscopy images were collected from the resin impregnated samples using an Olympus BX51 microscope fitted with a QImaging MicroPublisher 3.3 real-time viewing unit, and lenses of 5–100x magnification.

3.5.4 X-ray powder diffractometry

Powdered X-ray Diffraction (XRD) was used for identifying crystalline phases present within biochar. For XRD measurements, the biochar samples were powdered using a pestle and mortar and analysed using the X'Pert^3 Powder instrument (PANalytical, The Netherlands) between 2θ values of 5° to 70°, using steps of 0.1° and 8 s per step. Crystallographic compounds were identified by comparing the diffractogram peaks with a mineral database (International Centre for Diffraction Data – ICDD).

3.5.5 pH and electrical conductivity

Electrical conductivity (EC) measurements and pH were carried out using the International Biochar Initiative recommended method (Rajkovich et al., 2012). Briefly, 1g of washed biochar was equilibrated with 20 mL of ultrapure water for 1.5h on an orbital shaker (90 rpm) at 25°C. After equilibration, pH and EC measurements were carried out using probes and meter (model Eutech PC700) from Eutech Instruments (The Netherlands).

3.5.6 Quantitative metal analysis

The concentration of metals within the biochar samples was quantified following the EPA method 3052 (U.S. EPA, 1996) in triplicate. Briefly, 0.2 g of biochar were added to a microwave vessel with 2 mL of ≥69% HNO_3, 0.5 mL of ≥30% H_2O_2 and 0.5 mL of ultrapure water. Digestion took place within a microwave digestion unit (Mars 5, CEM, UK), held at 250 psi for 30 min. After dilution to < 5% HNO_3, elemental concentrations were determined using ICP-MS or ICP-AES.

3.5.7 Surface analysis

3.5.7.1 Boehm titrations

Total acidity was assessed using a Boehm titration method (Boehm, 2002). This method measures the amount of NaOH (or $NaHCO_3$ and Na_2CO_3) neutralised by the biochar – assumed to be solely due to surface functional groups on biochar – allowing for determination of the total acidity of the biochar. It has been reported that the method can lead to inaccurate results when assessing biochars (Fidel et al., 2013) as reactive ash and organic compounds can be gradually released and interfere with the neutralisation of the reactant solution. Therefore a modified Boehm titration method involving further washing steps (Tsechansky and Graber, 2014) was adopted in this thesis. The Boehm titration method used was as follows.

A ratio of ~0.8 g biochar to 40 mL of wash or reactant solution (0.05M NaOH) was used throughout. The method consisted of sample pre-treatment involving 2 consecutive acidic washes (0.05 M HCl) and 2 subsequent basic washes (0.05 M NaOH), each carried out for 24h on an orbital shaker. Following this the samples were washed 5 times with water before re-protonation of the surface acidic groups with a solution of 0.025 M HCl (24h on an orbital shaker) before a final 10 washes with ultrapure water – the samples were dried at 40°C under vacuum before equilibration with NaOH. The pre-treated samples were equilibrated with a 0.05 M NaOH solution for 24h. After equilibrium, the liquid extract was filtered using Whatman n°.1 filter paper and acidified using 0.05 M HCl at a 2:1 ratio (HCl:extract). The acidified extract was then titrated against a freshly standardised NaOH (0.05109 M) solution using phenolphthalein as an indicator. The standardisation was carried out with potassium biphthalate as the primary standard. The difference between the titrated volumes for the acidified extract and an acidified blank was assumed to be related to neutralisation by an equivalent concentration of total acidic groups on the biochar surface. These measurements were carried out in triplicate.

3.5.7.2 X-ray photoelectron spectroscopy

X-ray photoelectron spectroscopy (XPS) was performed, with the help of Dr. Santanu Ray at The University of Brighton, on biochar samples after slight crushing with the back of a spatula, using an ESCALAB 250 Xi system (Thermo Scientific) equipped with a monochromated Al Kα X-ray source, a hemispherical electron energy analyser, a magnetic lens and a video camera for viewing the analysis position. The standard analysis spot of ca. 900 × 600 μm^2 was defined by the microfocused X-ray source. Full survey scans (step size 1 eV, pass energy 150 eV, no of scans: 5, dwell time 50 mS) and narrow scans (step size 0.1 eV, pass energy 20 eV, no of scans: 10, dwell time 100 mS) of the C 1s (binding energy, BE ~ 285 eV) regions were acquired from three separate areas on each sample. Data were transmission function corrected and analysed using Thermo Avantage Software (Version 5.952) using a smart background.

3.5.7.3 Infrared spectroscopy

Fourier transform infrared spectroscopy (FTIR) was carried out on a Nicolet iS5 spectrometer with an iD1 transmission attachment (Thermo Scientific). Biochar samples were diluted to 1% weight with KBr and pressed into a disc before analysis – 20 scans were carried out with a resolution of 1 cm^{-1}.

3.6 Data analysis and statistics

All data was analysed with the use of Excel. Statistical analysis was carried out using Minitab 16 software. Significance was deemed for values of $p < 0.05$. ANOVA and t-test comparing means and t-correlation test were used to analyse the effect of the study-controlled parameters on the response measured. Outliers were identified using a Dixon's Q test. For principal component analysis, the data were scaled to between -1 and 1 in each series of experimental values to correct for differences between units of measurement.

4 Biochar as a complex system: methodological approaches for the characterisation of biochar structural and chemical properties

4.1 Introduction

Biochar is investigated and used for different environmental purposes including for soil amelioration, climate change mitigation, and water and soil remediation (Lehman and Joseph, 2009), where its potential effectiveness is informed and based on biochar physical and chemical characterisation. Therefore, accurate measurements of biochar properties are crucial. Within agronomy, assessment of pH, mineral content and nutrient availability for example, as well as identification of any potential contaminants that could leach to soil, are important to inform of potential biochar efficacy. For assessment of biochar for carbon sequestration applications, the stability or recalcitrance of the biochar-carbon is obviously a defining property required to be assessed with reliability.

The Official Methods of Analysis of the Association of Official Agricultural Chemists (AOAC) periodically publishes collections of procedures for the analysis of a wide variety of samples (AOAC, 2019). Some of these methods have been adopted as harmonised international reference methods by international organisations such as the International Union of Pure and Applied Chemistry (IUPAC) or the Codex Alimentarius Commission. But to the best of our knowledge, the AOAC has not published methods for the characterisation of biochar. The lack of standardised methods for the study of biochar has been overcome by adoption of methods designed for the characterisation of soil or other forms of carbon, but the translation of methods from these matrices to biochar can entail some error. Recently, some characterisation strategies of biochar have been included in a book (Singh et al., 2017), and there is also a set of standardised methods for the analysis of biochar, produced by the International Biochar Initiative (IBI, 2015). These documents outline methodological approaches to the study of biochar; however, it does not extend to

the discussion of some approaches that are relevant when assessing biochar for water treatment or other more specific environmental applications.

There are a myriad of physicochemical characteristics of biochar that can be important to assess. These include the analysis of surface area, porosity, surface charge, carbon chemistry, metal content and mineral speciation (both on the surface and in bulk). To some extent, these key biochar characteristics are all quantifiable, however, the complex nature of biochar can pose several problems when working to characterise them, such as inter- and intra-sample heterogeneity, changing properties over time, and brittleness of biochar particles. Hence, the complex nature of this type of widely used adsorbent (that is far from relatively stable homogenous carbons, or soil) should entail the use of a different set of analytical procedures. These should be used with the limitations of the technique and considered with the characteristics of the sample in mind. Careful consideration is required when developing experimental approaches to study critical biochar characteristics for particular applications. Therefore, the aim of this chapter is to investigate, experimentally, analytical approaches to the study of various biochar characteristics relevant to the use of biochar for water treatment applications, with techniques commonly available in environmental research laboratories. The strengths, limitations, and requirements of the analytical techniques assessed, for obtaining accurate measurements of biochar, are made from the study of 8 biochar materials.

4.2 Materials and methods

4.2.1 Chemicals and instrumentation

The reagents used for the digestion of biochar were HNO_3 and H_2O_2, as outlined in Chapter 3. KBr (of spectroscopic grade) was used to dilute the biochar samples for IR spectroscopy and was thoroughly dried before use. The instrumentation used for the characterisation of the biochar samples include SEM, SEM-EDS, light microscopy, XRD, FTIR, XPS, N_2 adsorption isotherms, and acid-microwave digestion and ICP analysis – all used as outlined in Chapter 3.

4.2.2 Biochar and sample preparation

Biochars (8) derived from 4 different feedstocks (wheat straw (WSP), oilseed rape straw (OSR), rice husk (RH) and *Miscanthus* straw (MSP)) pyrolysed at 2 treatment temperatures (550°C and 700°C) were investigated. These were prepared by the UK Biochar Research Centre (Mašek et al., 2018), received in 1 L sealed containers that were purged with N_2 after pyrolysis. The samples are referred to as WSP550, WSP700, OSR550, OSR700, RH550, RH700, MSP550 and MSP700.

Sample preparation steps were undertaken prior to the analysis of the physicochemical properties of biochar. For SEM, N_2 adsorption isotherms, and acid-microwave digestions, the biochars were crushed to particle sizes between 0.5–1mm using a pestle and mortar, and sieved with mesh sizes of 1 mm and 500 microns before being thoroughly washed with 200 bed volumes of ultrapure water through flow. This pre-treatment minimised uncontrolled release of ash that could block access to pores; allow exposing inner surfaces for its imaging with microscopy; impregnating the matrix with resin for light microscopy and SEM-EDX characterisation; and to allow degassing the sorbent and facilitate the adsorption of N_2 onto its exposed surface for the quantification surface area and porosity analysis.

Uncrushed biochar samples were embedded in resin for the visualisation of macroporosity through light microscopy and the SEM-EDS analysis of the polished surfaces. Two different hardeners were used to compare the final result of the polished surface. The procedure was as follows. The biochar sample was placed into a 25mm mould, where a mixture (4:1) of resin (RB158) and hardener (either Hardener IPD or DETDA), respectively, was added so as to cover the sample. The mould was then added to a vacuum impregnation unit where air was evacuated from the samples. Once the resin had reached a gel-like state it was placed on a hot plate at 50–60°C and allowed to cure overnight. Once cured, the samples were polished initially with a silicon carbide disc of 320 grit through to a 2000 grit silicon carbide disc each applied for 1 min with 50N of pressure, on an Abramin polishing machine. This

was then followed by diamond cloth polishing (from 6 micron for 12 min, through to 1 micron for 2 min), again with 50N of pressure.

For XRD characterisation of the biochar, the samples were crushed to a fine powder using a pestle and mortar to ensure equal orientation of crystalline material within the samples. For XPS analysis, the samples were crushed slightly using the back of a spatula. This was necessary to expose a moderately flat surface for analysis, with the average from 3 relatively large areas of the sample analysed in order to reduce the effects from differences in the 3D orientation of sample surfaces.

For the characterisation of the biochar samples with FTIR, the washed biochar samples were diluted (1% weight) with KBr; ground with a pestle and mortar, and 200mg of the diluted sample pressed to form a 1 cm radius biochar (in KBr) tablet. Boehm titrations were carried out as described in Chapter 3.

4.3 Results and discussion

The study biochars (8) offers a range of characteristics from a variety of feedstocks and treatment temperatures – this enables the study to encompass the analysis of samples possessing varying characteristics.

4.3.1 SEM and Light Microscopy – biochar structural properties

SEM is an important technique for visualising surface morphologies of solid samples, and when assessing adsorbents, is commonly used to qualitatively assess pore or crystal sizes within adsorbent structures. Quantitative analysis of micrographs is possible, but impracticable given the localised analysis provided and therefore the consequent high number of images required to have a representative sample from such a heterogeneous material such as biochar; similar limitations have been highlighted when attempting to use SEM for the quantitative analysis of nanoparticle sizes (Dudkiewicz et al., 2015). The spatial resolution of state-of-the-art SEM (~1nm), is about 10 times lower than what transmission

electron microscopy (TEM) offers for example (Mbundi et al., 2014), but this resolution is enough to image meso- and macropores within biochar, that can be important for adsorption processes. Another advantage of SEM with respect to TEM is that the former does not require ultrathin samples that can be penetrated with an electron beam – preparing samples for TEM thus requires some additional steps (milling, sieving, sonicating in ethanol) that will result in a deposit onto a grid from where nanostructure of the adsorbent can be imaged with great detail (Uchimiya et al., 2017). This technique can be considered largely unnecessary for analysis of biochar morphology.

SEM is a ubiquitous technique within materials chemistry and environmental science research. Figure 4.1 (A and B) show SEM micrographs of biochar samples pyrolysed from rice husk and wheat straw at 550°C and 700°C, respectively. From the micrographs, surface morphology is observed with some of the internal pores and structural characteristics visualised. However, there are several common problems that can be faced when assessing biochar structural properties with SEM. The observation of internal structure is only very localised, and this is aggravated by the fact that it is a heterogeneous material. From the study of several areas alone, it is hard to make assumptions of biochar pore structure, and there is no recommendation about the number of micrographs and magnification that would be advisable to have representative information from a biochar specimen. Given this limitation, SEM images will be used qualitatively in this thesis.

Additional difficulties with the study of biochar with SEM is that biochar can be extremely brittle and therefore it is challenging to expose its inner structures without either sample destruction or the introduction of artefacts. Additionally, biochar samples can be susceptible to charging under the electron beam. Even though the carbon proportion of the sample is conductive, the ash component and the fractured nature of biochar samples can lead to some portions of the mounted sample not being sufficiently grounded and therefore charging. Therefore, it was found that in most cases, coating biochar samples with a Au-Pd alloy was

necessary rather than simply mounting to a carbon adhesive pad, to ensure grounding. Additionally, the beam intensity was lessened for some localised areas or for high magnification, where smaller spot sizes are required to be used.

Light microscopy was investigated as an alternate characterisation technique for the qualitative assessment of biochar pore size and structure. To enable the visualisation of biochar pores, samples of biochar were embedded in resin, followed by a polishing stage to enable the visualisation of a flat surface. Figure 4.1 (C and D) show that biochar pore size can be very well assessed using light microscopy where the grey areas represent dead volume in the sample (i.e. resin). Although this technique has provided useful information from these samples, other samples that possess predominant micro- or mesoporosity characteristics would require a different approach as light microscopy could not provide the required magnification and SEM would be required for detailed imagery of their morphology (for meso- and microporous materials, N_2 adsorption isotherms can provide quantitative information regarding their size and distribution). For the study of agriculturally derived biochars pyrolysed at 550 and 700°C however, the porosity is determined to be predominantly macroporous in nature. Having both SEM and light microscopy imagery provides quite detailed, albeit qualitative, information of biochar morphology, porosity and presence of ash deposits.

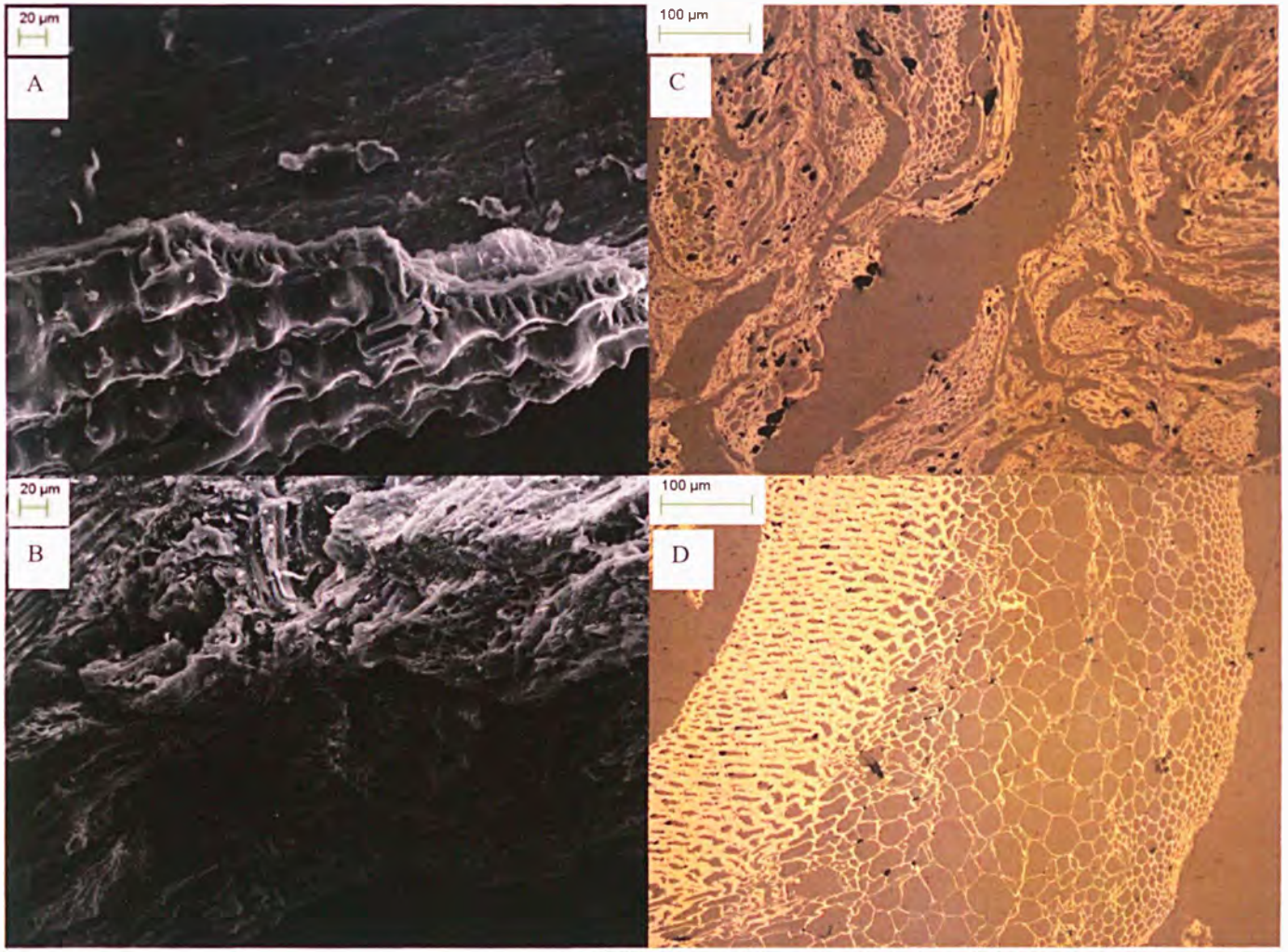

Figure 4.1 SEM micrographs of RH550 and WSP700 (A and B respectively) and light microscopy images of OSR550 and WSP550 (C and D respectively).

4.3.2 N_2 adsorption isotherms – surface area and porosity

N_2 adsorption isotherms at 77 K and BET analysis have become the standard in biochar surface area and porosity characterisation and the use of this technique has been derived from the analysis of activated carbons and other porous adsorbents. Biochars, however, are very different materials to activated carbons so the use of this technique may not always be valid. An example is illustrated in Figure 4.2, which shows N_2 adsorption isotherms for OSR550 biochar and GACs from two suppliers. The low adsorption of N_2 at low to medium relative pressure suggests that the biochar material lacks microporosity, however this lack of adsorption could also be related to a low heat of adsorption. This assumption however agrees with the SEM micrographs, where little evidence for micro- and mesoporosity was found, and light microscopy examination, which shows a largely macroporous structured material. In any case, the isotherm type would be classified as type III, i.e. indicative of a non-porous (i.e. lacking micro- and mesopores) sorbent with low adsorbent-adsorbate interaction energy.

When comparing the isotherms of the GAC and an example of a biochar sample (in Figure 4.2), the differences are apparent. The high level of adsorption at low relative pressures suggests that there is a high degree of microporosity present within the GAC samples, however this could also be related to higher adsorbent-adsorbate interaction energies. Mesoporosity, and specifically ink-bottle shaped pores are often indicated by hysteresis (between the adsorption and desorption branches), where at relative pressures just below 0.5 p/p_0 the hysteresis closes. For the biochar sample shown, there is a slight increase in desorption (i.e. a dip in the desorption branch) just below relative pressure of 0.5, indicating a degree of mesoporosity, however, it is also apparent that the hysteresis does not close. There is a relatively large hysteresis between the adsorption branch and desorption branch even at low relative pressures for the biochar's isotherm data, suggesting that a proportion of the adsorbed N_2 has become trapped in the biochar structure. This could be due to the

presence of residual ash in the sample that may move during the analysis, potentially causing artefacts, but could also be related to the gradual emptying of liquid N_2 from the Dewar vessel, or a slight leak in the system – pronounced due to the overall low volumes of N_2 gas adsorbed. The adsorbed quantity of gas adsorbed is in the range of 50–100 times more for the GAC sample, per gram of sample. The reproducibility of the analysis was tested by assessing the isotherms of the samples presenting open isotherm branches on > 6 times over 3 years. The method used to quantify BET and porosity with the BELSORP-miniII porosimeter (used in this thesis) was validated by measuring the same samples (GAC and a biochar samples) by an independent analyst and instrument (Quantrachrome porosimeter) at the University of Brighton. The result of the validation indicated that there was no difference between them.

From the fit to the BET model, we can determine that the biochar sample has a surface area of 3.43 m^2/g and a total pore volume 0.009 cm^3/g, which is low, compared with the activated carbons assessed (610 and 988 m^2/g from GACs used in the industry such as obtained from the tertiary treatment of Anglian Water, and Norit respectively), and for adsorbents more generally. The C value, which relates to the heat of adsorption, is positive in all cases and indicates that the use of the BET equation, in this case, is valid. However, due to the low surface area of the biochar sample, more sample weight is required to be used in the determination to avoid high instrumental error. For example, according to the specifications of the porosimeter used, the instrument achieves a measurement accuracy of ±1.5% for a total surface of 1 m^2 – in this case the biochar sample assessed had a total surface area of 1.17 m^2 and therefore we can assume higher accuracy than ±1.5%, but for samples of lower surface area (for example < 1 m^2/g) the sample weight required (i.e. > 1 g) for a similar level of accuracy would be higher than the capacity of the sample cell.

N_2 porosimetry is an important technique for the determination of surface area and analysis of meso- and microporosity of biochars. The analysis will be more suitable for biochars that

are free from ash where a total surface area of > ~1 m^2 can be achieved. Light microscopy is highly recommended for observing macroporosity and other techniques such as Hg-porosimetry could also have uses where quantitative data relating to the macroporosity of biochars is required.

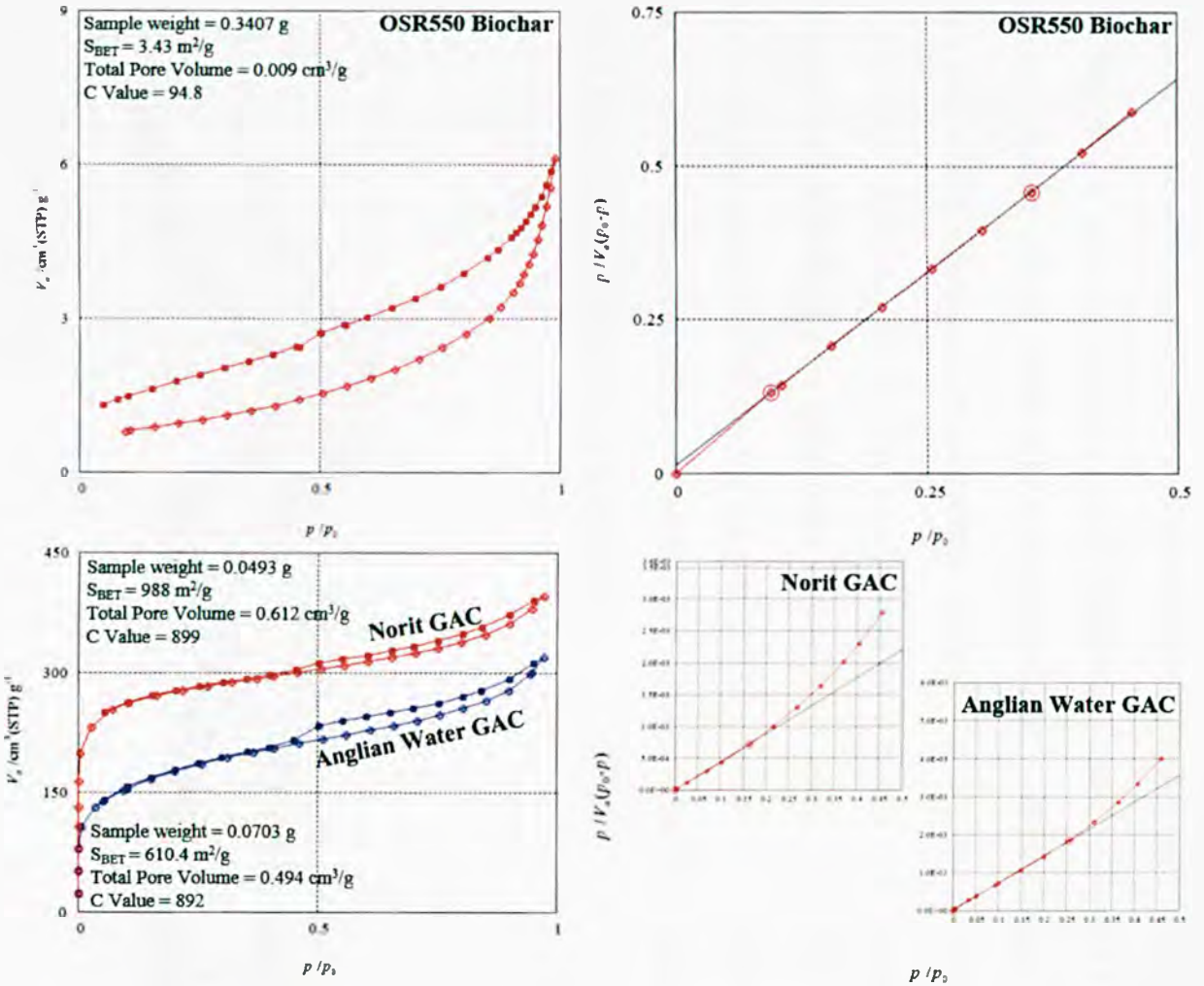

Figure 4.2 N_2 adsorption isotherms, carried out at 77K, of OSR550 biochar (top left) and Norit and Anglian Water supplied granular activated carbons (GAC) (bottom left). BET plots are shown on the right.

4.3.3 Mineral/metal content analysis – surface and in bulk

Knowledge of biochar mineral/metal content is important for various environmental applications. For the application of biochar as an adsorbent in water treatment, knowledge of both surface and bulk mineral/metal content and speciation is crucial. A common technique used in the literature for analysis of biochar mineral content is XRD. It can be useful for the identification of major crystalline phases in biochar (such as seen in Figure 4.3); however, it often does not give enough detail where there are limited amounts of crystalline material present and/or with limited crystallinity – diffractograms with broad peaks and limited information are commonly obtained. The oilseed rape straw biochar samples shown in Figure 4.3, represent samples with the highest mineral content amongst the study biochars derived from agricultural sources. XRD informs about the crystalline structures within a powdered sample and therefore is related to the bulk composition rather than crystalline material exposed on the surface and in pores. Additionally, this technique will not detect minority species due to its sensitivity.

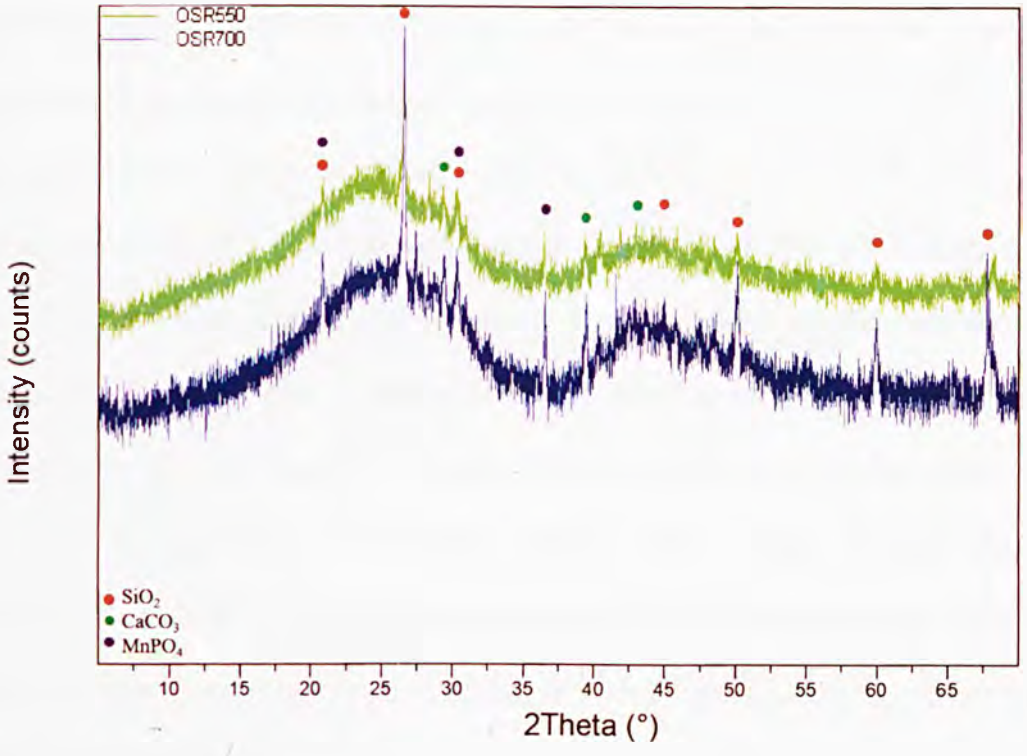

Figure 4.3 XRD diffractogram for OSR550 and OSR700 biochars.

SEM-EDS can have an important use for qualitative assessment of the elemental content of localised surface sites. It can be useful for identifying the major components of ash at the surface and within pores of biochar. For semi-quantitative analysis however, given that the signal/intensity of the EDS spectrum is affected by the angle of the sample and the interaction of the sample and the electron beam or x-ray emission, the sample must be polished flat. Without a flat surface, the x-ray intensity is dependent not only on the abundance of the element in that spot but on its position in the 3D structure of the sample. The resin impregnated and polished samples provided a flat cross-section of the biochar and were investigated with SEM-EDS; however, as it is a cross-section and only provides analysis of the bulk carbon, where in most cases the concentrations of the metal components were of too low concentration to be identified through the technique. This could be a useful approach to the study of biochars with higher mineral content, such as those produced through pyrolysis of sewage sludge and other feedstocks of higher metal/mineral content. The combination of XRD and SEM-EDS could provide useful information where applicable.

Another analytical technique investigated was XPS and although very useful for determining the atomic % coverage of localised sites and for the identification of some carbon functional groups, it was often difficult to identify specific inorganic phases through narrow scan data. Biochar samples were found to differentially charge – normally some sample charging occurs, which causes a drift in apparent binding energy and is normally compensated for by a correction based on the C1s narrow scan data. Bonds such as C-C and C-H, which are known to occur at very specific energies, are used as a correction for other peaks. However, due to the heterogeneous nature of the studied biochar samples, the correction for drift related to the C1s narrow scan was not equivalent to drift for mineral areas – i.e. carbon and mineral components of biochar react differently under the X-ray beam, similarly to when analysed through SEM.

Acid-microwave digestion of the study biochar samples was carried out using HNO_3, H_2O_2, and water, followed by determination by ICP-AES and ICP-MS. Acid-microwave digestion is a standard approach for quantifying bulk metal concentrations, for example in soils, and is the most accurate and precise route for quantitative analysis of biochar metal concentrations. Although data obtained has good precision, with relative standard deviations for most elemental concentrations being < 5%, without the use of a certified reference material, which was not found to be available, the data only has use for comparison between samples within the same study. Additionally, the total mass of metals can be of limited relevance because the fraction of them exposed remains unknown.

4.3.4 Surface chemistry

To know how a biochar material will interact with contaminants or nutrients in water and to understand the adsorbent/adsorbate system, at various pH values, it is important to know the surface chemistry. Fourier-transform infrared spectroscopy (FTIR) is a commonly used technique for the determination of bonds present within molecules and solid samples. It has found a use for the analysis of biochar in the literature (Lawrinenko et al., 2016; Liu et al., 2012), where solid dilution with KBr has been commonly employed. Figure 4.4 shows a FTIR spectrum for WSP550, in which bonds can be ascribed: N-H (at 3500–3300 and 1600 cm^{-1}); a broad round peak between ~3500–2000 cm^{-1} is most likely indicative of both carboxylic and alcohol/phenol O-H however could also indicate heterocyclic C (Keiluweit et al., 2010); aromatic C-H (3020 cm^{-1} and associated peaks around 800 cm^{-1}) and aliphatic C-H (2910 cm^{-1} and 2850 cm^{-1}); C=O (shoulder of peak at ~1690 cm^{-1}); aromatic C=C (1570 cm^{-1}); and C-O (1080 cm-1). This is qualitative information only, however where biochar samples are prepared into KBr discs using the same mass and disc thickness, data can be semi-quantitative – FTIR can be useful for determining surface changes to biochar over time or post-adsorption for example, and can be considered complementary to XPS, as a less

specific and less sensitive technique. For quantitative determination of surface chemistry other techniques, such as Boehm titrations can be used.

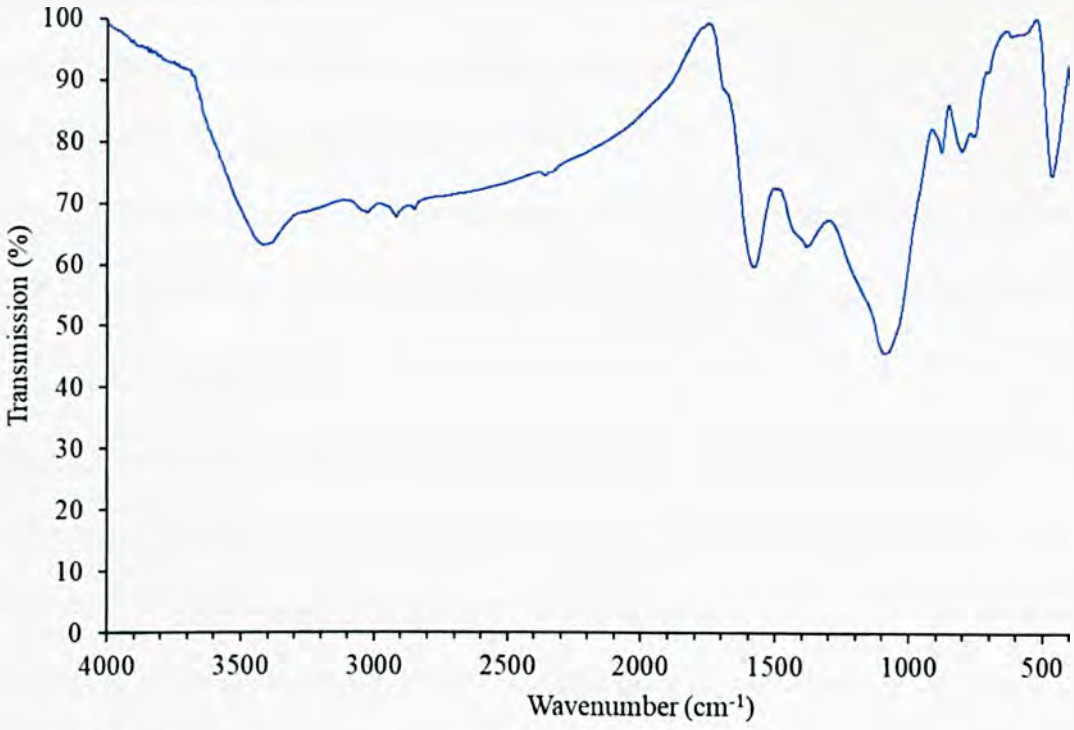

Figure 4.4 IR spectrum of WSP550, diluted to 1% weight with KBr.

Table 4.1 XPS C1s narrow scan data for WSP550 and atomic % values for the main carbon groups identified.

Name	Atomic %
Hydrocarbon (C-C, C-H)	62.09
Amine (C-N)	17.52
Alcohol (C-OH, C-O)	11.03
Amide (N-C=O)	6.4
Carboxylic acid (HO-C=O)	1.62
$(CO_3)^{2-}$	1.34

Two other techniques were investigated for quantitatively assessing biochar surface chemistry. The first one was XPS, where carbon narrow scan data obtained indicates the atomic % values for carbon in various bonds or groups (see Table 4.1). This data somewhat agrees with FTIR spectra obtained in that the same chemical bonds can be observed. The second technique investigated were Boehm titrations (Valente Nabais and Carrott, 2006), where biochar samples after several washing stages, were equilibrated with NaOH before being acidified and titrated to determine the concentration of oxygen-containing functional groups within the biochar sample. Boehm titrations are used and reported in Chapter 5.

4.4 Conclusions

There are a wide variety of approaches used for the characterisation of biochar, often that have been developed for use with other materials such as activated carbons or soils. Some commonly used techniques for biochar characterisation in the fields of materials and environmental chemistry include SEM and SEM-EDS for assessment of both structural and chemical characteristics of localised surface sites; N_2 adsorption isotherms and BET analysis for surface area and meso- and microporosity measurements; some more commonly used physicochemical analyses of metal content determination via acid-microwave digestion, pH and EC measurements; as well as FTIR analysis of surface chemistry.

As different approaches are required for characterising biochar for different environmental considerations, this research aimed to identify, improve and match key physicochemical characterisations that may be required when investigating biochar for environmental applications in water and soil. Biochars produced from 4 common feedstocks (wheat, oilseed rape and *Miscanthus* straw, and rice husk) were characterised through various techniques commonly present in environmental laboratories. It was found that whilst SEM and N_2 adsorption isotherms are valid for use with biochars and provide useful structural information, light microscopy analysis of resin impregnated, and polished samples provided a direct and much-improved identification of the macroporous structure of biochar samples.

However, microscopy techniques will be used qualitatively because its use for representative quantitative analysis would require treating a high number of images from the sample, given the high magnification power and the heterogeneity of biochar samples. Additionally, although it was not possible with the agriculturally derived biochars due to low inorganic content, SEM-EDS analysis of the polished surface could provide semi-quantitative information of the distribution of mineral content within biochar with higher overall concentration (mg/g range). Higher sensitivity in the analysis of metals will be achieved with ICP-MS and ICP-AES analysis of acid-microwave digested samples, but results will not represent the surface. XRD can then be used as a complementary technique to identify the crystalline phases in the bulk biochar sample (although again, the analysis will be limited to relatively high concentrations of crystalline phases).

Additionally, it was found that FTIR and XPS could give semi-quantitative data regarding the surface chemistry of the biochar samples studied here. The absence of reference materials and validated methodology still require the assessment of the analytical approach against matrices such as soil; and collaboration, even participation in inter-comparison exercises with other laboratories. The discussion and suggestions posed here act as a useful guide for environmental scientists characterising biochar for various environmental applications and are used throughout the rest of the thesis.

6 Modification of biochar

6.1 Introduction

In Chapter 5, it was established that concentrations of both Ca and Mg within the standard biochar materials were largely responsible for the removal of P from aqueous solutions. Although activation of these materials, leading to higher surface area and degree of porosity, inferred an increased uptake of P, the limited cationic content and overall negative surface charge of the biochars under wide pH range still limits P removal when compared with values in the literature. Additionally, the increased cost and CO_2 emissions associated with activation of biochar may be unsuitable for its adoption as a technology for larger scale use and application to soil. Section 2 discussed various feedstocks used specifically to produce biochar with increased ability to remove P from aqueous solution. These feedstocks included biomass with high concentrations of metal cations, such as marine macroalgae, sewage sludge and anaerobic digestate. Although some of these materials possess efficient removal of P after pyrolysis, the feedstock materials may be limited if considered for larger scale use (i.e. relatively unavailable, for example Mg-enriched tomato tissues, or having inconsistent physical or chemical properties over time, for example anaerobic digestate or sewage sludge), and often have significantly lower abilities to remove P compared with modified biochars in the literature.

From the literature and work carried out in Chapter 5, it can be generally assumed that biochar pyrolysed from most natural feedstocks, i.e. agricultural waste materials and most natural biomasses, would be relatively ineffective to adsorb P due to the myriad acidic oxygen containing functional groups such as carboxylic acids and phenols, of which a proportion of them will possess net negative charge under environmental pH values and basic pH resulting from the release of carbonates from biochar. The mineral component of biochar (found to be a main driver of any P adsorption in the research presented in Chapter 5) consisting of metal cations thought to interact with P (for example Ca and Mg), are often

found in forms associated with native phosphate, carbonates, sulphur compounds and oxides. These anions may be thought of as occupying and competing for the few adsorption sites available to P species.

From an extensive review of adsorbents for P uptake, marine macroalgae stands out as an effective biochar feedstock that may enable efficient removal of P, whilst being potentially practical for use at larger scales. Chemical modification of biochar and biochar feedstock can make the sorbent's effectiveness at recovering P less dependent on the natural composition of the biomass. Chemical modification followed by several authors to derive an effective biochar-based material for P recovery are compiled in Table 6.1. Here, chemical modification of biochar and feedstock is discussed and will be the basis for proposing the direction of the investigation of preparation of new materials for the efficient removal of P from wastewater in the thesis.

Table 6.1 Overview of preparation conditions of biochar and respective performance in the removal of P.

Feedstock	Pyrolysis temperature (°C)	Pre-pyrolysis modification	Post-pyrolysis modification	Other Notes	Max P removal capacity (mg P/L)	Reference
Biosolids	700	$Ca(OH)_2$ (up to 20%) and activated carbon (10% as microwave susceptor)	-	Microwave pyrolysis	147.1	(Antunes et al., 2018)
Biosolids	700	-	-	10% activated carbon added as microwave susceptor. Microwave pyrolysis	14.1	(Antunes et al., 2018)
Water hyacinth	450	$FeCl_3$ / $FeCl_2$ co-precipitation	-		5.1	(Cai et al., 2017)
Orange peel	400	$FeCl_3$ / $FeCl_2$ co-precipitation	-		0.2	(Chen et al., 2011)
	700	as above	-		1.2	
Crab shell	up to 900	-	-	Biochar naturally calcium-rich. High removal of P for crab shell biochar pyrolysed at 800 and 900	*100% and 63% removal of P from P solutions and biogas effluent, respectively.	(Dai et al., 2017)

Feedstock	Pyrolysis temperature (°C)	Pre-pyrolysis modification	Post-pyrolysis modification	Other Notes	Max P removal capacity (mg P/L)	Reference
Corncob	300	$MgCl_2$ and $CaCl_2$ solutions	-	Tested at extremely high initial P concentrations (up to 4000mg/L)	294.2	(Fang et al., 2015)
	450	as above	-		315.3	
	600	as above	-		326.6	
Maize straw	300	-	-		2.3	(Feng et al., 2017)
	300	$CeCl_3$ solution used at pH 10	-		77.5	
Cypress sawdust	400	$MgCl_2$ solutions	-		43.5	(Haddad et al., 2018)
	500	as above	-		58.8	
	600	as above	-		66.7	
Cotton stalk	350	-	Granulation and Fe_2O_3 loading to macroporous granular biochar		< 1	(Jing et al., 2015)
Peanut shell	700	-	-		7.6	(Jung et al., 2015)

Feedstock	Pyrolysis temperature (°C)	Pre-pyrolysis modification	Post-pyrolysis modification	Other Notes	Max P removal capacity (mg P/L)	Reference
Marine macroalgae	600	-	-	High maximum capacity (620.6 mg P/L) is established from a higher initial concentration range.	3.4	(Jung and Ahn, 2015)
	600	Electric field	-		7.8	
	600	$MgCl_2$	-		15.5	
	600	$MgCl_2$ + electric field	-		23.8 (or 620.6)	
Marine macroalgae (Undaria pinnatifida roots)	400	-	-		20.9–32.6 (10–30°C)	(Jung et al., 2016)
Sugarcane leaves	550	-	Soaking in $Mg(NO_3)_2$ and $Al(NO_3)_3$ solution to prepare LDH	Mg/Al layered double hydroxide ratios of 2:1, 3:1 and 4:1.	53.4	(R. Li et al., 2016a)
					72.1	
					81.8	
Poultry manure	350	$MgCl_2$ solution	-		250.8	(Novais et al., 2018a)
	650	as above	-		163.6	
Sugarcane straw	350	as above	-		17.7	
	650	as above	-		17.6	

Feedstock	Pyrolysis temperature (°C)	Pre-pyrolysis modification	Post-pyrolysis modification	Other Notes	Max P removal capacity (mg P/L)	Reference
Poultry manure	350	-	Modified by soaking with various concentrations $AlCl_3$ before drying.	Determining maximum adsorption of Al on biochar for determining the optimum concentration for the modifying solution.	701.7	(Novais et al., 2018b)
Sugarcane straw	350	-			759.0	
Sesame straw	600	-	HCl		0	(Park et al., 2015)
	600	-	H_2SO_4		0	
	600	-	H_3PO_4		0	
	600	-	KOH (followed by re-pyrolysis)		0	
	600	-	$ZnCl_2$ (followed by re-pyrolysis)		15.5	
	600	-	K_2SO_4 (followed by re-pyrolysis)		0	

Feedstock	Pyrolysis temperature (°C)	Pre-pyrolysis modification	Post-pyrolysis modification	Other Notes	Max P removal capacity (mg P/L)	Reference
Presscake	250 (hydrochar) - 650	-	-		< 10% removal from a 400 mg/L initial concentration for all samples	(C. A. Takaya et al., 2016)
Municipal waste		-	-			
Commercial oak		-	-			
Greenhouse waste		-	-			
Oak wood		-	-			
Bamboo	600	-	Mg and Al or Fe chloride, co-precipitation to form LDHs		172	(Wan et al., 2017)
Flour	800	Amended with $Ca(OH)_2$ in various ratios.	-		175.1–249.9 for ratios of 1:4–1:1 $Ca(OH)_2$:flour.	(Wang et al., 2018)
Oak sawdust	500	$LaCl_3$ solution	-		142.7	(Z. Wang et al., 2015)
Oak sawdust	500	-	Biochar immersed in to suspension of precipitated La (La solution adjusted to pH 10). Further calcined at 400°C		46.4	(Wang et al., 2016)

Feedstock	Pyrolysis temperature (°C)	Pre-pyrolysis modification	Post-pyrolysis modification	Other Notes	Max P removal capacity (mg P/L)	Reference
Corn stalk	600	LDH co-precipitation of:				(Yang et al., 2019)
		Ni/Fe	-		78.3	
		Mg/Al	-		152.1	
		Zn/Al	-		64.9	
Mg-enriched tomato tissues	600	-	-		103.8	(Yao et al., 2013)
Anaerobically digested sugar beet tailings	600	-	-		43.4 (given as 133085 mg PO_4^{3-}/kg	(Yao et al., 2011b)
Sugar beet tailings	600	Mg	-		272.33 (given as 835mg PO_4^{3-})	(M. Zhang et al., 2012)
Bamboo	unknown	-	Chitosan used to fix zero-valent iron particles to surface		40–96% removal from 12 mg P/L for differing ratios of ZVI particles	(Zhou et al., 2014)
Wheat straw	500	Bi_2O_3 and HCl	-		125.4	(Zhu et al., 2016)

Feedstock	Pyrolysis temperature (°C)	Pre-pyrolysis modification	Post-pyrolysis modification	Other Notes	Max P removal capacity (mg P/L)	Reference
Bamboo	600	Boiled in dilute ammonia solution and added to ferric nitrate solution in water and ethanol, dried and repeated three times.	-		2.85 –3.08 (temperatures of 25–45°C)	(Zhu et al., 2018)

6.1.1 Chemical modification of biochar feedstock

Modification of biochar feedstock or biochar (i.e. pre- or post-pyrolysis modification, respectively) infer additional approaches to tailor biochar characteristics for enabling the effective removal of P – this has so far been largely achieved through increasing the cationic content of the feedstock or biochar material itself, through various approaches (Figure 6.1). Modification or amendment of the feedstock pre-pyrolysis is the most common approach and can also be achieved through amendment with materials such as metal precipitates, for example $Ca(OH)_2$ (Antunes et al., 2018; Wang et al., 2018) or waste materials such as iron ochre (Shepherd et al., 2017). The modification of biochar post-pyrolysis in comparison has been less explored but includes similar techniques such as soaking biochar in concentrated metal solutions and drying, but also extends to the precipitation of specific crystalline phases such as metal hydroxides or layered double hydroxides (LDH), or affixing specific particles to biochar, for example zerovalent iron particles affixed to biochar using chitosan (Zhou et al., 2014). The modification route chosen should be congruent with environmental use which is often large in scale (in terms of geographic area or volume of land or water to treat) and therefore low cost and simplicity when manufacturing and utilising modified biochars needs to be prioritised. It is additionally important that the biochar material is environmentally compatible and does not confer detrimental impacts to soil or the aquatic environment with its use.

Figure 6.1 Three common routes to derive biochar with effective ability for the capture of P from aqueous solution. The red circles indicate cationic species with availability to interact with P. Biochar images adapted from (Mašek et al., 2018).

6.1.1.1 Cationic impregnation of biochar

Metal impregnation of biochar is an effective and relatively simple technique for optimising biochar materials for effective P capture. It is generally achieved through soaking of feedstock material or biochar in a concentrated metal solution, followed by the pyrolysis stage or drying, respectively. Takaya et al. (2016a), employed various approaches for the chemical modification of oak biochar. In most cases, modification with a $MgCl_2$ solution, which was followed by a second pyrolysis stage, was superior when compared to other chemical modifiers such as H_2O_2 or KOH. $MgCl_2$ was also found to be superior to $FeCl_3$, in terms of P removal (C. A. A. Takaya et al., 2016). Jung and Ahn, (2015) also focused on modifications with Mg, and employed a combination of a $MgCl_2$ solution and a graphite electrode-based electric field to modify marine macroalgae pre-pyrolysis – the resulting biochar had an enhanced porosity as well as a dispersion of nanosized MgO particles, which enabled removal of P to as high as 620 mg P/g.

Both $MgCl_2$ and $CaCl_2$ solutions were used to modify ground corncob before pyrolysis at 300, 450 and 600°C (Fang et al., 2015). The resulting biochar materials had nanosized CaO and MgO particles present on the surfaces of the biochar and achieved a maximum removal of up to 326.6 mg P/g from biogas fermentation liquid, however the biochar material possessed only limited effectiveness at lower initial concentrations compared with other studies. The desorption ability was assessed with extractions in both deionised water and dilute citric acid – although the release of P was found to be low, < 2% of the adsorbed P released per extraction, the material could consistently release P over 6 extractions and was found to be more effective in releasing P in acidic conditions. This suggests that the material could have potential for the slow release of P in acidic soils. Novais et al. (2018a) established the maximum capacity of poultry manure and sugarcane straw-derived biochars pyrolysed at 350 °C for Al (as $AlCl_3$). The biochars then saturated with Al had maximum adsorption capacities of 702 and 759 mg P/g respectively. The same feedstocks modified through soaking in $MgCl_2$ pre-pyrolysis at 350 and 650°C, could remove up to 250.8 mg P/g and 17.7 mg P/g for the poultry manure and the sugarcane straw based biochars, respectively (Novais et al., 2018a), suggesting that the feedstock material used, the interplays between the feedstock/biochar and the metal cation employed, as well as the pyrolysis temperature reached, can all have important impacts over the effectiveness of the resulting biochar-based material to capture P. In both studies, the kinetic rate was not established.

Other metals used to modify biochar include: a sesame straw biochar modified with Zn post-pyrolysis followed by a second activation stage at 600°C (maximum adsorption capacity of 15.5 mg P/L) (Park et al., 2015); oak sawdust modified with lanthanum before pyrolysis at 500°C (maximum capacity of 142.7 mg P/L) (Z. Wang et al., 2015); and bamboo modified with $Fe(NO_3)_3$ after boiling the biomass in a dilute ammonia solution before pyrolysis at 600°C (adsorption capacity from 2.85–3.08 mg P/g) (Zhu et al., 2018). From review, Fe-impregnated biochar materials tend to have lower effectiveness to adsorb P from solution

when compared with Mg, Ca or Al used as modifiers. Al may have toxic effects if applied to soil (especially in acidic soil environments) (Poschenrieder et al., 2008) and if released in toxic amounts, so Ca or Mg may be preferable in many cases, being effective but also low cost, abundant and environmentally compatible in most cases. However, although the maximum adsorption capacity can be very high, from review, the kinetic rate associated with P removal using cation-impregnated biochars can still be relatively slow (though significantly higher than for biochar produced from unmodified feedstocks) or have relatively low removal efficiency at low initial concentration. For instance, up to 6 hours was taken to reach equilibrium using corncob biochar modified with Ca and Mg, removing ~80% of P from fermentation liquid at an initial concentration of 62 mg P/L (Fang et al., 2015), and up to 4 hours to reach equilibrium with La-modified oak sawdust biochar, removing ~65% of PO_4^{3-} from an initial concentration of 61.3 mg PO_4^{3-}/L (Z. Wang et al., 2015). Providing that the material is low cost to produce, it may be more practical to derive materials that possess rapid removal kinetics and high removal efficiency at lower initial concentrations, even if this is to the detriment of maximum adsorption capacity.

6.1.1.2 Metal (hydr)oxides and layered double hydroxides biochar composites

Metal hydroxides can be synthesised relatively simply through various approaches, but the most common and facile is co-precipitation. Co-precipitation of metal hydroxides involves the formation of the precipitate by increasing pH in a solution containing metal cations. The addition of biochar/biochar feedstock to the solution of metal cations at basic pH, can lead to the in-situ growth of metal hydroxides to the surfaces and pores of the material. Metal oxides can then be synthesised through the calcination of metal hydroxides, however in the case of biochar-based composites, this can be achieved through the pyrolysis process if modified pre-pyrolysis. Precipitating metals to biochar may have benefits over the simpler approach of soaking the feedstock/biochar before pyrolysing/drying, as specific crystalline

phases can be derived; the precipitation can be tailored to derive micro- and nanoparticles; and a material with a higher resulting inorganic component could be derived as the process is not necessarily limited by the adsorption capacity of the biochar/feedstock for the chosen metal ion, rather biochar acts as a seed for the precipitation process. Small micro- and nanoparticles of precipitate are favoured due to the known enhancement to adsorptive efficiency and the kinetic rate, due to increases in surface area/volume ratio and potential of novel reactivity in the nanoscale.

Feng et al. (2017), modified maize with a $CeCl_3$ suspension maintained at pH 10 or above, before pyrolysing at temperatures between 300–600°C. Nanoparticles of cerium oxide were present on the surfaces of the biochar, with the material pyrolysed at 300°C able to remove up to 77.5 mg PO_4^{3-}/g. The biochar-based material also possessed rapid removal kinetics, reaching equilibrium within 60–90 minutes. Wang et al. (2016b), prepared biochar from oak sawdust pyrolysed at 500°C before immersion in a suspension of precipitated La (La solution adjusted to pH 10). The material was further calcined at 400°C and had a maximum capacity of 46.4 mg P/g and was able to remove over 81% of P within 2 hours. P adsorption was found to decrease at higher pH values, which is commonly reported due to the disabling of ligand exchange mechanisms and electrostatic attractions as pH is increased (L. Zhang et al., 2012), with any adsorption limited to Lewis acid-base interactions (Figure 6.2). However, some precipitates do not follow this trend. Ca hydroxides in particular are often found to be relatively unaffected by pH or even display higher rates of removal at higher pH values (Fang et al., 2015; Wang et al., 2018). For example, Wang et al. (2018) showed that as well as adsorption capacity increasing at high pH with a calcium-flour biochar, the kinetic rate was also quicker. This is due to precipitation of hydroxyapatite ($Ca_5(PO_4)_3(OH)$) being a predominant mechanism for removal, which is hindered at lower pH values, since P exists with lower charge (as HPO_4^{2-} or $H_2PO_4^-$) and there are less OH^- groups able to react, with more required (highlighted in the equation below).

$$3PO_4^{3-} + 5Ca^{2+} + OH^- \rightarrow Ca_5(PO_4)_3(OH)\downarrow$$

$$3HPO_4^{2-} + 5Ca^{2+} + 4OH^- \rightarrow Ca_5(PO_4)_3(OH)\downarrow + 3H_2O \quad (1)$$

$$3H_2PO_4^- + 5Ca^{2+} + 7OH^- \rightarrow Ca_5(PO_4)_3(OH)\downarrow + 6H_2O$$

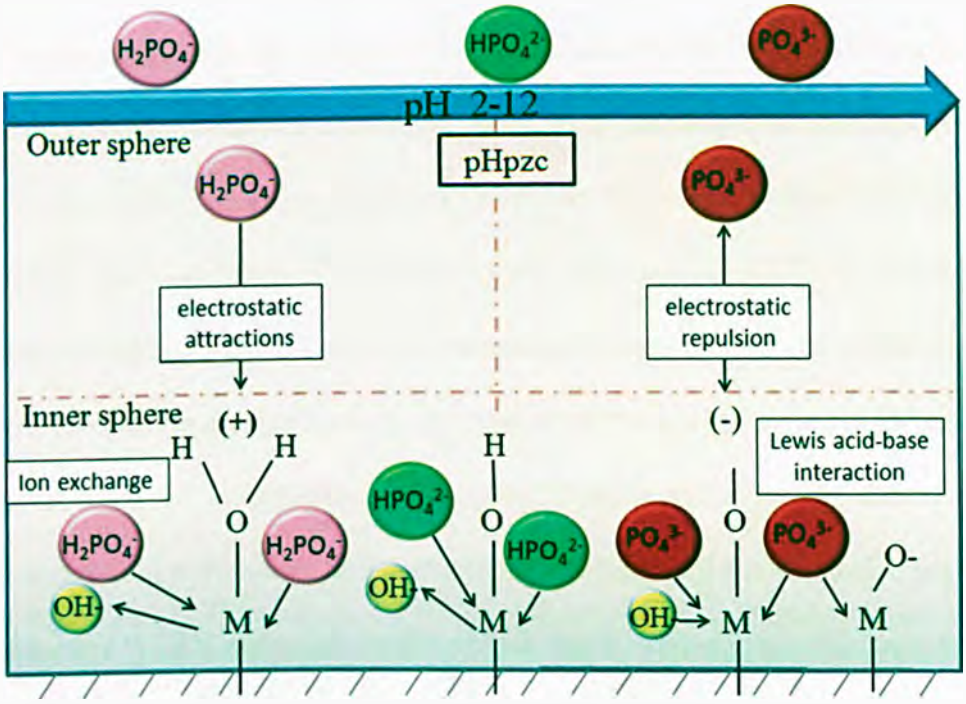

Figure 6.2 Adsorption mechanisms of P to metal (hydr)oxides. Taken from (M. Li et al., 2016).

As the pH of biochar tends to be basic, Ca-based modification may be beneficial because the environmental pH that enables optimal conditions for the Ca-based component of the material to achieve efficient P removal matches the native pH of the biochar material. However, high calcium content and pH of biochar has been shown to be detrimental to the release of P in soil (Buss et al., 2018). In many cases, developing effective biochar-based materials may entail matching the metal modification to biochar structures with a pH value at which the adsorbent species can be most effective (either in terms of maximum adsorption

capacity, kinetic rate, or resulting bioavailability of the recovered P). These factors are often not considered, with many studies overlooking the kinetic rate of P capture, the pH-related changes to P removal efficiency or the resulting availability of the recovered P.

Another group of precipitates that are investigated are layered double hydroxide (LDH) or hydrotalcite-like compounds. LDHs are a class of anionic clay, based on layers of positively charged brucite-like sheets balanced by intercalated anions (see Figure 6.3), having the general formula $[M_{1-x}^{2+}M_x^{3+}(OH)_2]^{x+}(A^{n-})_{x/n}\cdot mH_2O$. Where M^{2+} and M^{3+} are di- and trivalent cations, respectively, the value of x is the molar ratio of $M^{3+}/(M^{2+}+M^{3+})$ and A is the intercalated anion with charge n (Goh et al., 2008). They can be synthesised relatively simply through various approaches including urea hydrolysis, the sol-gel method and hydrothermal synthesis but most commonly via co-precipitation (Theiss et al., 2016). Co-precipitation of LDHs involves adding base to a solution containing a mixture of di- and trivalent metals, as well as the intended intercalated anion. Adsorption of P to LDHs can occur through various mechanisms such as electrostatic interactions, ligand exchange and Lewis acid-base interactions (similar to P capture with metal (hydr)oxides-based composites), but due to their unique structure, LDHs may additionally unlock anion exchange mechanisms, which may enhance the capture or release of P and be overall beneficial for P recovery.

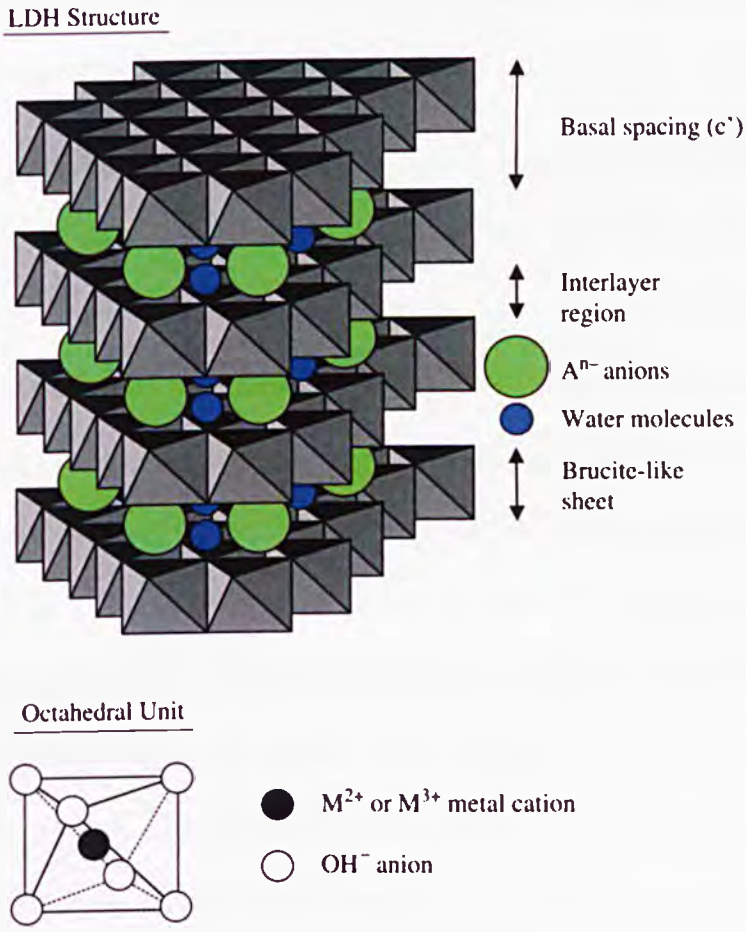

Figure 6.3 The structure of layered double hydroxides. From (Goh et al., 2008).

Several researchers have precipitated LDH materials within biochar/biochar feedstock and investigated them for the capture of P. Yang et al. (2019) precipitated 3 different LDHs (Ni-Fe, Mg-Al and Zn-Al) to corn stalk before pyrolysis at 600°C. The Zn-Al LDH-biochar composite was found to be superior where at pH 5 it had a maximum adsorption capacity of 152.1 mg P/g, and relatively quick removal kinetics made up of a rapid initial rate followed by slower removal with equilibrium reached after > 12 h. Removal efficiency under environmental/wastewater-relevant conditions (at 25°C and 10 mg P/L initial concentration) however was relatively low with < 90% removal of P. Zhang et al. (2014), prepared a Mg-Al-Cl-LDH-hydrochar composite material via hydrothermal treatment of cottonwood in a

suspension containing $MgCl_2$ and $AlCl_3$ at pH 10. The prepared material enabled removal of P to over 386 mg PO_4^{3-}/g and reached equilibrium very rapidly (within 1 hour) – much faster than found for many other biochar-based materials.

Li et al. (2016b) prepared several Mg-Al-NO_3-LDH-functionalised biochars from sugarcane leaves post-pyrolysis (with Mg:Al ratios of 2:1, 3:1 and 4:1). When investigated for the capture of P it was found that maximum adsorption of P was 53.4, 72.1 and 81.8 mg P/g with increasing Mg content – the composite with higher Mg content possessed high removal efficiency at low initial concentrations and rapid kinetics (equilibrium reached in < 30 minutes). Similarly, Wan et al. (2017), modified a biochar produced from bamboo at 600°C post-pyrolysis, with a Mg-Al-Cl LDH. Equilibrium could be reached within 1 hour from both 10 and 50 mg P/L initial concentrations and the isotherm data showed high removal rates at initial concentrations ≤ 50 mg P/L. The P-enriched composite was then shown to enhance seedling growth when compared to a control. Studies indicate that LDH-based biochar composites can be highly effective with rapid removal kinetics in many cases. From the literature it appears that calcination of biochar-LDH materials is not necessary for enabling high effectiveness and that modification of biochar post-pyrolysis through co-precipitation processes to create the metal hydroxide/LDH material is enough and potentially lower cost and an overall more facile approach.

6.1.1.3 Magnetic biochar composites

One common problem with the application of adsorbents is the recovery of the material from the liquid phase once saturated. Several researchers have aimed to solve this through the development of magnetic biochar materials by amendment with magnetite, thereby allowing for the magnetic recovery of the biochar-based material post-adsorption. Magnetic biochars derived from orange peel and water hyacinth were prepared by soaking the feedstock in a 1:1 ratio of ferrous and ferric chlorides before increasing the pH to 10, to initiate co-

precipitation (Cai et al., 2017; Chen et al., 2011). Pyrolysis was then carried out at various temperatures to derive the magnetic biochar-based materials, which had nanosized iron oxide particles on the surfaces of the material. The capture of P however was found to be relatively low with maximum capacities of 5.1 and 1.2 mg P/g for the water hyacinth and orange peel based biochars pyrolysed at 450°C and 700°C, respectively. The water hyacinth-based biochar however was highly efficient, able to remove > 90% of P from low initial concentrations in both batch and column studies – this demonstrates that there is potential for the material be effective in recovering P from a tertiary treatment stage of a WWTP process or from eutrophic water (both of which have low initial concentrations but demand efficient removal to protect surface water), providing the material could be produced with low cost. By impregnating a sugarcane residue feedstock with both ferrous chloride and magnesium chloride solutions before pyrolysis at 550°C, Li et al. (2016c) enabled a maximum removal capacity for P of 121.3 mg P/g, with the biochar-based material also possessing magnetic properties and therefore separation ability. Similarly, Koilraj and Sasaki (2016) found that they could enhance Fe_3O_4 particles through amendment with a Mg_2-Al-NO_3-LDH, which increased the maximum adsorption capacity for P from 4.6 to 33.4 mg P/g. Although the material was not incorporated into a biochar-based matrix, it indicates that by using the magnetic properties of Fe_3O_4 in conjunction with other phases, a material can be made more effective for capturing P. Studies on the use of magnetic biochar for the capture of phosphate are still limited. Whilst there may be potential for such phases to be incorporated into biochar to provide effective P capture, where suitable particle sizes of biochar-based materials can be achieved (i.e., > ~2mm), a biochar-based composite may be applied in a column or through flow apparatus, eliminating the need for a material to be applied in batch mode and subsequently be recovered.

6.1.1.4 Research opportunities

The modification of biochar (rather than the modification of the feedstock) had been relatively unexplored when this study started. This synthetic approach for preparing a composite with enhanced properties for P recovery, can offer high control over its properties and lead to a low-cost sorbent that could be applied for large scale applications and make a measurable impact in P recovery from wastewater. Porous carbon materials such as biochars can act as a suitable matrix and a host to precipitated adsorbent species with greater capacity to adsorb P than biochar itself. It was demonstrated in Chapter 5 that biochars were limited for the uptake of P and did not offer competitive performance with respect to other technologies.

The inherent structure of biochar containing relatively low surface area but interconnected macropores has potential for water treatment and its use in soil. The benefits to embedding adsorbent species within a biochar matrix over the use of the pure species capturing P is that: (1) the inorganic materials on its own, such as a synthesised metal (hydr)oxide, tend to form in powdered or crystal forms and therefore do not allow the through flow of solutions when applied as a filtration media, causing high backpressure when packed in columns. (2), where the end use of the saturated adsorbent is application to soil, small particles and powders may be more easily degraded, reduce the control release of P and/ or leached to surface and ground water – exacerbating the issue of eutrophication.

In this chapter, biochars' inherent properties beneficial for soil amendment such as its water holding capacity and structure that can be penetrated by roots to access nutrients have been enhanced through the in-situ precipitation of metal (hydr)oxides and LDHs. Here, it is proposed that when biochar with porosity and negative surface charge is added into solution with cations, adsorption can occur on the surface biochar which will then lead to in situ growth of metal hydroxides with the addition of strong basic media. By changing the

synthesis conditions, precipitate forms may be controlled to increase the surface reactivity and sorption of P.

6.2 Materials and methods

6.2.1 Materials

Biochar OSR550 (particle size, 0.5–1 mm) was used in all experiments. The description of its preparation can be found in Chapter 3. Chemicals used were: NaOH (98.5%), $CaCl_2$ (96%), $FeCl_3$ (97%) and $MgCl_2$ (96%), supplied from Fisher; $Ce(NO_3)_3 \cdot 6H_2O$ (99.5%) was used and supplied by ACROS Organics. Ultrapure water was used in all experiments.

6.2.2 Preparation of metal biochar composites

A range of biochar-metal composites (11) with well differentiated composition were synthesised (outlined in Table 6.2). The metal hydroxide modification method (samples A–H) was adapted from reported co-precipitation reactions (for example in Harvey and Rhue, (2008)), and was carried out as follows. A total of 5 mmol metal/g biochar was used in the syntheses across composites to compare both the effectiveness of the precipitate in removing P and of the modification method employed. Where more than one type of metal is included in the inorganic precipitate, the combined amount of metal used was 5 mmol, divided equally between the metals incorporated. The metal salts were added, together with 2 g of OSR550 biochar, to 10 mL of ultrapure water in a round bottomed flask at 40 °C. The reaction was left for 10 min under moderate magnetic stirring before adding 10 mL, 11.7 mL or 15 mL of 2 M NaOH solution dropwise, for the M^{2+}, M^{2+}/M^{3+} (as in the case of sample F) or M^{3+} ions used respectively. The mixture was then cooled, while keeping stirring constant, in a water bath until reaching 25°C. The mixture was filtered through Whatman n°.1 paper and dried under vacuum at 60°C for 24 h. Samples A–F underwent thermal treatment at 300°C for 2h to investigate the effect on P recovery by differing precipitate morphologies and crystallinity; this was carried out in a covered crucible to minimise burn-off of carbon from the material. Samples G–N did not undergo such treatment and were stored after drying only.

Table 6.2 Overview of the biochar composites prepared in this chapter.

Sample	Attempted precipitation	Metals salts added	Heat treatment at 300°C
A	$Ca(OH)_2$	Ca	Yes
B	$Ca/Mg(OH)_2$	Ca, Mg	Yes
C	$Mg(OH)_2$	Mg	Yes
D	$Fe(OH)_3$	Fe	Yes
E	$Ce(OH)_3$	Ce	Yes
F	$Ca/Fe/Mg(OH)_{2/3}$	Ca, Mg, Fe	Yes
G	$Fe(OH)_3$	Fe	No
H	$Ce(OH)_3$	Ce	No
I	Ca-Fe-Cl LDH	Ca, Fe	No
J	Mg-Fe-Cl LDH	Mg, Fe	No
K	Ca-Ce-NO_3 LDH	Ca, Ce	No

In addition to the procedures listed in above, the preparation of LDHs was also attempted (samples I–K) through a slightly different approach. This was carried out as follows. As above, a total of 5 mmol of metal/g of biochar was used and added to 2 g of biochar in 10 mL of ultrapure water in a round bottomed flask. The variant involved heating the suspension of metals in solution with biochar to 80°C before adding 10mL of 2 M NaOH. The suspension was kept under these reaction conditions and stirred for a further 2 days at 80 °C before cooling, filtering and drying as above (without heat treatment applied after the precipitation).

6.2.3 Characterisation of the composites

The structure and composition of the modified biochars was analysed to confirm that the modification had been successful. The samples were coated with Au-Pd alloy, prior SEM analysis, to improve sample conductivity (decrease surface charging). SEM-EDS allowed confirmation of the precipitates and the metals contained within them – where possible,

powder-XRD was used to indicate the crystalline phases present within the modified biochar structures and compare between unmodified and modified OSR550 materials. These characterisations were carried out as described in Chapter 3.

6.2.4 Study of the uptake of P by the composites

The P removal efficiency of the prototypes was tested from an initial P concentration of 10 mg P/L in batch mode – this is more representative of a wastewater-relevant initial concentration. The pH of the P solution was uncontrolled but initially at pH ~ 7.5. In triplicate, 0.2 g of composite was added to 40 mL of the P containing solution which was shaken at 90 rpm on an orbital shaker for 48 h at 25 °C. The suspensions were filtered (0.22 µm PES syringe filters, Merck Millipore, Ireland) before being analysed by ICP-AES.

6.2.5 Study on P leaching from the metal biochar composites

All composites were centrifuged and subsequently kept at 40 °C under vacuum until dry (constant weight) post-adsorption. The dried composites (0.1 g, n=3) were individually immersed in aqueous solutions (10 mL) for 2 h (at 90 rpm on an orbital shaker, 25°C). The leaching study was carried out at pH 5 and 8 to represent both a highly acid and highly alkaline soil solution. The pH was buffered using acetic acid and tris at a 0.01M concentrations for pH 5 and 8 respectively, with a 0.01M $CaCl_2$ background ionic concentration present in all extractions. This test is adapted from the assessment of P availability from soil (Houba et al., 1986).

6.4 Results and discussion

OSR550 biochar was chosen as the matrix and host to the precipitated species as it is a widely available biomass throughout the UK. Additionally, it presented a higher degree of macroporosity from SEM micrographs obtained and light microscopy analysis (Chapters 4 and 5).

6.4.1 Metal hydroxide precipitation with thermal treatment

A total of 6 samples were synthesised through the precipitation of metal hydroxide/s followed by thermal treatment at 300°C. Their uptake of P from 10 mg P/L is shown in Figure 6.4.

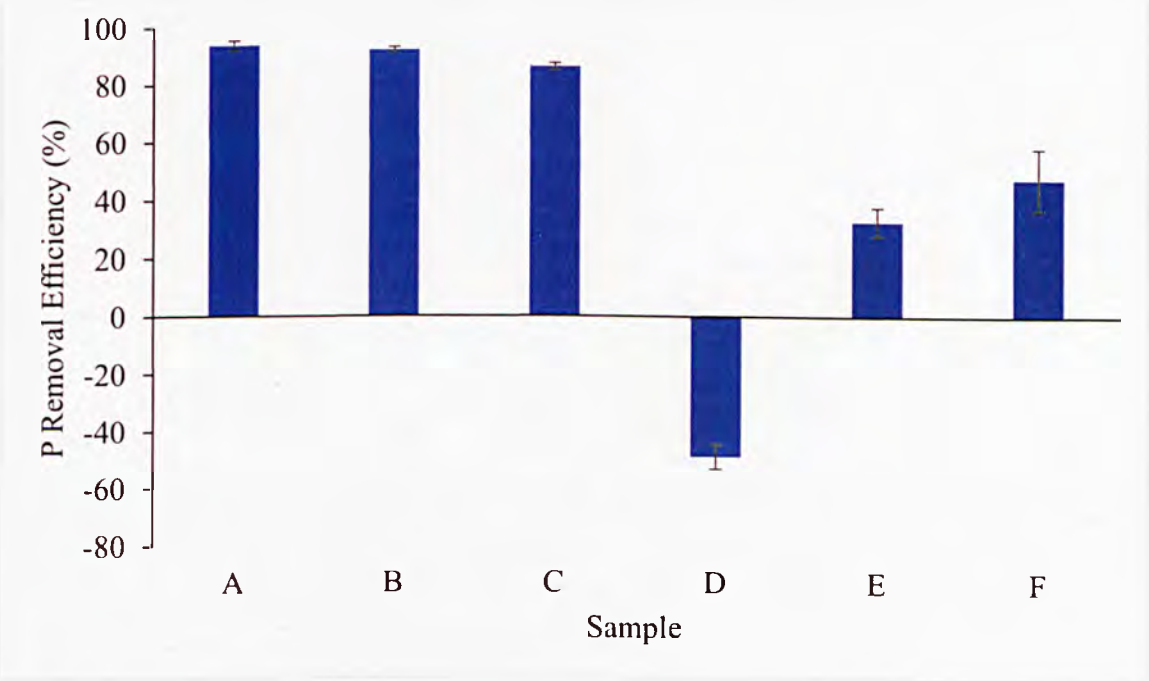

Figure 6.4 Comparison of the P removal efficiencies of composite samples of OSR550 biochar (modified with): A ($Ca(OH)_2$), B ($Ca/Mg(OH)_2$), C ($Mg(OH)_2$), D ($Fe(OH)_3$), E ($Ce(OH)_3$)and F ($Ca/Mg/Fe(OH)_{2/3}$). Removal of P from ultrapure water at an initial concentration of 10 mg P/L and a sorbent dose of 0.2 g / 40 mL. Error bars correspond to standard deviations, n=3.

The highest P removal was offered by composites containing Ca (hydr)oxides (samples A and B). A P removal of > 90% was obtained from the 10 mg/L initial concentration

representing removal of P to < 1 mg/L, equating to discharge limits often required by WWTPs. The Mg-modified sample (C), has a removal of ~86%, which is less than that of the Ca-modified composites with Mg or on its own (B and A respectively, Figure 6.4). The Fe(III)-modified composite (D) has no ability to remove P and releases more P than removing equating to the negative removal efficiency seen in Figure 6.4. It is suggested that the heat treatment applied has converted the $Fe(OH)_3$ (suggested compound present) into a more unreactive form (suggested to be FeO(OH)) as it has become dehydrated. Additionally, the heating at 300°C for 2 hours may have altered the carbonaceous internal structure and unlocked some more of the native-P from the biochar component of the composite, which leads to release of P (hence negative removal efficiency shown in Fig. 6.4 D). Chen et al., (2011) similarly found a limited ability for an Fe^{2+}/Fe^{3+} modified orange peel biochar; Zhang et al., (2009) showed that removal of P with a Fe-Mn binary oxide adsorbent was pH dependant with the greatest adsorption occurring at acidic pH (3–6). Due to the basic nature of the biochar samples this may be a limiting factor. Fe(III) incorporated into a composite that also contains Ca and Mg (see F in Figure 6.4), had a limited capability to remove P. Similarly, the composite containing Ce(III) (E) only removed 33 % of P from this initial concentration. This could also be due to changes in the crystallinity or crystal structure; however, the temperature is not enough to form oxides – the release of P from the altered biochar component may also have an important influence on this result.

Figure 6.5 illustrates the very different morphologies of composites A–C with SEM micrographs. Sample A, modified with $Ca(OH)_2$, presents relatively small particle sizes (aggregates of < 1 μm diameter particles) of the inorganic precipitate that is occupying the surfaces and macropores of the material without fully blocking them, as intended. When Mg was precipitated as the only cation present (C), it appears to just coat the biochar surfaces and pores without any obvious order or crystallinity. Sample B (Ca and Mg precipitated

together) shows even coverage of the surface but is not in particulate form like seen in sample A.

The results obtained show different crystallinities that form from the incorporation of different divalent metals. The differences in the uptake of P using these materials also indicates differences in reactivity between di- and trivalent metal/s, and so far indicates that divalent metal species (Ca, Mg) are more effective in the removal of P when precipitated to the biochar matrix (potentially due to the basic pH limiting adsorption to trivalent species); divalent species are more amenable to be precipitated into crystalline forms within biochar; or, the heat treatment is detrimental to the M^{3+} species' ability to remove P.

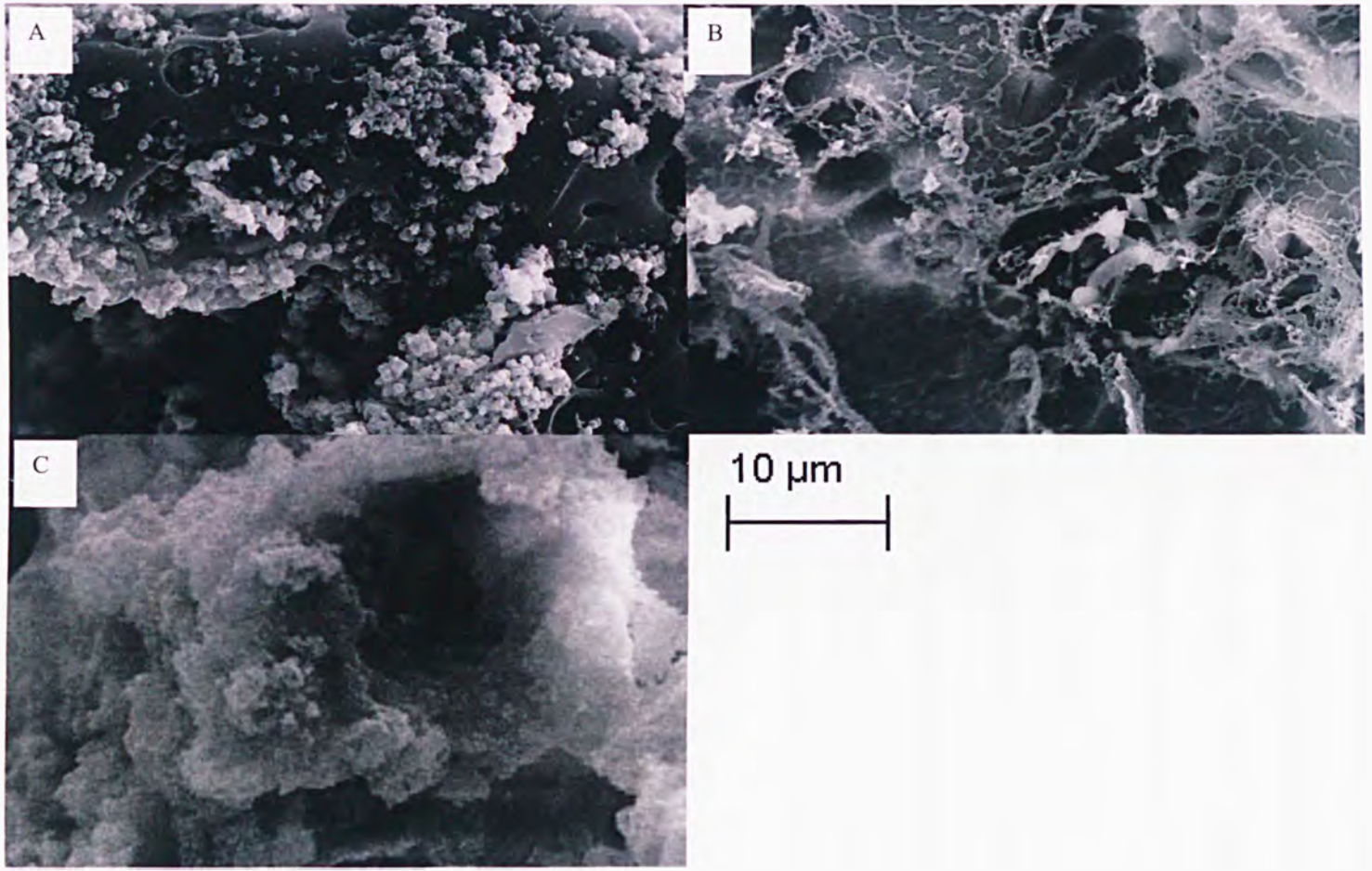

Figure 6.5 SEM micrographs of composites (modified with): A ($Ca(OH)_2$), B ($Ca/Mg(OH)_2$) and C ($Mg(OH)_2$) with heat treatment.

6.4.2 Metal hydroxide precipitation without thermal treatment

The thermal treatment applied during the precipitation of metal hydroxides could influence the structure of the inorganic precipitate and P removal efficiency. To investigate further such effects within the composites containing trivalent metal species, biochar modifications were carried out with Fe(III) and Ce(III) again that did not include the heat treatment stage (sample G and H). Figure 6.6 shows a comparison between Fe(III)- and Ce(III)-modified composites with and without the application of a heat treatment stage.

As is shown, both Fe(III) and Ce(III) incorporated into biochar composites where in absence of heat treatment had a significantly higher removal of P ($p < 0.05$) from an initial concentration of 10 mg/L. The Fe(III)-modified sample removes 48% and the Ce(III) modified sample removed 99.7% of the P. A removal of P of > 99% represents reduction of P to < 0.1 mg P/L, which is well below most P discharge limits required by legislation.

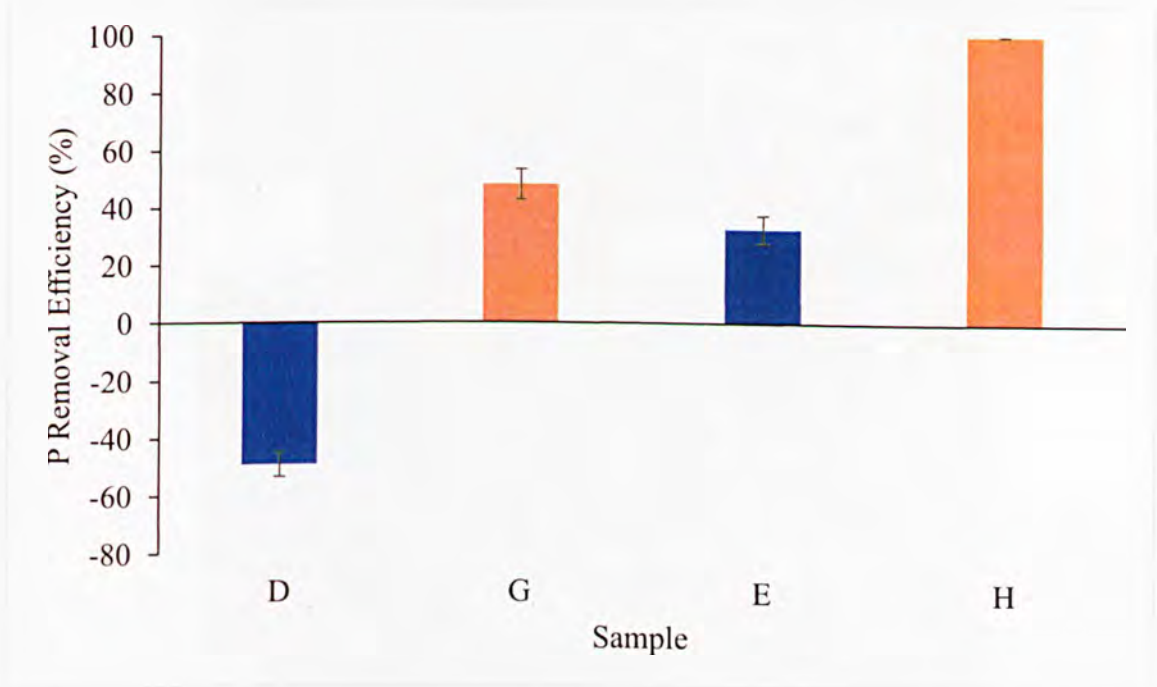

Figure 6.6 Comparison of the P removal efficiencies of composite samples (biochar modified with): D ($Fe(OH)_3$ – heat treated at 300°C), G ($Fe(OH)_3$), E ($Ce(OH)_3$ – heat treated at 300°C) and H ($Ce(OH)_3$). Removal from an initial concentration of 10 mg P/L in ultrapure water and a sorbent dose of 0.2 g / 40 mL. Error bar correspond to standard deviation, n=3.

This study suggests that the heat treatment stage is not required to derive an effective composite material and can have an overall negative effect on the ability of these prototypes to remove P. Additionally, as thermal treatment would infer additional cost and energy requirement, further studies in this thesis will not include thermal treatment. Upon inspection of several micrographs from these samples (Figure 6.7), the Fe precipitate does not appear to be crystalline whereas the Ce-modified material possesses more ordered clumps of crystals (< 1 μm). It could be suggested that Fe(III)-based precipitates of higher crystallinity/smaller particle size could have an increased ability but this is not investigated further.

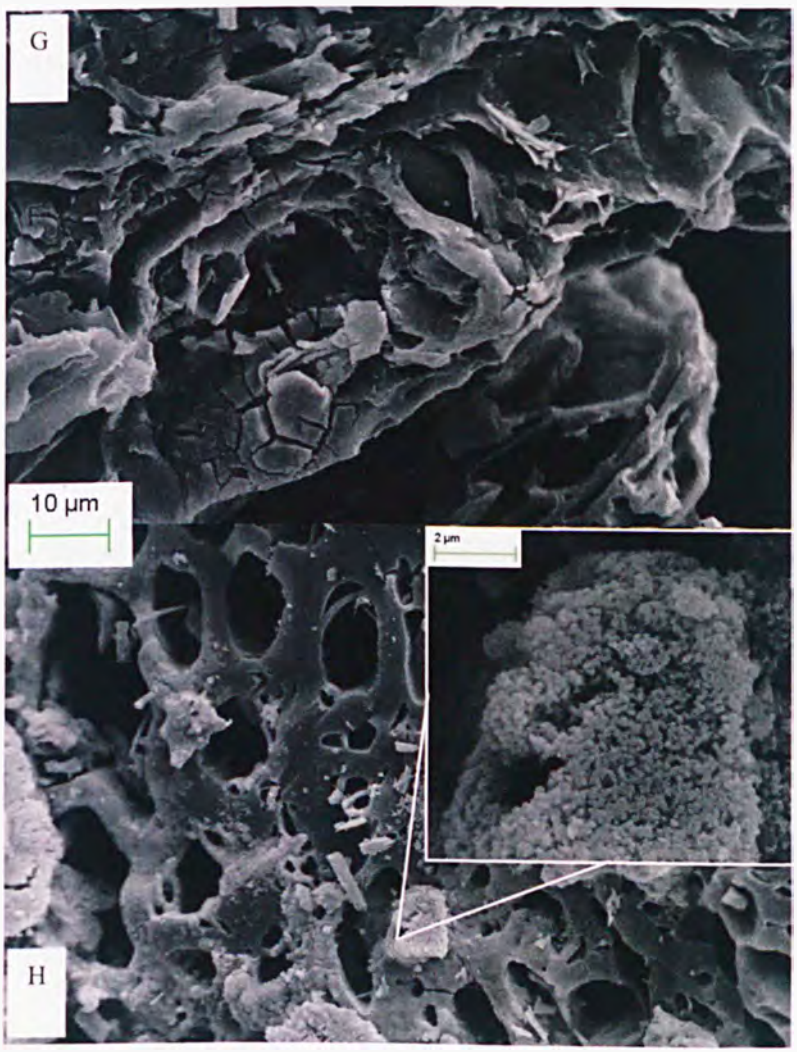

Figure 6.7 SEM micrographs of composites (biochar modified with): G ($Fe(OH)_3$) and H ($Ce(OH)_3$) without heat treatment.

6.4.3 Towards the formation of layered double hydroxide structures within biochar

LDHs could increase the selective removal of P. This work tried to prepare novel LDHs onto biochars. The LDHs included metals with known affinity for P, and the structure of the LDH could provide some selectivity in the uptake of P, which would be beneficial for applications that involve the removal/recovery of P from complex matrices such as wastewater and soil, giving prolonged efficiency to the sorbent.

Figure 6.8 shows the removal of P from the initial 10 mg P/L solution with LDH-modified composites. The Ca-Fe-Cl-LDH (A) has significantly ($p < 0.05$) higher removal of P than Mg included in the LDH with Fe (B). These were both synthesised using chloride salts meaning the theorised mechanism for the uptake would be exchange of chloride ions for phosphate (either as HPO_4^{2-}, or $H_2PO_4^-$ – dependent upon pH) in addition to other electrostatic interactions and/or ligand exchange of OH^- in the structure.

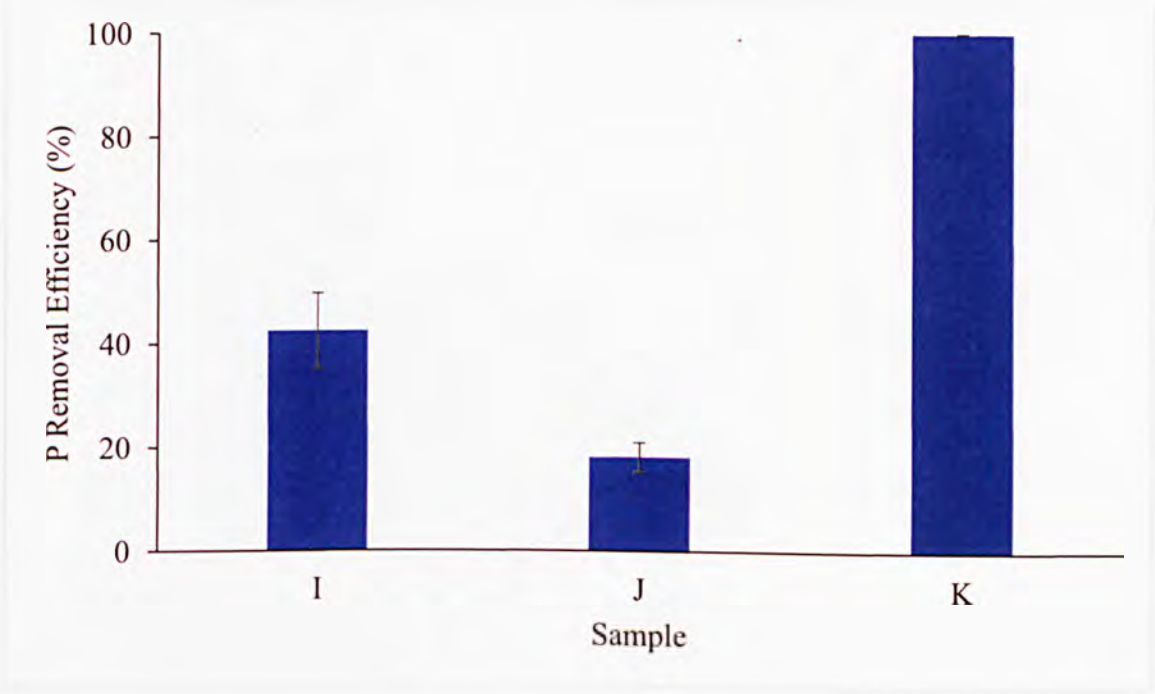

Figure 6.8 Comparison of the P removal efficiencies from spiked water of composite samples (biochar modified with): I (Ca-Fe-Cl-LDH), J (Mg-Fe-Cl-LDH) and K (Ca-Ce-NO_3-LDH). Removal from an initial concentration of 10 mg P/L and a sorbent dose of 0.2 g / 40 mL.

XRD analysis indicated amorphous structures amongst these LDH (showing broad bands possibly dominated by the contribution of biochar). The SEM micrographs shown in Figure 6.9 do not show much evidence for crystallinity either, however do show that the precipitates are quite evenly distributed throughout the biochar structure without blocking the existing macropores. It is possible that the amount of inorganic precipitate analysed (among the powdered composite) was not enough given the sensitivity the technique used. The proposed Ce-based LDH had very high removal of P, similarly to the $Ce(OH)_3$-modified OSR550 biochar without heat treatment (H). This implies that the structure of both Ce precipitates allows for efficient chemisorption of P.

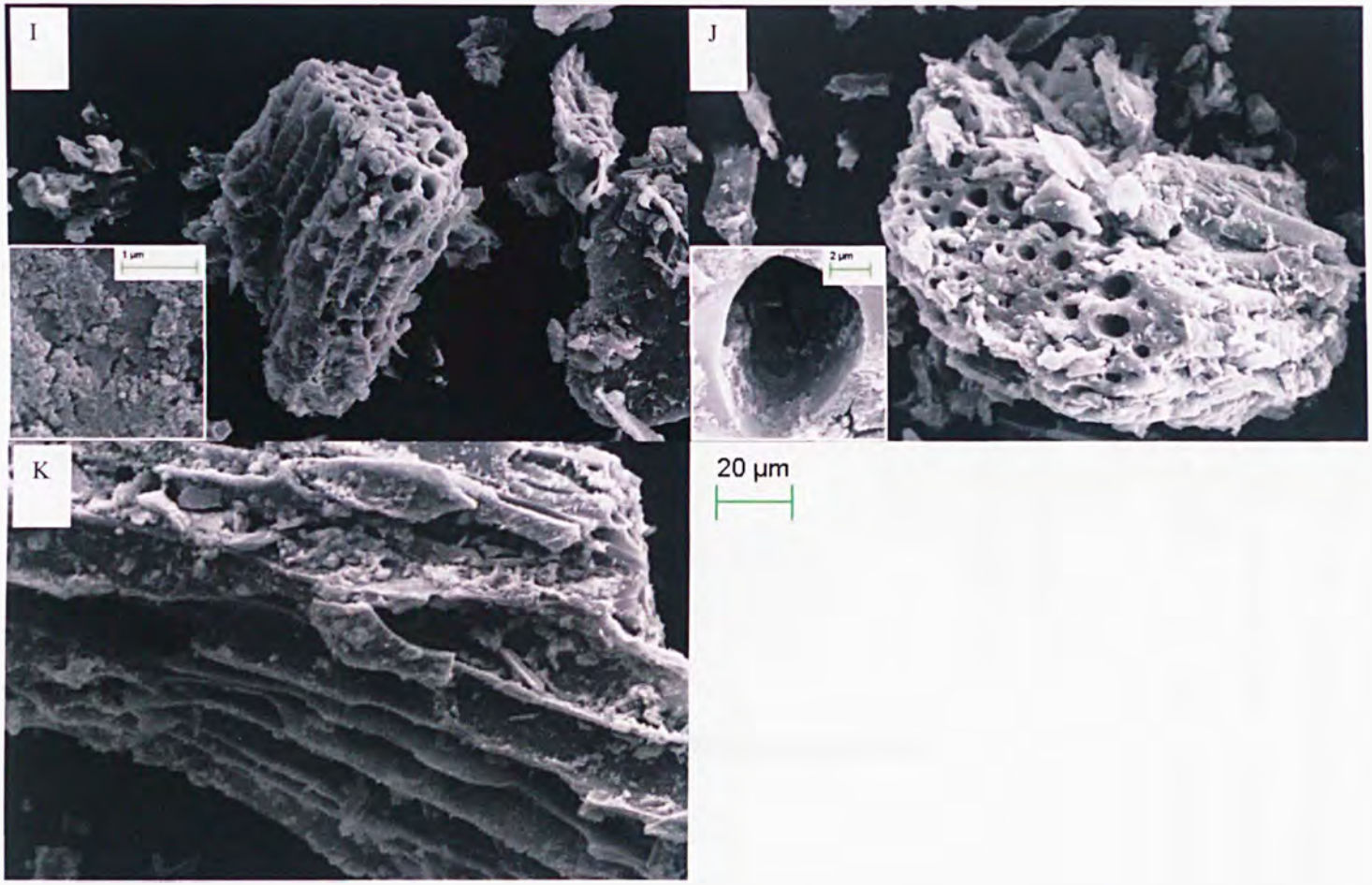

Figure 6.9 SEM micrographs of composites (biochar modified with): I (Ca-Fe-Cl-LDH), J (Mg-Fe-Cl-LDH) and K (Ca-Ce-NO_3-LDH).

6.4.3.1 P release from the metal biochar composites

A P leaching study was carried out (as described in section 6.2.5) to determine and compare the P availability between the composites after the uptake of P. This study, in combination with the P uptake study, gives a good overview of the modified prototypes in terms of P recovery (uptake and release) and enables an informed choice of modification to take forward for further enhancement and study (Chapter 7), in a more practical sense.

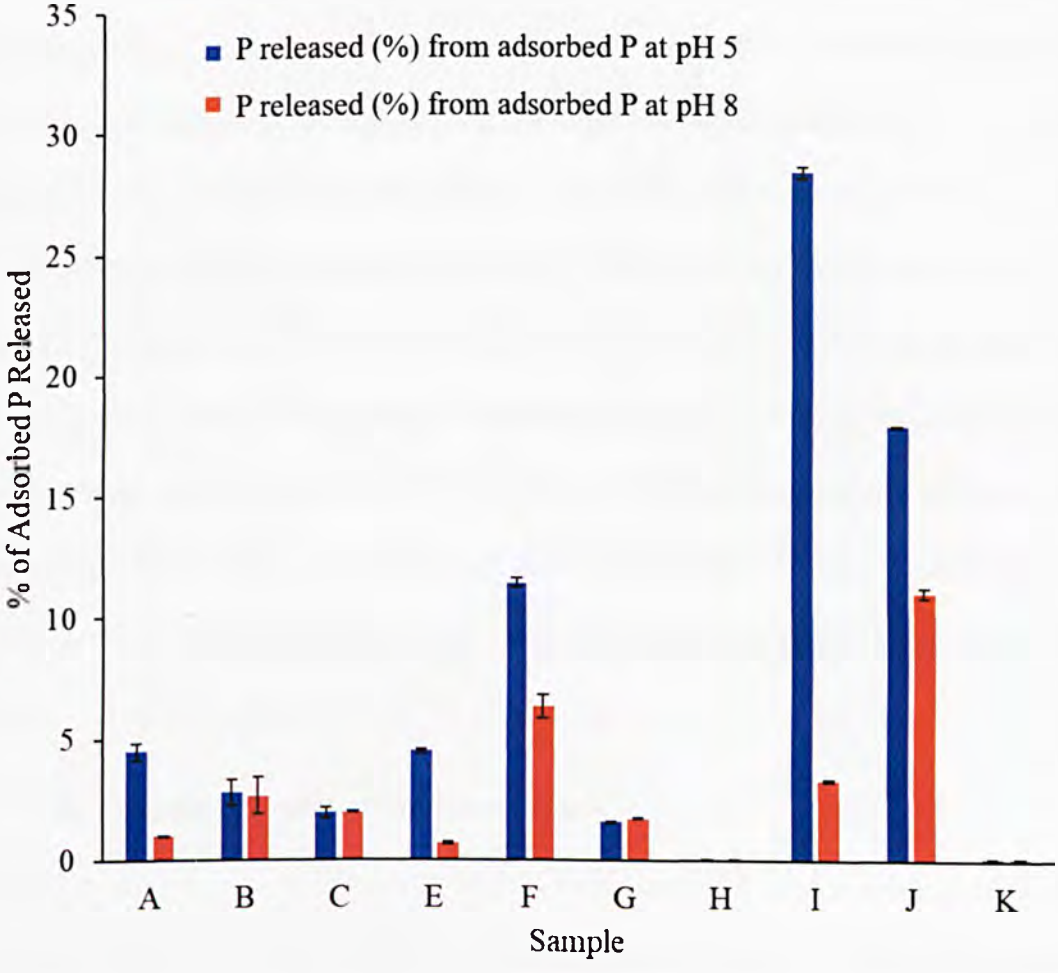

Figure 6.10 P released (% of the P removed) from the composites after adsorption of P from 10 mg P/L at pH 5 (blue) and pH 8 (orange). Error bars correspond to the SD, n=2.

Figure 6.10 shows markedly different P release characteristics between the composites after adsorption of P from 10 mg P/L. Of the Ca and Mg hydroxide modified samples (A, B and C), it is apparent that samples B and C (modified with Ca/Mg, and just Mg, respectively)

have equivalent release of P at both pH 5 and 8 whereas the composite modified with just Ca has significantly ($p < 0.05$) higher release (% of the P adsorbed) at pH 5 compared with pH 8. This could be due to the known greater affinity of P for Ca at higher pH values. This finding is important given that there is literature reported where the presence of Ca within biochar is highlighted as a detrimental property for P release (Buss et al., 2018). It appears that precipitating Ca and Mg together is beneficial.

Among the LDH-modified composites, release from the Ca-Fe-Cl-LDH and the Mg-Fe-Cl-LDH composites (I and J respectively) are both significantly ($p < 0.05$) higher at pH 5 than any of the other samples at pH 5, indicating that there is a higher availability of P from these proposed layered structures post-adsorption – this requires further study, however others have found gradual and controlled release of P from LDH structures intercalated with phosphate (Benício et al., 2017), when precipitated on their own. Composites modified with Ce show a low release of the adsorbed P (samples H and K). This is most likely due to the lower solubility of $Ce(PO_4)$ ($7.434x10^{-11}$ g / 0.1 L at 20°C) compared with various forms of calcium phosphate (0.002–1.8 g / 0.1 L at 20°C) for example. Sample E (modified with $Ce(OH)_3$ and heat treated) shows moderate release of P especially at pH 5 however the initial uptake of P from this sample was low (< 35%).

6.5 Choice of prototype and conclusions

The ideal composite would have both effective removal of P, and a subsequent high P-availability/release, for it to be effective for the purpose of P recovery. Effective removal of P from solution may, in many cases, be to the detriment of P release in soil. Both effective removal and release of P could be mediated by a pH change (e.g. removal of P under basic conditions, with the release of P from the composite driven by an acidic soil environment). From the results obtained, it is apparent that $Ca(OH)_2$ precipitation is an effective modification approach to derive a composite with effective (> 90%) removal of P from 10 mg P/L. When precipitated with Mg, the release characteristics indicate similar release at pH

5 and 8 – this may give the composite more flexibility to deliver P under various soil environments. Release of P from the LDH structures incorporating Ca and Mg, was significantly higher than the other composites synthesised at pH 5, and also higher at pH 8 compared with most composites. Although the removal of P using these materials was lower, it is apparent from the literature that these structures can be effective for P removal – precipitation of LDHs with higher crystallinity or with a different intercalated anion may derive better removal, whilst retaining similar P release characteristics. Ce modification is highly effective in removing P (> 99% removal from 10 mg P/L), however the material does not possess the ability to effectively release P. However, Ce-modified biochar could be suggested to be a highly effective P removal technique, where recovery is not required or removal down to very low concentrations is required. In summary, three composites are chosen for further study: $Ca/Mg(OH)_2$-, $Ce(OH)_3$- and Ca-Fe-NO_3-LDH-modified OSR550 biochar.

However, several changes to the composite synthesis will be undertaken: (1) leaving the biochar and metal solution equilibrating for 48 hr instead of 10 mins: this is to allow for further diffusion of the metal cations within the biochar structure; (2) no heat treatment will be applied after the precipitation procedure: thermal treatment during the precipitation of LDHs was found to be ineffective and its avoidance will prevent burn off of the biochar component and release of native-P; (3) instead of using a magnetic bar, a vortex stirrer will be used to minimise the breakup of the biochar particles.

7 Practical application of biochars and its modification for the recovery of P from model aqueous samples and wastewater

7.1 Introduction

Wastewater treatment consists of primary and secondary treatment to reduce contaminants and P concentrations down to safe levels permissible for discharge (Melia et al., 2017, Chapter 2). P removed through chemical or biological techniques may often be suitable for reuse providing organic and chemical contaminants are minimised to safe levels and P is suitably available for its bioavailability in soil – this can be achieved through anaerobic digestion, pyrolysis or thermochemical treatments. Struvite precipitation, as a technology capable of P recovery and direct reuse, is mainly operated within the anaerobic digestate stream from biological sludge. As legislation ensures that most WWTPs remove P to levels < 1 mg P/L before discharge to receiving waters, WWTPs may require a tertiary treatment stage to provide final polishing of effluents before discharge. A tertiary treatment technology that is capable of both removing P to levels < 1 mg P/L, or even as low as < 0.5 mg P/L and enables the safe reuse of the recovered P is now important for increasing the future sustainable use of P and for the protection of environmental waters from eutrophication.

Composite materials synthesised in the previous chapter show potential for forming part of such a treatment stage. It is suggested that a material such as a biochar-based composite could be applied as an effective filter medium in a column through flow setting. However, before suggesting the application of such a material as proposed, it is important that more information is gathered of the ability of the composite; such as adsorption kinetics, maximum adsorption capacity and the ability to recover P from matrixes other than ultrapure water.

The aim therefore of this chapter is to establish the practical ability of the 3 chosen composites ($Ca/Mg(OH)_2$-, $Ce(OH)_3$-, and Ca-Fe-NO_3-LDH-modifed OSR550 biochar) to recover P, in terms of P adsorption kinetics, isotherm studies (maximum P adsorption

capacity and effect of initial P concentration) and removal from wastewater effluent in order to suggest the materials to be technologically and practically capable in recovering P from WWTP effluent.

7.2 Materials and methods

OSR550 biochar is used as the matrix to host the precipitated species. NaOH (98.5%), $Ca(NO_3)_2 \cdot 4H_2O$ (99%), $Fe(NO_3)_3 \cdot 9H_2O$ (> 99%) and $Ce(NO_3)_3 \cdot 6H_2O$ (99.5%) (supplied by ACROS Organics) are used in this chapter.

7.2.1 Synthesis

The synthetic approach is approximately the same method as used in Chapter 6. However, the synthesis here has been scaled up and slight changes have been made, as justified in section 6.5. For the Ca/$Mg(OH)_2$ - and the $Ce(OH)_3$ -modified composites, the method is as follows. OSR550 biochar (15 g) was added to 100 mL of ultrapure water with a total of 75 mmol of the metal ion (in the case of the Mg/Ca-modified sample this was evenly split to be 37.5 mmol Ca and 37.5 mmol Mg). This was left shaking for 48hr before heating the suspension to 40°C. Under agitation via a vortex stirrer, 100 mL of 1.5 M NaOH solution was added dropwise. Once mixed, the suspension was cooled in a water bath to room temperature before filtering and rinsing with Whatman n°.1 filter paper and ultrapure water. The samples were dried at 50 °C under vacuum before analysis. The Ca/$Mg(OH)_2$ - and the $Ce(OH)_3$ -modified composites are referred to as composite A and B, respectively, in this chapter.

For the Ca-Fe-NO_3-LDH composite, the method is as follows. OSR550 biochar (15 g) was added to 100 mL of ultrapure water with 50 mmol of Ca and 25 mmol of Fe (both as nitrate salts). This was left shaking for 48h before heating the suspension to 80°C. Under agitation via a vortex stirrer, 100 mL of 1.5 M NaOH solution was added dropwise. Once mixed, the 200 mL suspension was continually heated at 80°C for a further 72 hours before cooling in

a water bath to room temperature, filtering and rinsing with Whatman n°.1 filter paper and ultrapure water. The samples were dried at 50 °C under vacuum before analysis. The Ca-Fe-NO_3-LDH composite is referred to as sample C in this chapter.

7.2.2 Characterisations

SEM and SEM-EDS analysis were carried out as described in Chapter 3. This was to visualise the distribution and morphology of the inorganic precipitates; determine the stability of the material as a composite pre- and post-adsorption; to qualitatively determine what metals were present in the precipitates; and to confirm where the P was adsorbing to. XRD analysis was also carried out to observe if crystal structures and their crystallinities could be elucidated and was carried out as outlined in Chapter 3.

7.2.3 Adsorption studies

The general P adsorption process carried out for the isotherm and kinetic studies detailed below is outlined in Chapter 3, using 0.2 g of composite per 40 mL of P containing solution. Na_2HPO_4 was used as the source of P in all adsorption studies.

7.2.3.1 Isotherms

Adsorption isotherms were carried out to establish the effect of initial concentration of P on the adsorption capacity, allowing the heat of adsorption and maximum capacity of the composites to be determined. Initial concentrations used were 1.2, 5.8, 11.7, 20.5, 43.7, 60.3, 117.2 and 230.2 mg P/L. Adsorption was carried out in duplicate – additional adsorption points were included if any values were > ±5% from the mean value. The experimental data obtained was fitted to Langmuir and Freundlich adsorption isotherm models (outlined in Table 7.1).

Table 7.1 Adsorption isotherm models, and parameters determined. Q_{max} (mg P/ g) represents the maximum adsorption capacity and *b* represents an equilibrium constant (Langmuir model). C_{eq} and q_{eq} are the concentrations (mg P/ L) and quantities adsorbed (mg P/ g) at equilibrium respectively. *K* and *n* are Freundlich model constants.

Isotherm model	Equation	Linear Plot	Parameters
Langmuir	$q_{eq} = \frac{q_{max} b C_{eq}}{1 + bC_{eq}}$	C_{eq}/q_{eq} vs. C_{eq}	q_{max}=1/slope b=q_{max}/intercept
Freundlich	$q_{eq} = KC_{eq}^{1/n}$	log q_{eq} vs. log C_{eq}	log K=intercept 1/n=slope

7.2.3.2 Kinetics

A kinetics study was carried out to determine the length of time taken for the composites to remove P from solution. This was carried out from an initial concentration of 5 mg P/L, which could be considered as representative of wastewater. Adsorption was carried out with individual samples for the various time periods including, 15 and 30 seconds, 1, 5, 10, 20, 30, 60, 120 and 480 minutes, and were carried out in duplicate. The experimental data was fitted to pseudo-first- and pseudo-second-order models (Ho and McKay, 1998). Kinetic data was first plotted according to the linearization of the models, to find the model parameters.

Table 7.2 Kinetic model equations applied, and parameters determined. The kinetic constants determined for the respective model were k_1 and k_2, where q_t and q_e are the quantities adsorbed (mg P / g) at time (*t*).

Kinetic model	Linear form	Plot	Parameters
Pseudo-first-order	$\log(q_e - q_t) = \log(q_e) - \frac{k_1}{2.303} t$	$\log(q_e - q_t)$ vs time	k_1=-2.303xslope
Pseudo-second-order	$\frac{t}{q_t} = \frac{1}{k_2 q_e^2} + \frac{1}{q_e} t$	$\frac{t}{q_t}$ vs time	q_e=1/slope k_2=slope^2/intercept

7.2.3.3 Uptake of P from wastewater

Final effluent was sourced from Reading WWTP, where secondary treatment and tertiary sand filtration is operated, and used as a matrix to determine P adsorption in order to inform the more practical potential for the composites to recover P. The adsorption was carried out as described in Chapter 3 from: (1) the existing P concentration in the effluent (0.36 mg P/L); (2) the wastewater effluent spiked to 1.1 mg P/L, and; (3) the wastewater effluent spiked to 5.3 mg P/L. Na_2HPO_4 was used as the source of P in the spiked effluent. The solutions had an initial pH of ~ 7.5 and was uncontrolled in all experiments.

7.3 Results and discussion

7.3.1 Characterisations

The composites were inspected after their use and compared with their initial characteristics. This was carried out through SEM and SEM-EDS, examples of which are given in Figures 7.1–7.3. The SEM micrographs indicate that the composites are stable, with the precipitate component maintaining adhered to the biochar surfaces and pores post-adsorption. The micrograph with higher magnification in Figure 7.3 indicates nano-features within the Ca-Fe-NO_3-LDH precipitates, which may have been formed due to the longer thermal treatment of several days that was applied; features of this scale are commonly reported with synthesised LDHs (Kuang et al., 2010). This is a desirable morphology to have for an adsorbent as it enables higher reactivity and surface area – it would be preferable for all three composites to have such structures potentially enhancing the performance of the sorbent – this would be a focus of further work. SEM-EDS indicates the elemental components of the precipitates and that: (1) the precipitate is composed of the intended metals; (2) P is being adsorbed to the precipitate component of the composites as theorised; and (3) P is not being adsorbed to the carbon component.

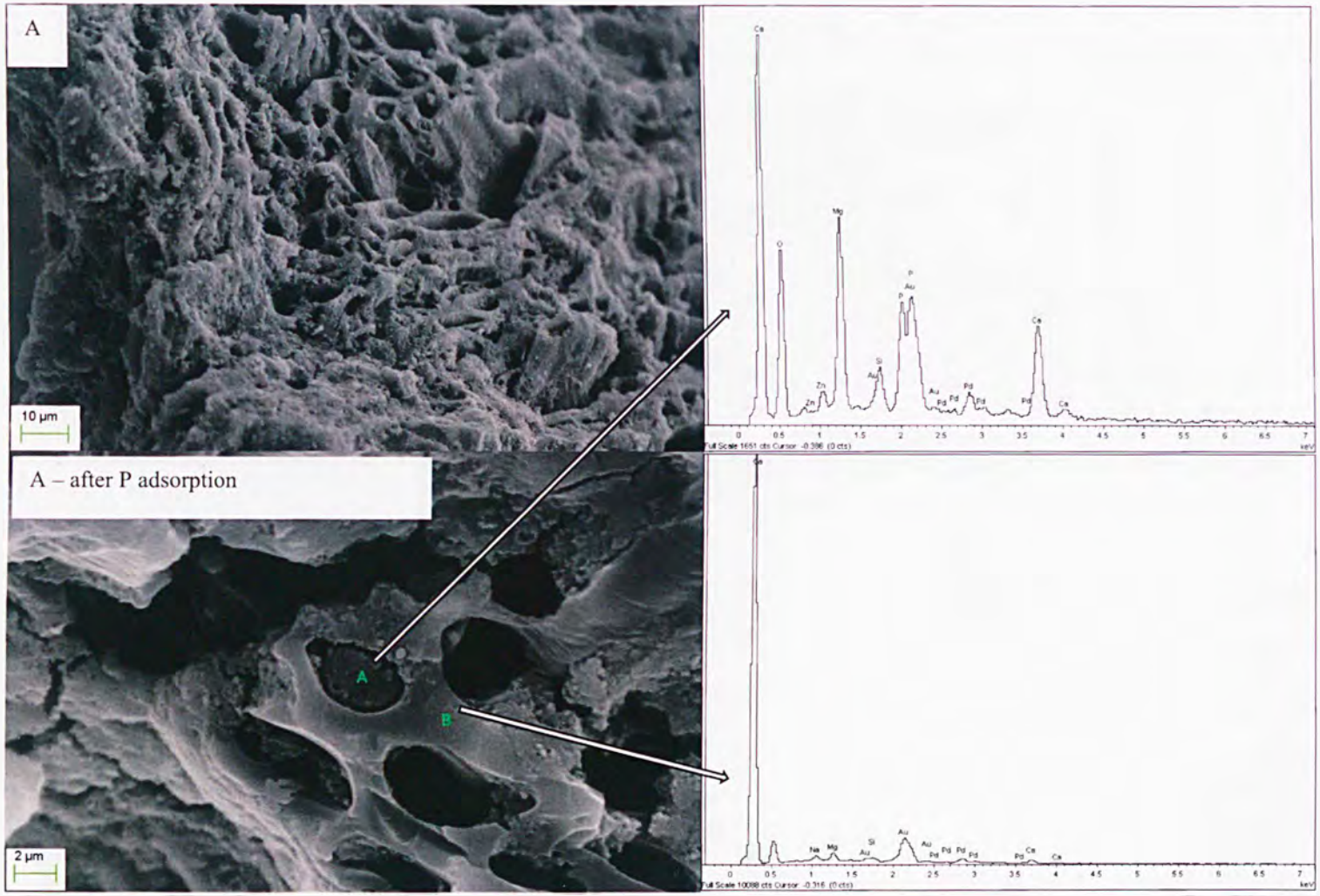

Figure 7.1 SEM and SEM-EDS micrographs and spectra, respecively, of Ca/$Mg(OH)_2$ -modified OSR550 biochar before and after adsorption of P. Both micrograph and spectra of composite, taken after adsorption of P, is of the sorbent saturated with P at its maximum capacity.

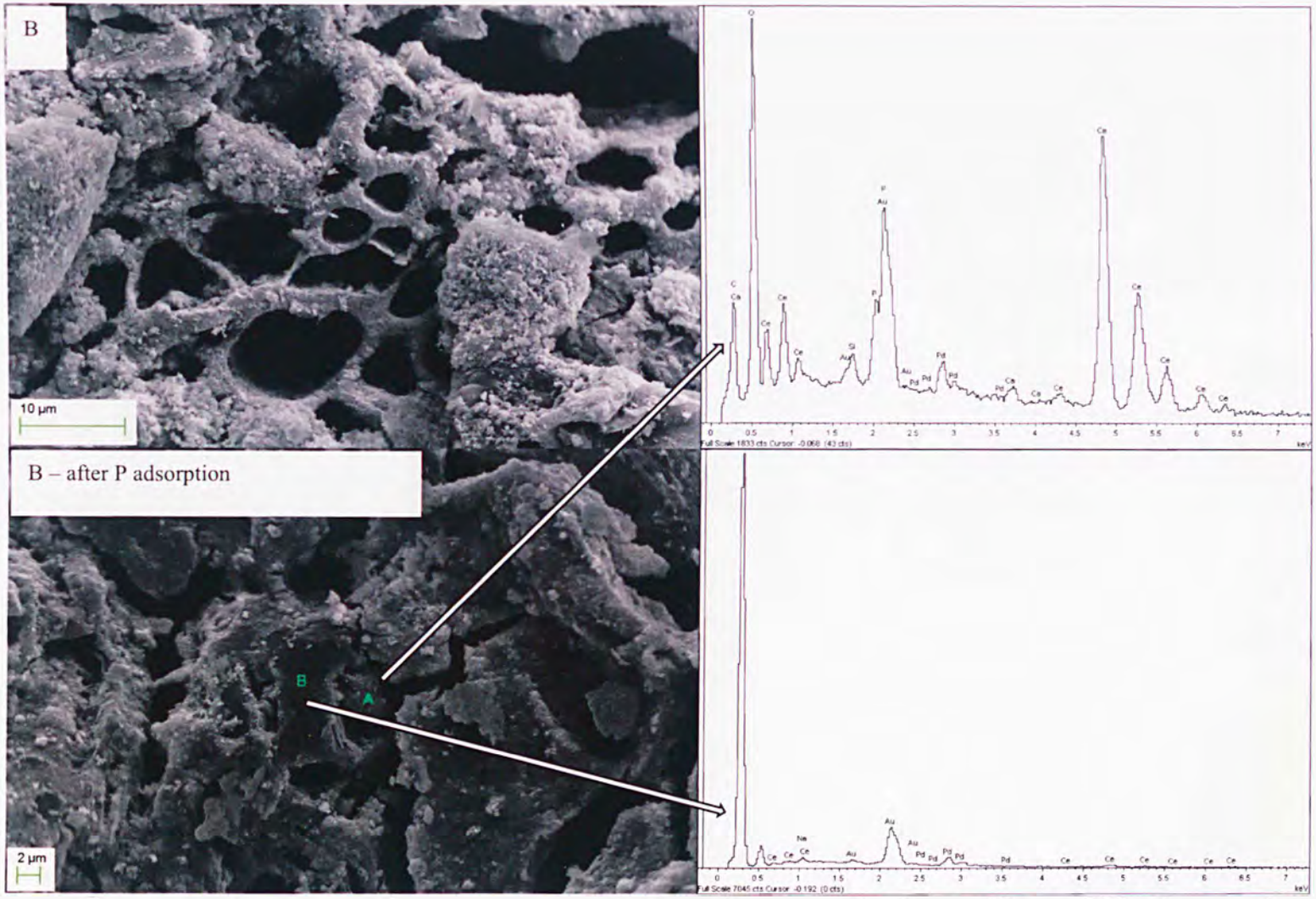

Figure 7.2 SEM and SEM-EDS micrographs and spectra, respecively, of $Ce(OH)_3$ -modified OSR550 biochar before and after adsorption of P. Both micrograph and spectra of composite, taken after adsorption of P, is of the sorbent saturated with P at its maximum capacity.

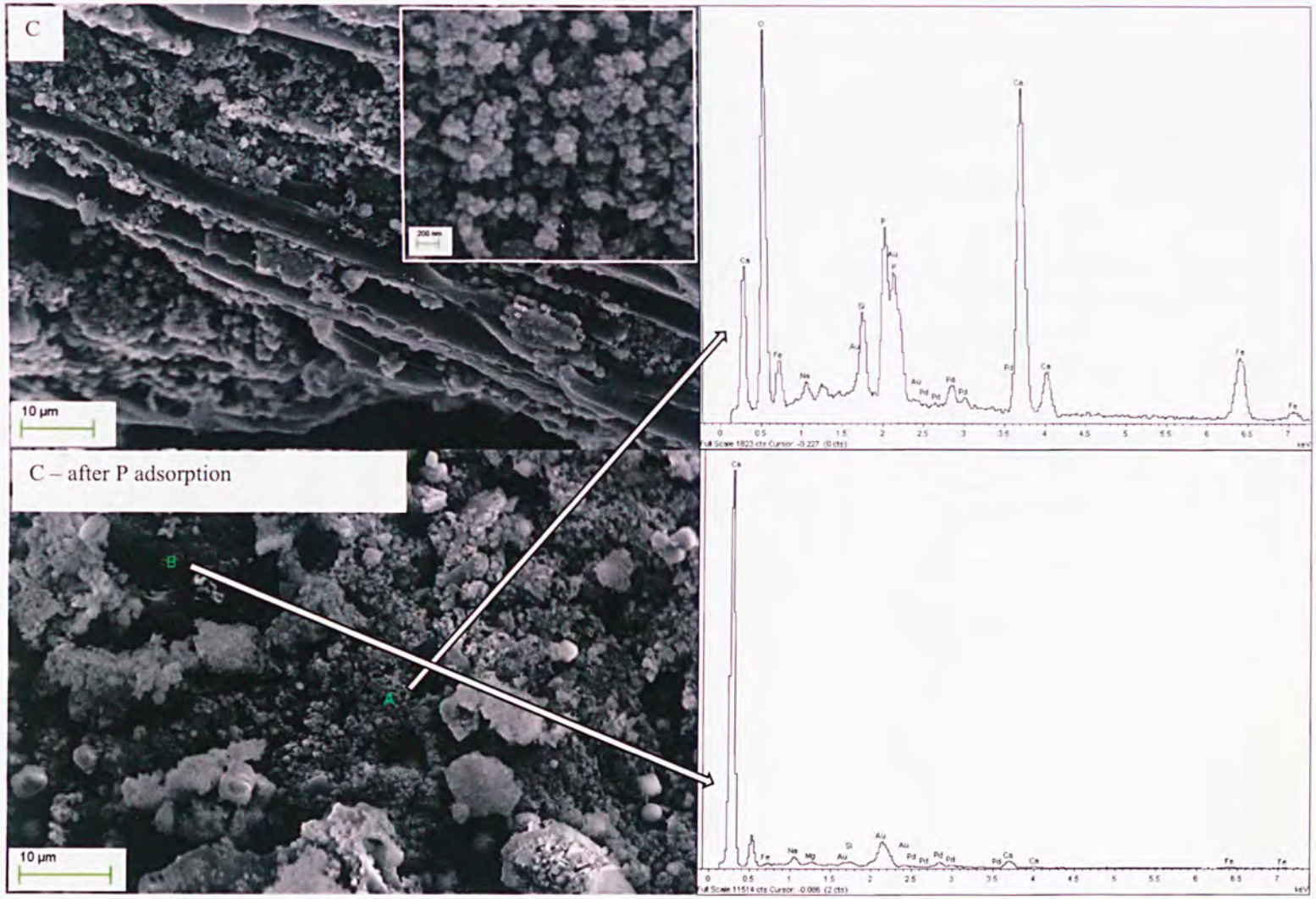

Figure 7.3 SEM and SEM-EDS micrographs and spectra, respecively, of Ca-Fe-NO_3-LDH -modified OSR550 biochar before and after adsorption of P. Both micrograph and spectra of composite, taken after adsorption of P, is of the sorbent saturated with P at its maximum capacity.

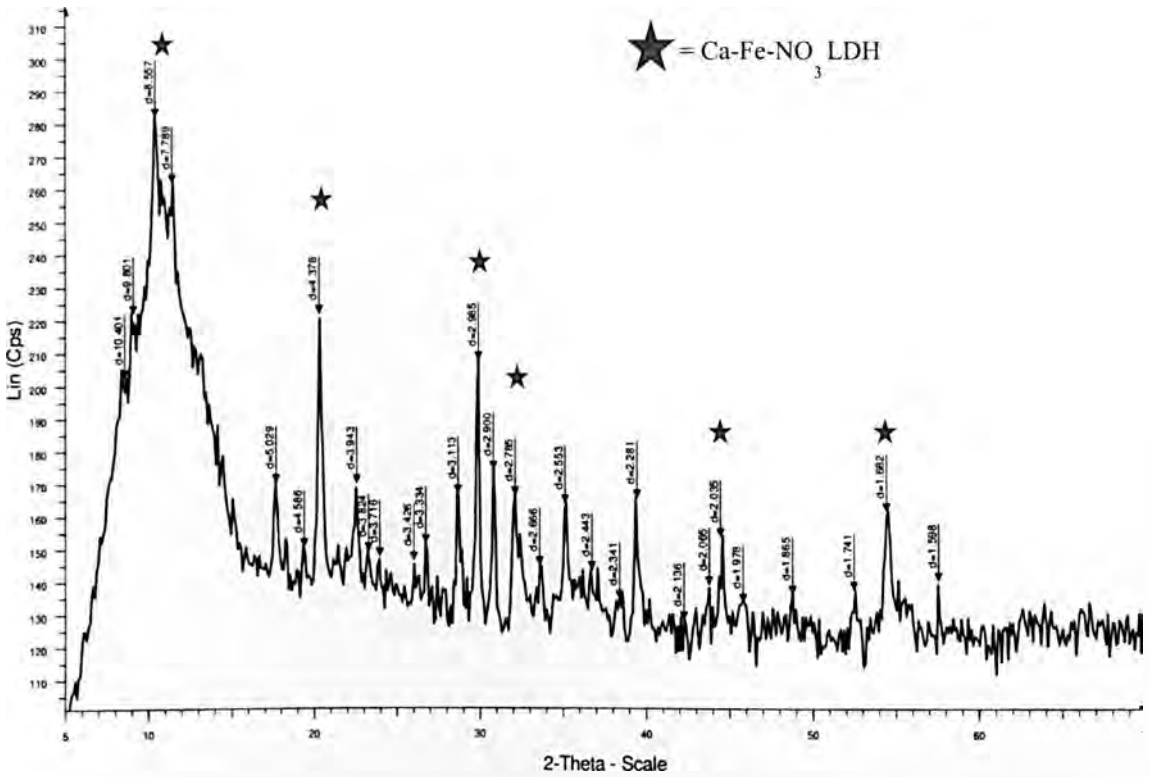

Figure 7.4 XRD diffractogram of Ca-Fe-NO_3-LDH-modified biochar composite

Figure 7.4 shows an XRD diffractogram of the Ca-Fe-NO_3-LDH-modified OSR550 biochar composite. This diffractogram confirms that the crystalline structure of the LDH has been successfully synthesised: peaks at 2θ angles of ~11°, ~20°, ~30°, ~32°, ~44° and ~55° agreeing with diffractogram data reported in Woo et al., (2011), where the LDH was prepared (and not the composite). In the previous chapter, the precipitation of crystalline LDH structures was unsuccessful, with XRD data indicating a high degree of amorphous structures. Changing the synthesis to incorporate NO_3^- as opposed to Cl^- may have allowed for a more facile synthesis of this structure, which has a relatively high degree of crystallinity and nano-features (indicated in Figure 7.3). There are many other phases present within the composite, indicated by the various other peaks left unassigned. These may be native components of the biochar matrix or side products of the precipitation process – these will be inevitable features when modifying biochar in this way due to their complex makeup.

7.3.2 Isotherms

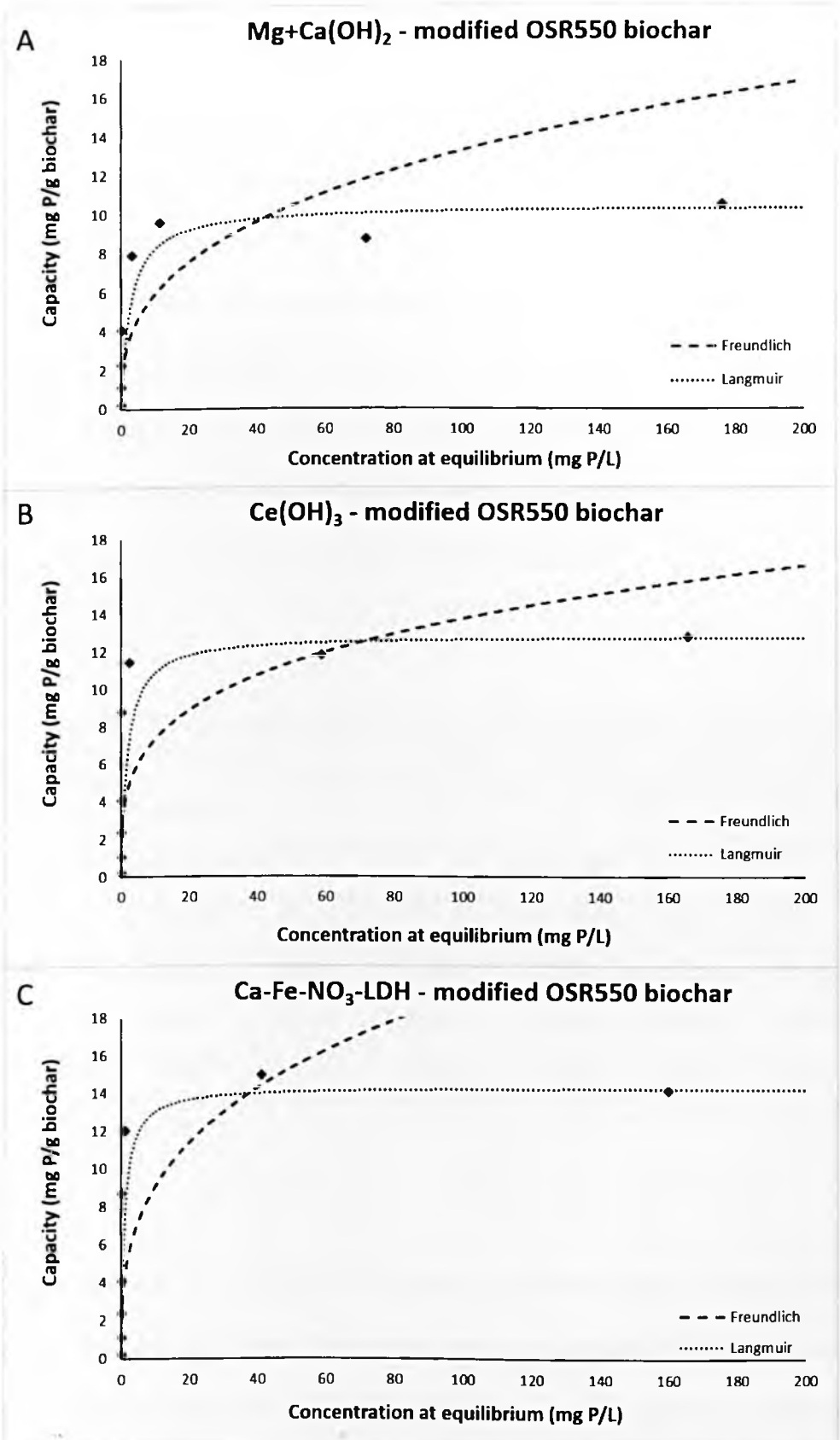

Figure 7.5 P adsorption isotherms for prototype adsorbents. Conditions of adsorption in batch mode: 200mg adsorbent and 40 mL P solution, on orbital shaker at 90 rpm, 48h contact time, room temperature (25°C).

Adsorption isotherms for the three composites are shown in Figure 7.5, where the effect that the initial P concentration has over the adsorption capacity of the materials can be observed. All three composites possess high heats of adsorption and are well fitted to Langmuir isotherm model (r^2 values of 0.994, 0.998 and 0.999 for samples A, B and C, respectively). The Langmuir model calculates the maximum adsorption capacities to be 10.4, 12.8 and 14.3 mg P/g for the three composites. These values are quite modest but compare well to some maximum adsorption capacity values reported in the literature (for example in R. Li et al., (2016a)) – see Table 6.1. It may be the case that employing a lower adsorbent dose or conducting isotherms at a lower controlled pH value could result in a higher predicted maximum capacity. However, provided that the material could be prepared with low cost, it could be applied on a larger scale, negating its moderate capacity.

Table 7.3 Freundlich and Langmuir isotherm data for the three metal biochar composites. 1/n and K are Freundlich constants which correspond to adsorption intensity and adsorption capacity respectively. Q_{max} is the Langmuir maximum adsorption capacity, b corresponds to the heat/energy of adsorption.

Composite modification	Freundlich			Langmuir		
	r^2 value	1/n	K	r^2 value	Q_{max}	b
$Ca/Mg(OH)_2$	0.593	0.347	2.668	0.994	10.37	0.386
$Ce(OH)_3$	0.358	0.271	3.935	0.998	12.84	0.557
Ca-Fe-NO_3-LDH	0.443	0.325	4.299	0.999	14.33	1.012

The Langmuir isotherm is characterised by monolayer adsorption onto a surface with finite adsorption sites that are equivalent. The b values indicate that the LDH-modified composite possesses the highest heat of adsorption followed by the $Ce(OH)_3$ -modified sample, with the $Ca/Mg(OH)_2$ -modified composite having the lowest heat of adsorption but still high when compared with most isotherm data reported throughout in the literature (Fang et al.,

2015). The high energy in the adsorption of P with the LDH-modified sample may originate from the nano-scale features present within the precipitated phases and/or specific chemisorption.

7.3.3 Kinetics

Adsorption rate is one of the most important factors when designing adsorption systems. Figure 7.6 shows the adsorption kinetics for the removal of P from a 5 mg P/L initial concentration for the three composites studied. All three composites possess very rapid removal of P, reaching equilibrium in < ~5 minutes in all cases. The $Ce(OH)_3$ -modified composite represents the most rapid removal of P, followed by the $Ca/Mg(OH)_2$ -modified sample, the Ca-Fe-NO_3-LDH -modified composite has the slowest removal of P of the 3 composites. As the LDH-modified composite has higher crystallinity and nano-features it would be assumed that this material would have more rapid kinetics, as this has been found in many other adsorption studies. However, it is not the case here – this may indicate that there are different mechanisms responsible for the adsorption of P such as diffusion-limited processes, or that lower crystallinity (or polycrystallinity) can be a beneficial feature for rapid removal of P.

Many kinetic models have been suggested and applied to the adsorption of contaminants from water, including pseudo-first- and pseudo-second-order models. When applied to the experimental data obtained, they can help to define rate constants and equilibrium capacities, as well as suggesting adsorption mechanisms and the overall complexity of the adsorption process. The kinetic modelling was done through linearization of the models to determine the fit and key parameters. All three composites' kinetics are well described by a pseudo-second-order model (Table 7.4), with the predicted equilibrium capacity being very close to the experimental equilibrium capacity. These composites possess much faster kinetic rates than other LDH materials precipitated (for example Wan et al., (2017)), and other

composites more generally (Wang et al., 2016). This may be due to the fact these composites present a high proportion and accessibility of the inorganic precipitate when compared with biochar-based materials prepared through a pre-pyrolysis modification approach. Additionally, the high pH present especially with Ca and Mg hydroxides may be limiting the composites to removal mechanisms happening at these pH values (i.e. ~10), which may occur at a rapid rate compared with others, for example ion exchange mechanisms that are unlikely to occur at basic pH.

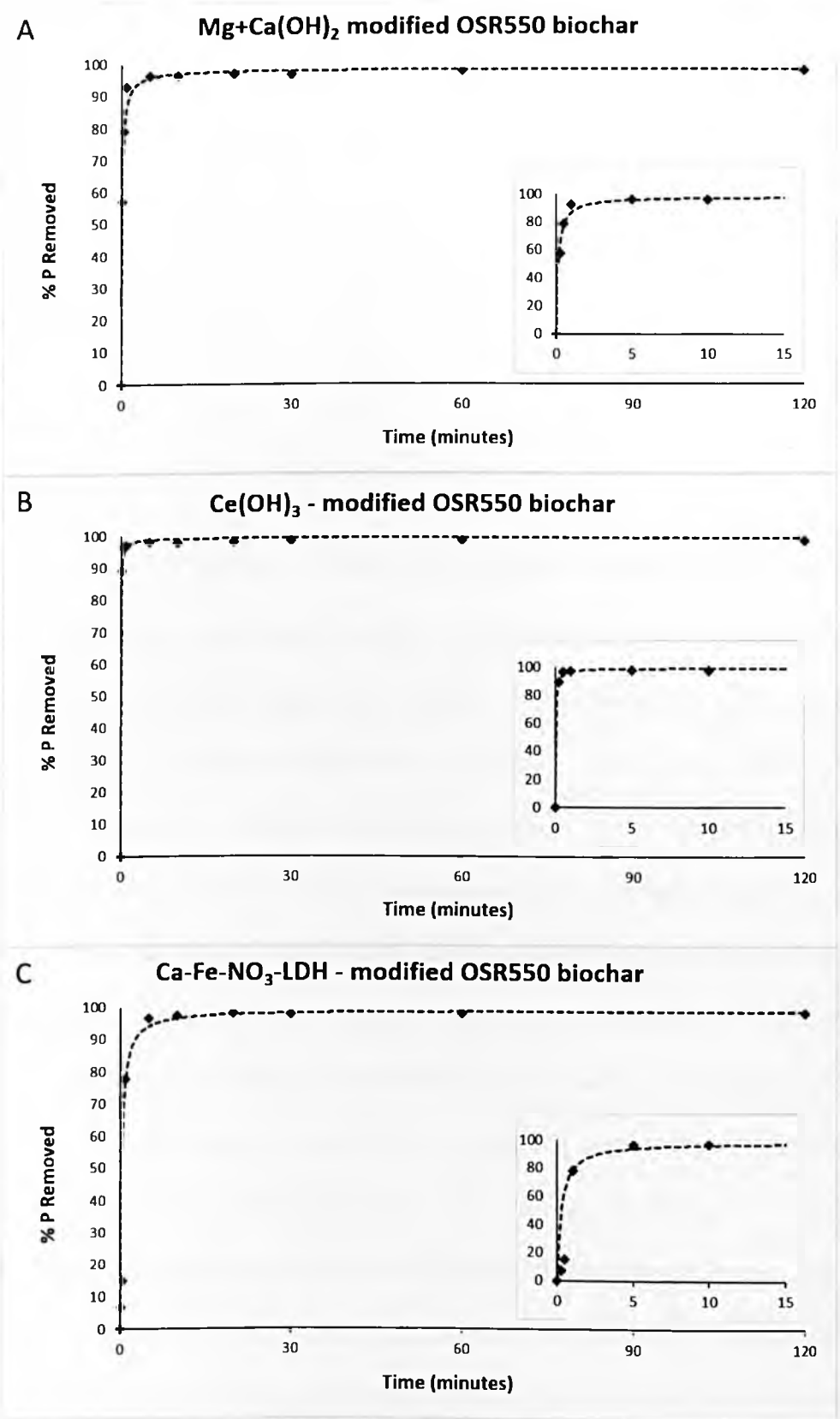

Figure 7.6 P removal kinetics for prototype adsorbents from an initial concentration of 5 mg P/L in ultrapure water – larger figure shows 0–120 minutes, smaller figure shows 0–15 minutes. Points show experimental data; the dashed line represents the pseudo-second-order kinetic modelled data. Conditions: 200mg adsorbent dose and 40 mL P solution.

Table 7.4 Pseudo-first and pseudo-second-order kinetic model data for the three composite samples.

Composite modification	Pseudo-first-order parameter		Pseudo-second-order parameters		
	r^2 value	k_1 (min^{-1})	r^2 value	k_2 (L mg^{-1} min^{-1})	Q_{eq} (mg P/g)
$Ca/Mg(OH)_2$	0.949	0.51	0.999	7.81	0.971
$Ce(OH)_3$	0.951	1.12	0.999	36.8	0.982
$Ca\text{-}Fe\text{-}NO_3\text{-}LDH$	0.727	0.03	0.999	3.75	0.980

7.3.4 Uptake of P from wastewater and practical considerations

Wastewater effluent collected from Reading WWTP is used to assess the removal of P from a realistic matrix. It is very important to identify if the composites can remove P from relevant matrices other than ultrapure water. Figure 7.7 shows the removal of P from wastewater effluent at 3 different initial concentrations. It is apparent that the three composites can remove P to < 0.5 mg P/L in all cases, apart from the $Ca/Mg(OH)_2$ -modified composite (from the highest initial concentration), which is evidently most effected by the change in matrix (ultrapure water compared with wastewater effluent) – this may be as a result of there being a presence of competing anions, such as carbonates, sulphates or nitrates, however these were not analysed. The $Ce(OH)_3$ composite is highly effective in removing P from all three initial concentrations (to < 17 µg/L in each case – i.e. the LOD of the ICP-AES instrument used) whereas the LDH-modified composite is much less efficient at removing P from the higher initial concentration (removal to 0.37 mg/L) but achieves removal to 19.7 µg/L and 38.8 µg/L from the lower and middle initial concentrations tested.

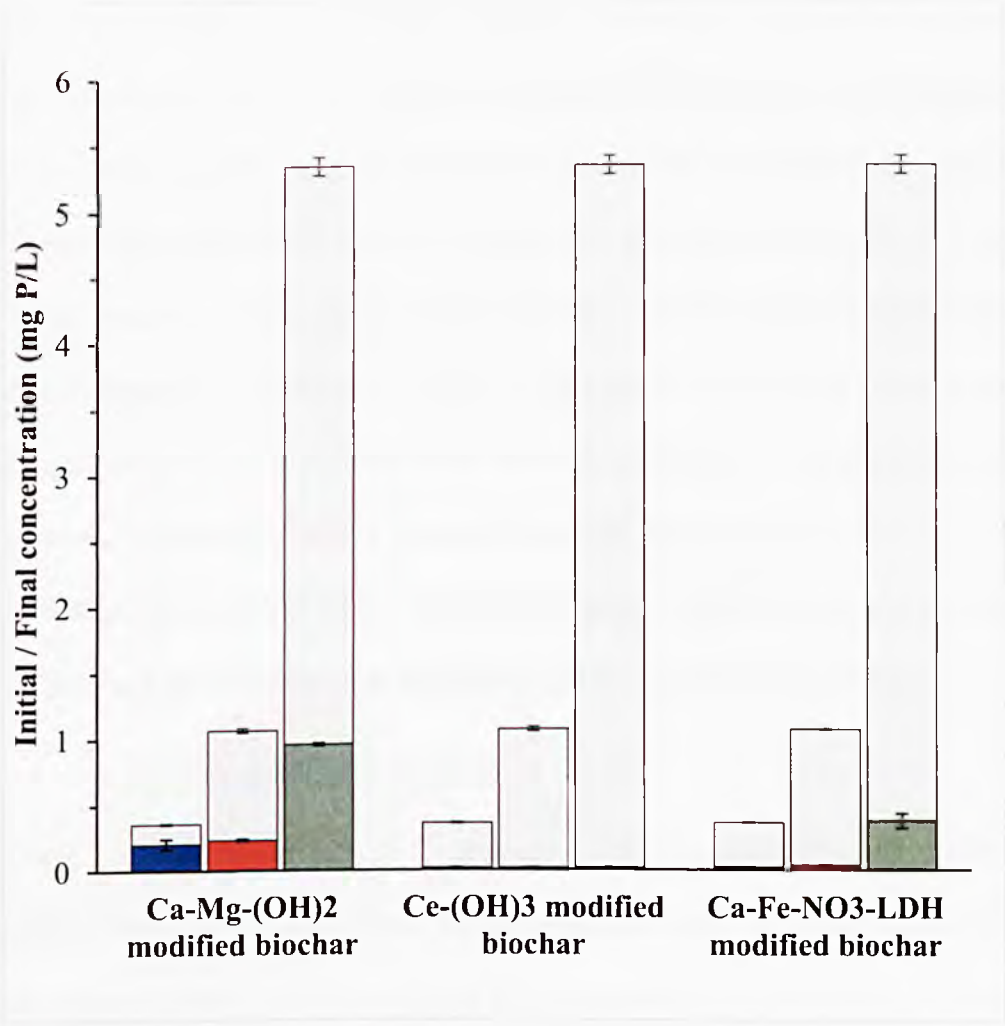

Figure 7.7 Uptake of P from final wastewater effluent (Reading WWTP) at 3 different concentrations: non-spiked at 0.36 mg P/L (blue), spiked at 1.1 mg P/L (orange) and spiked at ~5.3 mg P/L (grey). 0.2 g adsorbent dose and 40 mL P solution. n=2.

The wastewater effluent had a native P concentration of 0.36 mg P/L and this would represent one realistic application for these materials – to recover P from final effluent before discharge to the environment (i.e. tertiary treatment). Recovering P from here minimises the potential for the adsorption of other potentially toxic contaminants (as they will have been removed at an earlier point in the treatment process) and reduces P to very low concentrations suitable for discharge without risk to the environment. Assuming maximum capacities of 10.4, 12.8 and 14.3 mg/g for the three composites (A, B and C) (derived from the Langmuir isotherm model) and an initial concentration of 0.36 mg P/L, theoretically, 1 kg of composite could continually remove P from 28.89, 35.56 and 39.72 m^3 of final

wastewater effluent, respectively. This may not be practical for the recovery of P from WWTPs at large scale, as it would either require the filter media to be changed too frequently or for an excessively large amount of the material to be employed at once. For example, Thames Water reportedly treat 2.8 billion litres of wastewater per day in London (Thames Water, no date), which would require between ~70–100 tonnes of material to be used per day. However, for treatment of wastewaters (including industrial sources) and potentially eutrophic water too, at smaller scales, then the application could potentially be found to be practical, especially if the P saturated material had a market value. This would be an important test to undertake in a throughflow setup in further work and would be important before the potential scale of application could be suggested to be practical.

7.4 Discussion and conclusions

These materials, modified with $Ca/Mg(OH)_2$, $Ce(OH)_3$ and Ca-Fe-NO_3-LDH, possess high affinity for P in lab-scale tests from deionised water and final wastewater effluent – maximum capacity of up to 14.3 mg P/g composite, and quick kinetics. However, studies with a wider range of wastewater conditions, and of P release in soil, would have to be conducted to determine their effectiveness for P recovery from a wastewater process. In soil, as $Ca(OH)_2$ is slightly soluble the $Ca/Mg(OH)_2$ and LDH structures would be assumed to be broken down especially within more acidic environments such as slightly acidic soils or local environments surrounding roots that are known to have higher acidity (Rengel and Marschner, 2005). We can propose that the material would work as a slow release P fertiliser with the additional benefits to soil of the native biochar component. As fertiliser regulation in the EU is under review (Huygens et al., 2017) and set to include recovered ashes, chars and precipitates, the material could be suggested as a recovered fertiliser. Further work would investigate the bioavailability of the recovered phosphate in soil or field studies.

8 Summary and Conclusions

The recovery of P from wastewater to agriculture, is becoming critical to ensure that future P use is sustainable – both minimising the eutrophication of surface waters and ensuring that future demand for P can be met. WWTPs represent a significant opportunity for the recovery of P, and although there are several technologically proven routes for its successful recovery (such as struvite precipitation and thermochemical treatment of sewage sludge residues), these technologies are currently limited to large-scale treatment plants while issues remain in reducing P down to < 1 mg P/L before discharge. Overall, the recovery of P through struvite crystallisation, a well-developed approach, can be limited to < 25% recovery of the influent P load unless chemical extraction is applied. There is now a need for new technological options that can both remove P down to lower concentrations and provide its recovery in forms that are suitable for direct reuse as recovered fertiliser. The use of biochar-based materials, as P-adsorbents, is attractive due to the native soil ameliorant properties of biochar – biochar-based materials can become part of the solution to increase and enhance the overall recovery of P from WWTPs.

For the accurate measurement of biochar physicochemical properties it was important to establish what analytical techniques could be used and that they were suitable for biochars. Through initial work carried out with biochar pyrolysed from a range of biomass, it was identified that the study biochars possessed macroporosity, were brittle, and were observed to release ash – this posed several issues when trying to accurately assess key biochar characteristics. SEM, light microscopy and N_2 adsorption isotherms could all be useful for the determination of biochar structural properties, however no one technique on its own provides a high enough level of information. Similarly, when assessing biochar mineral/metal content, it was found that a combination of XRD, acid-microwave digestion and ICP-MS/ICP-AES analysis, and SEM-EDS all had important applications in determining the inorganic content of biochar on the surface and in bulk. XPS alongside

Boehm titration and IR spectroscopy gave a good indication of biochar surface chemistry. These analytical techniques (and modifications to them) were used throughout the rest of the thesis and will contribute to establishing methodology for the characterisation of biochar that are relevant for its environmental uses.

The study biochars (that were unmodified, but size graded and washed) pyrolysed from: sewage sludge, wheat straw, oilseed rape straw, *Miscanthus* straw, soft wood and rice husk at 550°C and 700°C had a very limited ability to capture P from water (< 0.8 mg P/g biochar), with most of the agriculturally derived biochars possessing a higher release of native P than adsorbing from solution. However, it was determined that overall, P removal was pH-related and dependent upon concentrations of Ca and Mg in particular. Increases to surface area and micro- and mesoporosity through activation in CO_2 at 800°C, increased P removal to < 1.2 mg P/g (although no significant correlation was found between surface area and P removal $p > 0.05$). This removal was still extremely limited when compared to biochar in the literature with higher cationic content. This initial work was important and contributes new insights of biochar-P interaction to the field. Unmodified biochar has only limited potential for being incorporated into a P recovery process due to limited adsorption capacity in most cases. Some natural feedstocks, such as marine macroalgae, do however show potential in the literature but the removal of P must be shown to be effective in terms of kinetics and efficiency from lower initial concentrations. Whilst some unmodified biochars are demonstrated to have high maximum adsorption capacities (corn and sugarcane bagasse, for example) they require unrealistic initial P concentrations and are largely inefficient for use in environmental or wastewater settings (where the initial concentration is < 10 mg P/L).

The aim was then to derive modified biochars through novel approaches to overcome limitations observed in the existing unmodified biochars. There are now a wide variety of approaches in the literature for modifying biochar for the aim of capturing P. Through a second literature review, it was found that most modification of biochar, for an increased

affinity for P, is carried out through either pre-pyrolysis modification (mostly via soaking of the feedstock in a metal solution before pyrolysis), or post-pyrolysis modification, again through soaking in concentrated metal solutions and drying or a second pyrolysis stage. The approach taken in this thesis was to precipitate specific inorganic phases, thought to interact with P (based on the studies carried out in Chapter 5, and preliminary testing) to the surfaces and pores of biochar derived from oilseed rape straw biochar pyrolysed at 550°C. It was important that the particle size of the resulting composite was suitable for use as filtration media. The benefits of this approach was that micro- and nanoparticles could be formed through changes to the precipitation technique, and a material with an overall higher mineral/metal content could be derived. Modification with various phases, incorporating Ca, Mg, Fe and Ce, were carried out and tested for the recovery of P from wastewater-relevant concentrations, in terms of their removal and then subsequent release characteristics at two pH values. In terms of the single and mixed metal hydroxide modifications, Fe was found to be the least effective (<50% removal of P from a 10 mg P/L initial concentration), with Ce- and Ca-incorporated phases showing the best performance in terms of P removal (> 95% removal from a 10 mg P/L initial concentration), when incorporated into the biochar structure. The LDH materials, although initially unsuccessful in terms of its crystallinity and P removal (compared with the single and mixed metal hydroxides), showed a clearly different, and an overall relatively larger release of the adsorbed P. Incorporating a secondary heating stage after precipitation was found to decrease the removal of P especially with the Fe and Ce based modifications and the LDH structures. Therefore, it was deemed that the formation of metal phases post-adsorption, with subsequent washing and drying stages was enough in deriving biochar-based materials with increased abilities to recover P.

The release/availability of P is as important as its uptake, and it was important to assess the relative P leaching intensity between the prototype materials post-adsorption. The P release study carried out gave information of the relative recovery of P (0–28% of the adsorbed P

released after one extraction) and therefore allowed for the choice of prototype materials to carry forward for further testing. From the assessment of the overall P recovery with the prepared prototype materials, three composite materials were chosen to be synthesised further – $Ca/Mg(OH)_2$, $Ce(OH)_3$ and Ca-Fe-NO_3-LDH modified OSR550 biochar. The $Ca/Mg(OH)_2$ composite offers a low cost and practical material and can be considered as being environmentally compatible. The $Ce(OH)_3$ composite offers extremely high removal (> 99% from an initial concentration of 10 mg P/L) and is worthy of study as a novel material (even if considered for removal only). Finally, the Ca- Fe-NO_3-LDH composite possessed the highest removal of P, when compared with the other LDH materials that were attempted to be synthesised.

The three prototype materials were synthesised in larger amounts through slightly modified approaches to attempt to gain a higher level of crystallinity and smaller particle sizes. Work undertaken in Chapter 7 demonstrates that the LDH material was successfully synthesised, with particles possessing features in the nano-range, and demonstrated an improved performance to remove P. Through isotherm and kinetic testing, it was found that all three materials possessed very rapid kinetic rates of removal, high heats of adsorption, and have maximum adsorption capacities of 10.4, 12.8, and 14.3 mg P/g composite, for the $Ca/Mg(OH)_2$, $Ce(OH)_3$, and Ca-Fe-NO_3-LDH composites respectively – these values agree well to values reported in the literature. The final experiment carried out demonstrated the ability of the prototypes to remove P from tertiary wastewater collected from Reading WWTP. In most cases, the three composites could remove P to < 0.5 mg P/L. The $Ca/Mg(OH)_2$ composite was most effected by the change in matrix (ultrapure water to wastewater effluent). The $Ce(OH)_3$ composite could remove P from various initial concentrations to < 17 µg/L (i.e. the LOD of the technique) within the wastewater matrix.

More research is needed to establish the bioavailability or release characteristics of P in these recovered forms within soil and in pot/field trials. Future research would establish the

effectiveness of the P-saturated biochar materials as fertiliser in a variety of soil conditions and plants, to determine if they may be more suited to certain applications or could be applied more widely. The composition of these materials work, having quick kinetics and high heats of adsorption, but it will be important to carry forward this work where further testing and development could be undertaken in an industrial setting – IP is currently being reviewed by KU. Ideally these composites would be applied and compared to the efficacy of existing treatment technologies such as struvite crystallisation, on the overall recovery of P in WWTPs. These materials can also be tested for the removal of similar anions to phosphate, such as arsenate (work is being undertaken on a new research project within the team, stemming from work undertaken in this thesis). Further material development of these composites would include increases to the overall particle size (to ensure compatibility with existing treatment processes) and to the porosity of the composite/matrix whilst aiming to decrease the crystalline size of the inorganic component. Selectivity in adsorption processes is important, and competition between several species in wastewater could be assessed; checked to ensure that the uptake and potential leaching of toxic compounds from wastewater does not occur at levels deemed unsafe for the environment or human health.

Work undertaken in this thesis has developed several novel biochar-based composites and demonstrated their potential to remove P from wastewater effluents, able to achieve rapid kinetics and efficiency at low initial concentration - it is important that we now take the next step in establishing the potential of using biochar materials to capture and reuse P.

9 References

Ahmad, M., Rajapaksha, A.U., Lim, J.E., Zhang, M., Bolan, N., Mohan, D., Vithanage, M., Lee, S.S., Ok, Y.S., 2014. Biochar as a sorbent for contaminant management in soil and water: a review. Chemosphere 99, 19–33. doi:10.1016/j.chemosphere.2013.10.071

Antunes, E., Jacob, M. V, Brodie, G., Schneider, P.A., 2018. Isotherms, kinetics and mechanism analysis of phosphorus recovery from aqueous solution by calcium-rich biochar produced from biosolids via microwave pyrolysis. Journal of Environmental Chemical Engineering 6, 395–403.

Association of Official Agricultural Chemists (AOAC), 2019. Official Methods of Analysis of AOAC International, 21st. ed. ed. AOAC International, Gaithersburg Maryland.

Barrett, E.P., Joyner, L.G., Halenda, P.P., 1951. The Determination of Pore Volume and Area Distributions in Porous Substances. I. Computations from Nitrogen Isotherms. Journal of the American Chemical Society 73, 373–380. doi:10.1021/ja01145a126

Benício, L.P.F., Constantino, V.R.L., Pinto, F.G., Vergütz, L., Tronto, J., da Costa, L.M., 2017. Layered Double Hydroxides: New Technology in Phosphate Fertilizers Based on Nanostructured Materials. ACS Sustainable Chemistry & Engineering 5, 399–409. doi:10.1021/acssuschemeng.6b01784

Boehm, H.P., 1994. Some aspects of the surface chemistry of carbon blacks and other carbons. Carbon 32, 759–769. doi:10.1016/0008-6223(94)90031-0

Boehm, H.P., 2002. Surface oxides on carbon and their analysis: A critical assessment. Carbon 40, 145–149. doi:10.1016/S0008-6223(01)00165-8

Břendová, K., Tlustoš, P., Száková, J., Habart, J., 2012. Biochar Properties From Different Materials of Plant Origin. European Chemical Bulletin 1, 535–539.

Brunauer, S., Emmett, P.H., Teller, E., 1938. Adsorption of Gases in Multimolecular Layers.

Journal of the American Chemical Society 60, 309–319. doi:10.1021/ja01269a023

Buss, W., Assavavittayanon, K., Shepherd, J.G., Heal, K. V., Sohi, S., 2018. Biochar Phosphorus Release Is Limited by High pH and Excess Calcium. Journal of Environment Quality 47, 1298. doi:10.2134/jeq2018.05.0181

Cai, R., Wang, X., Ji, X., Peng, B., Tan, C., Huang, X., 2017. Phosphate reclaim from simulated and real eutrophic water by magnetic biochar derived from water hyacinth. Journal of Environmental Management 187, 212–219.

Cantrell, K.B., Hunt, P.G., Uchimiya, M., Novak, J.M., Ro, K.S., 2012. Impact of pyrolysis temperature and manure source on physicochemical characteristics of biochar. Bioresource technology 107, 419–28. doi:10.1016/j.biortech.2011.11.084

Chen, B., Chen, Z., Lv, S., 2011. A novel magnetic biochar efficiently sorbs organic pollutants and phosphate. Bioresource technology 102, 716–23. doi:10.1016/j.biortech.2010.08.067

Chen, T., Zhou, Z., Han, R., Meng, R., Wang, H., Lu, W., 2015. Adsorption of cadmium by biochar derived from municipal sewage sludge: Impact factors and adsorption mechanism. Chemosphere 134, 286–293. doi:10.1016/j.chemosphere.2015.04.052

Choi, J.W., Lee, S.Y., Lee, S.H., Kim, J.E., Park, K.Y., Kim, D.J., Hong, S.W., 2012. Comparison of surface-modified adsorbents for phosphate removal in water. Water, Air, and Soil Pollution 223, 2881–2890. doi:10.1007/s11270-011-1072-6

Correll, D.L., 1998. The Role of Phosphorus in the Eutrophication of Receiving Waters: A Review. Journal of Environment Quality 27, 261–266. doi:10.2134/jeq1998.00472425002700020004x

Crombie, K., Mašek, O., Cross, A., Sohi, S., 2015. Biochar - synergies and trade-offs between soil enhancing properties and C sequestration potential. GCB Bioenergy 7,

1161–1175. doi:10.1111/gcbb.12213

Dai, L., Tan, F., Li, H., Zhu, N., He, M., Zhu, Q., Hu, G., Wang, L., Zhao, J., 2017. Calcium-rich biochar from the pyrolysis of crab shell for phosphorus removal. Journal of Environmental Management 198, 70–74.

Dudkiewicz, A., Boxall, A.B.A., Chaudhry, Q., Mølhave, K., Tiede, K., Hofmann, P., Linsinger, T.P.J., 2015. Uncertainties of size measurements in electron microscopy characterization of nanomaterials in foods. Food Chemistry 176, 472–479. doi:10.1016/j.foodchem.2014.12.071

Egle, L., Rechberger, H., Zessner, M., 2015. Overview and description of technologies for recovering phosphorus from municipal wastewater. Resources, Conservation and Recycling 105, 325–346. doi:10.1007/s00506-013-0127-x

EPA, U.S., 1996. Method 3052. Microwave Assisted Acid Digestion of Siliceous and Organically Based Matrices. doi:10.1016/j.aqpro.2013.07.003

European Commission, 2000. Council Directive 2000/60/EC of the European Parliament and of the Council establishing a framework for the Community action in the field of water policy. Official Journal of the European Communities L327, 1–72.

European Sustainable Phosphorus Platform (ESPP), 2017. Austria opts for manadatory phosphorus recovery from sewage sludge [WWW Document]. European Sustainable Phosphorus Platform. URL http://phosphorusplatform.eu/scope-in-print/news/1396-austria-manadatory-p-recovery (accessed 7.13.17).

Fang, C., Zhang, T., Li, P., Jiang, R., Wu, S., Nie, H., Wang, Y., 2015. Phosphorus recovery from biogas fermentation liquid by Ca-Mg loaded biochar. Journal of Environmental Sciences 29, 1–9. doi:10.1016/j.jes.2014.08.019

Feng, Y., Lu, H., Liu, Y., Xue, L., Dionysiou, D.D., Yang, L., Xing, B., 2017. Nano-cerium

oxide functionalized biochar for phosphate retention: preparation, optimization and rice paddy application. Chemosphere 185, 816–825.

Fidel, R.B., Laird, D. a., Thompson, M.L., 2013. Evaluation of Modified Boehm Titration Methods for Use with Biochars. Journal of Environment Quality 42, 1771. doi:10.2134/jeq2013.07.0285

Food and Agriculture Organization of The United Nations (FAO), 1983. Simple Technologies for Charcoal Making, in: FAO Forestry Paper 41. FAO, Rome, Italy.

Gámiz, B., Velarde, P., Spokas, K.A., Celis, R., Cox, L., 2019. Changes in sorption and bioavailability of herbicides in soil amended with fresh and aged biochar. Geoderma 337, 341–349. doi:10.1016/j.geoderma.2018.09.033

Goh, K.H., Lim, T.T., Dong, Z., 2008. Application of layered double hydroxides for removal of oxyanions: A review. Water Research 42, 1343–1368. doi:10.1016/j.watres.2007.10.043

Haddad, K., Jellali, S., Jeguirim, M., Trabelsi, A.B.H., Limousy, L., 2018. Investigations on phosphorus recovery from aqueous solutions by biochars derived from magnesium-pretreated cypress sawdust. Journal of Environmental Management 216, 305–314.

Hale, S.E., Lehmann, J., Rutherford, D., Zimmerman, A.R., Bachmann, R.T., Shitumbanuma, V., O'Toole, A., Sundqvist, K.L., Arp, H.P.H., Cornelissen, G., 2012. Quantifying the total and bioavailable polycyclic aromatic hydrocarbons and dioxins in biochars. Environmental Science and Technology 46, 2830–2838. doi:10.1021/es203984k

Harvey, O.R., Rhue, R.D., 2008. Kinetics and energetics of phosphate sorption in a multi-component Al(III)-Fe(III) hydr(oxide) sorbent system. Journal of Colloid and Interface Science 322, 384–393. doi:10.1016/j.jcis.2008.03.019

Ho, Y.S., McKay, G., 1998. Sorption of dye from aqueous solution by peat. Chemical Engineering Journal 70, 115–124. doi:10.1016/S1385-8947(98)00076-X

Houba, V.J.G., Novozamsky, I., Huybregts, A.W.M., van der Lee, J.J., 1986. Comparison of soil extractions by 0.01 M CaCl2, by EUF and by some conventional extraction procedures. Plant and Soil 96, 433–437. doi:10.1007/BF02375149

Huygens, D., Saveyn, H., Eder, P., Sancho, L.D., 2017. DRAFT STRUBIAS Technical Proposals – DRAFT nutrient recovery rules for recovered phosphate salts, ash-based materials and pyrolysis materials in view of their possible inclusion as Component Material Categories in the Revised Fertiliser Regulation.

International Biochar Initiative (IBI), 2015. Standardized Product Definition and Product Testing Guidelines for Biochar That Is Used in Soil. International Biochar Initiative 23. doi:http://www.biochar-international.org/characterizationstandard. 22

Jing, R., Nan, L., Lei, L., Jing-Kun, A., Lin, Z., Nan-Qi, R., 2015. Granulation and ferric oxides loading enable biochar derived from cotton stalk to remove phosphate from water. Bioresource Technology 178, 119–125. doi:10.1016/j.biortech.2014.09.071

Jung, K.-W., Ahn, K.-H., 2015. Fabrication of porosity-enhanced MgO/biochar for removal of phosphate from aqueous solution: Application of a novel combined electrochemical modification method. Bioresource Technology 200, 1029–1032. doi:10.1016/j.biortech.2015.10.008

Jung, K.-W., Kim, K., Jeong, T.-U., Ahn, K.-H., 2016. Influence of pyrolysis temperature on characteristics and phosphate adsorption capability of biochar derived from waste-marine macroalgae (Undaria pinnatifida roots). Bioresource Technology 200, 1024–1028. doi:http://dx.doi.org/10.1016/j.biortech.2015.10.016

Jung, K.W., Hwang, M.J., Ahn, K.H., Ok, Y.S., 2015. Kinetic study on phosphate removal

from aqueous solution by biochar derived from peanut shell as renewable adsorptive media. International Journal of Environmental Science and Technology 12, 3363–3372. doi:10.1007/s13762-015-0766-5

Jung, S.H., Kim, J.S., 2014. Production of biochars by intermediate pyrolysis and activated carbons from oak by three activation methods using CO2. Journal of Analytical and Applied Pyrolysis 107, 116–122. doi:10.1016/j.jaap.2014.02.011

Kätterer, T., Roobroeck, D., Andrén, O., Kimutai, G., Karltun, E., Kirchmann, H., Nyberg, G., Vanlauwe, B., Röing de Nowina, K., 2019. Biochar addition persistently increased soil fertility and yields in maize-soybean rotations over 10 years in sub-humid regions of Kenya. Field Crops Research 235, 18–26. doi:10.1016/j.fcr.2019.02.015

Keiluweit, M., Nico, P.S., Johnson, M., Kleber, M., 2010. Dynamic molecular structure of plant biomass-derived black carbon (biochar). Environmental Science and Technology 44, 1247–1253. doi:10.1021/es9031419

Klasson, K.T., Uchimiya, M., Lima, I.M., 2014. Uncovering surface area and micropores in almond shell biochars by rainwater wash. Chemosphere 111, 129–34. doi:10.1016/j.chemosphere.2014.03.065

Koilraj, P., Sasaki, K., 2016. Fe3O4/MgAl-NO3 layered double hydroxide as a magnetically separable sorbent for the remediation of aqueous phosphate. Journal of Environmental Chemical Engineering. doi:10.1016/j.jece.2016.01.005

Kuang, Y., Zhao, L., Zhang, S., Dong, M., Xu, S., 2010. Morphologies, Preparations and Applications of Layered Double Hydroxide Micro-/Nanostructures. Materials 3, 5220–5235. doi:10.3390/ma3125220

Lawrinenko, M., Laird, D.A., Johnson, R.L., Jing, D., 2016. Accelerated aging of biochars: Impact on anion exchange capacity. Carbon 103, 217–227.

doi:10.1016/j.carbon.2016.02.096

Lehman, J., Joseph, S., 2009. Biochar for Environmental Management: Science and Technology, 1st Editio. ed. Earthscan.

Lehmann, J., 2007. A handful of carbon. Nature 447, 143–144. doi:10.1038/447143a

Li, M., Liu, J., Xu, Y., Qian, G., Li, M., Xu, Y., 2016. Phosphate adsorption on metal oxides and metal hydroxides : A comparative review. Environmental Reviews 332, 1–58. doi:10.1139/er-2015-0080

Li, R., Wang, J.J., Zhou, B., Awasthi, M.K., Ali, A., Zhang, Z., Gaston, L.A., Lahori, A.H., Mahar, A., 2016a. Enhancing phosphate adsorption by Mg/Al layered double hydroxide functionalized biochar with different Mg/Al ratios. Science of the Total Environment 559, 121–129. doi:10.1016/j.scitotenv.2016.03.151

Li, R., Wang, J.J., Zhou, B., Awasthi, M.K., Ali, A., Zhang, Z., Lahori, A.H., Mahar, A., 2016b. Recovery of phosphate from aqueous solution by magnesium oxide decorated magnetic biochar and its potential as phosphate-based fertilizer substitute. Bioresource Technology 215, 209–214. doi:10.1016/j.biortech.2016.02.125

Li, X., Shen, Q., Zhang, D., Mei, X., Ran, W., Xu, Y., Yu, G., 2013. Functional Groups Determine Biochar Properties (pH and EC) as Studied by Two-Dimensional13C NMR Correlation Spectroscopy. PLoS ONE 8. doi:10.1371/journal.pone.0065949

Liu, P., Liu, W.J., Jiang, H., Chen, J.J., Li, W.W., Yu, H.Q., 2012. Modification of bio-char derived from fast pyrolysis of biomass and its application in removal of tetracycline from aqueous solution. Bioresource Technology 121, 235–240. doi:10.1016/j.biortech.2012.06.085

Long, F., Gong, J.L., Zeng, G.M., Chen, L., Wang, X.Y., Deng, J.H., Niu, Q.Y., Zhang, H.Y., Zhang, X.R., 2011. Removal of phosphate from aqueous solution by magnetic

Fe-Zr binary oxide. Chemical Engineering Journal 171, 448–455. doi:10.1016/j.cej.2011.03.102

Lou, K., Rajapaksha, A.U., Ok, Y.S., Chang, S.X., 2016. Pyrolysis temperature and steam activation effects on sorption of phosphate on pine sawdust biochars in aqueous solutions. Chemical Speciation and Bioavailability 28, 42–50. doi:10.1080/09542299.2016.1165080

Lozano-Castelló, D., Calo, J.M., Cazorla-Amorós, D., Linares-Solano, A., 2007. Carbon activation with KOH as explored by temperature programmed techniques, and the effects of hydrogen. Carbon 45, 2529–2536. doi:10.1016/j.carbon.2007.08.021

Lua, A.C., Yang, T., Guo, J., 2004. Effects of pyrolysis conditions on the properties of activated carbons prepared from pistachio-nut shells. Journal of Analytical and Applied Pyrolysis 72, 279–287. doi:10.1016/j.jaap.2004.08.001

Mašek, O., Buss, W., Sohi, S., 2018. Standard Biochar Materials. Environmental Science and Technology 52, 9543–9544. doi:10.1021/acs.est.8b04053

Mbundi, L., Gallar-Ayala, H., Khan, M.R., Barber, J.L., Losada, S., Busquets, R., 2014. Advances in the Analysis of Challenging Food Contaminants, 1st ed, Advances in Molecular Toxicology. Elsevier B.V. doi:10.1016/b978-0-444-63406-1.00002-7

Melia, P.M., Cundy, A.B., Sohi, S.P., Hooda, P.S., Busquets, R., 2017. Trends in the recovery of phosphorus in bioavailable forms from wastewater. Chemosphere 186, 381–395. doi:http://dx.doi.org/10.1016/j.chemosphere.2017.07.089

Morse, G.K., Brett, S.W., Guy, J. a., Lester, J.N., 1998. Review: Phosphorus removal and recovery technologies. Science of the Total Environment 212, 69–81. doi:10.1016/S0048-9697(97)00332-X

Naushad, M., Khan, M.R., ALOthman, Z.A., AlSohaimi, I., Rodriguez-Reinoso, F., Turki,

T.M., Ali, R., 2015. Removal of BrO3− from drinking water samples using newly developed agricultural waste-based activated carbon and its determination by ultra-performance liquid chromatography-mass spectrometry. Environmental Science and Pollution Research 22, 15853–15865. doi:10.1007/s11356-015-4786-y

Novais, S.V., Zenero, M.D.O., Tronto, J., Conz, R.F., Cerri, C.E.P., 2018a. Poultry manure and sugarcane straw biochars modified with MgCl2 for phosphorus adsorption. Journal of Environmental Management 214, 36–44.

Novais, S.V., Zenero, M.D.O.O., Barreto, M.S.C., Montes, C.R., Cerri, C.E.P., 2018b. Phosphorus removal from eutrophic water using modified biochar. Science of the Total Environment 633, 825–835. doi:10.1016/j.scitotenv.2018.03.246

Park, J.H., Ok, Y.S., Kim, S.H., Cho, J.S., Heo, J.S., Delaune, R.D., Seo, D.C., 2015. Evaluation of phosphorus adsorption capacity of sesame straw biochar on aqueous solution: influence of activation methods and pyrolysis temperatures. Environmental Geochemistry and Health 37, 969–983. doi:10.1007/s10653-015-9709-9

Poschenrieder, C., Gunsé, B., Corrales, I., Barceló, J., 2008. A glance into aluminum toxicity and resistance in plants. Science of the Total Environment 400, 356–368. doi:10.1016/j.scitotenv.2008.06.003

Rajapaksha, A.U., Chen, S.S., Tsang, D.C.W., Zhang, M., Vithanage, M., Mandal, S., Gao, B., Bolan, N.S., Ok, Y.S., 2016. Engineered/designer biochar for contaminant removal/immobilization from soil and water: Potential and implication of biochar modification. Chemosphere 148, 276–291. doi:10.1016/j.chemosphere.2016.01.043

Rajkovich, S., Enders, A., Hanley, K., Hyland, C., Zimmerman, A.R., Lehmann, J., 2012. Corn growth and nitrogen nutrition after additions of biochars with varying properties to a temperate soil. Biology and Fertility of Soils 48, 271–284. doi:10.1007/s00374-

011-0624-7

Rengel, Z., Marschner, P., 2005. Nutrient availability and management in the rhizosphere: exploiting genotypic differences. New Phytologist 168, 305–312. doi:10.1111/j.1469-8137.2005.01558.x

Salame, I.I., Bandosz, T.J., 2001. Surface Chemistry of Activated Carbons: Combining the Results of Temperature-Programmed Desorption, Boehm, and Potentiometric Titrations. Journal of colloid and interface science 240, 252–258. doi:10.1006/jcis.2001.7596

Schoumans, O.F., Bouraoui, F., Kabbe, C., Oenema, O., van Dijk, K.C., 2015. Phosphorus management in Europe in a changing world. Ambio 44, 180–192. doi:10.1007/s13280-014-0613-9

Shafizadeh, F., 1984. The Chemistry of Pyrolysis and Combustion. Advances in Chemistry 207, 489–529. doi:10.1021/ba-1984-0207.ch013

Shepherd, J., Joseph, S., Sohi, S., Heal, K., 2017. Biochar and enhanced phosphate capture: Mapping mechanisms to functional properties. Chemosphere. doi:10.1016/j.chemosphere.2017.02.123.This

Shrivastava, A., Gupta, V.B., 2011. Methods for the determination of limit of detection and limit of quantitation of the analytical methods. Chronicles of Young Scientists 2, 21. doi:10.4103/2229-5186.79345

Singh, B., Arbestain, M.C., Lehmann, J., 2017. Biochar: A Guide to Analytical Methods. CRC Press.

Sjöström, E., 1993. Wood chemistry: Fundamentals and Applications, Second Edi. ed, New York. Academic Press, London.

Stoddard, J.L., Van Sickle, J., Herlihy, A.T., Brahney, J., Paulsen, S., Peck, D. V., Mitchell,

R., Pollard, A.I., 2016. Continental-Scale Increase in Lake and Stream Phosphorus: Are Oligotrophic Systems Disappearing in the United States? Environmental Science and Technology 50, 3409–3415. doi:10.1021/acs.est.5b05950

Sun, J., Lian, F., Liu, Z., Zhu, L., Song, Z., 2014. Biochars derived from various crop straws: Characterization and Cd(II) removal potential. Ecotoxicology and Environmental Safety 106, 226–231. doi:10.1016/j.ecoenv.2014.04.042

Takaya, C.A., Fletcher, L.A., Singh, S., Anyikude, K.U., Ross, A.B., 2016. Phosphate and ammonium sorption capacity of biochar and hydrochar from different wastes. Chemosphere 145, 518–527. doi:10.1016/j.chemosphere.2015.11.052

Takaya, C.A.A., Fletcher, L.A.A., Singh, S., Okwuosa, U.C.C., Ross, A.B.B., 2016. Recovery of phosphate with chemically modified biochars. Journal of Environmental Chemical Engineering 4, 1156–1165. doi:10.1016/j.jece.2016.01.011

Thames Water, no date. The sewage treatment process [WWW Document]. URL https://cycles.thameswater.co.uk/Accessible/The-sewage-treatment-process

Theiss, F.L., Ayoko, G.A., Frost, R.L., 2016. Synthesis of layered double hydroxides containing Mg2+, Zn2+, Ca2+ and Al3+ layer cations by co-precipitation methods—A review. Applied Surface Science 383, 200–213. doi:10.1016/j.jnucmat.2010.11.101

Tsechansky, L., Graber, E.R., 2014. Methodological limitations to determining acidic groups at biochar surfaces via the Boehm titration. Carbon 66, 730–733. doi:10.1016/j.carbon.2013.09.044

Tu, Y.J., You, C.F., 2014. Phosphorus adsorption onto green synthesized nano-bimetal ferrites: Equilibrium, kinetic and thermodynamic investigation. Chemical Engineering Journal 251, 285–292. doi:10.1016/j.cej.2014.04.036

Uchimiya, M., Pignatello, J.J., White, J.C., Hu, S.-T., Ferreira, P.J., 2017. Structural

Transformation of Biochar Black Carbon by C60 Superstructure: Environmental Implications. Scientific Reports 7, 1–11. doi:10.1038/s41598-017-12117-9

Uchimiya, M., Wartelle, L.H., Klasson, K.T., Fortier, C.A., Lima, I.M., 2011. Influence of Pyrolysis Temperature on Biochar Property and Function as a Heavy Metal Sorbent in Soil. Journal of Agricultural and Food Chemistry 59, 2501–2510.

Valente Nabais, J.M., Carrott, P.J.M., 2006. Chemical Characterization of Activated Carbon Fibers and Activated Carbons. Journal of Chemical Education 83, 436. doi:10.1021/ed083p436

Van Zwieten, L., Kimber, S., Morris, S., Chan, K.Y., Downie, A., Rust, J., Joseph, S., Cowie, A., 2009. Effects of biochar from slow pyrolysis of papermill waste on agronomic performance and soil fertility. Plant and Soil 327, 235–246. doi:10.1007/s11104-009-0050-x

Wan, S., Wang, S., Li, Y., Gao, B., 2017. Functionalizing biochar with Mg–Al and Mg–Fe layered double hydroxides for removal of phosphate from aqueous solutions. Journal of Industrial and Engineering Chemistry 47, 246–253. doi:10.1016/j.jiec.2016.11.039

Wang, C., Wang, Y., Herath, H.M.S.K., 2017. Polycyclic aromatic hydrocarbons (PAHs) in biochar – Their formation, occurrence and analysis: A review. Organic Geochemistry 114, 1–11. doi:10.1016/j.orggeochem.2017.09.001

Wang, S., Kong, L., Long, J., Su, M., Diao, Z., Chang, X., Chen, D., Song, G., Shih, K., 2018. Adsorption of phosphorus by calcium-flour biochar: Isotherm, kinetic and transformation studies. Chemosphere 195, 666–672.

Wang, Xinjun, Chen, J., Kong, Y., Shi, X., 2014. Sequestration of phosphorus from wastewater by cement-based or alternative cementitious materials. Water Research 62, 86–96. doi:10.1016/j.watres.2014.05.021

Wang, Xinggang, Lü, S., Gao, C., Xu, X., Zhang, X., Bai, X., Liu, M., Wu, L., 2014. Highly efficient adsorption of ammonium onto palygorskite nanocomposite and evaluation of its recovery as a multifunctional slow-release fertilizer. Chemical Engineering Journal 252, 404–414. doi:10.1016/j.cej.2014.04.097

Wang, Y., Lin, Y., Chiu, P.C., Imhoff, P.T., Guo, M., 2015. Phosphorus release behaviors of poultry litter biochar as a soil amendment. Science of The Total Environment 512–513, 454–463. doi:10.1016/j.scitotenv.2015.01.093

Wang, Z., Guo, H., Shen, F., Yang, G., Zhang, Y., Zeng, Y., Wang, L., Xiao, H., Deng, S., 2015. Biochar produced from oak sawdust by Lanthanum-involved pyrolysis for adsorption of ammonium, nitrate and phosphate. Chemosphere 119, 646–653.

Wang, Z., Shen, D., Shen, F., Li, T., 2016. Phosphate adsorption on lanthanum loaded biochar. Chemosphere 150, 1–7. doi:10.1016/j.chemosphere.2016.02.004

Woo, M.A., Woo Kim, T., Paek, M.J., Ha, H.W., Choy, J.H., Hwang, S.J., 2011. Phosphate-intercalated CaFe-layered double hydroxides: Crystal structure, bonding character, and release kinetics of phosphate. Journal of Solid State Chemistry 184, 171–176. doi:10.1016/j.jssc.2010.11.003

Xie, J., Wang, Z., Lu, S., Wu, D., Zhang, Z., Kong, H., 2014. Removal and recovery of phosphate from water by lanthanum hydroxide materials. Chemical Engineering Journal 254, 163–170. doi:10.1016/j.cej.2014.05.113

Yang, F., Zhang, S., Sun, Y., Tsang, D.C.W., Cheng, K., Sik, Y.S.O., 2019. Assembling biochar with various layered double hydroxides for enhancement of phosphorus recovery. Journal of Hazardous Materials 365, 665–673.

Yang, H., Yan, R., Chen, H., Lee, D.H., Zheng, C., 2007. Characteristics of hemicellulose, cellulose and lignin pyrolysis. Fuel 86, 1781–1788. doi:10.1016/j.fuel.2006.12.013

Yao, Y., Gao, B., Chen, J., Yang, L., 2013. Engineered biochar reclaiming phosphate from aqueous solutions: Mechanisms and potential application as a slow-release fertilizer. Environmental Science and Technology 47, 8700–8708. doi:10.1021/es4012977

Yao, Y., Gao, B., Inyang, M., Zimmerman, A.R., Cao, X., Pullammanappallil, P., Yang, L., 2011a. Biochar derived from anaerobically digested sugar beet tailings: characterization and phosphate removal potential. Bioresource technology 102, 6273–8. doi:10.1016/j.biortech.2011.03.006

Yao, Y., Gao, B., Inyang, M., Zimmerman, A.R., Cao, X., Pullammanappallil, P., Yang, L., 2011b. Removal of phosphate from aqueous solution by biochar derived from anaerobically digested sugar beet tailings. Journal of hazardous materials 190, 501–7. doi:10.1016/j.jhazmat.2011.03.083

Yuan, H., Lu, T., Wang, Y., Chen, Y., Lei, T., 2016. Sewage sludge biochar: Nutrient composition and its effect on the leaching of soil nutrients. Geoderma 267, 17–23. doi:10.1016/j.geoderma.2015.12.020

Zhang, G., Liu, H., Liu, R., Qu, J., 2009. Removal of phosphate from water by a Fe-Mn binary oxide adsorbent. Journal of Colloid and Interface Science 335, 168–174. doi:10.1016/j.jcis.2009.03.019

Zhang, L., Zhou, Q., Jianyong, L., Chang, N., Wan, L., Chen, J., 2012. Phosphate adsorption on lanthanum hydroxide-doped activated carbon fiber. Chemical Engineering Journal 185–186, 160–167. doi:10.1016/j.cej.2012.01.066

Zhang, M., Gao, B., Fang, J., Creamer, A.E., Ullman, J.L., 2014. Self-assembly of needle-like layered double hydroxide (LDH) nanocrystals on hydrochar: characterization and phosphate removal ability. RSC Advances 4, 28171. doi:10.1039/c4ra02332c

Zhang, M., Gao, B., Yao, Y., Xue, Y., Inyang, M., 2012. Synthesis of porous MgO-biochar

nanocomposites for removal of phosphate and nitrate from aqueous solutions. Chemical Engineering Journal 210, 26–32. doi:10.1016/j.cej.2012.08.052

Zhou, Y., Gao, B., Zimmerman, A.R., Chen, H., Zhang, M., Cao, X., 2014. Biochar-supported zerovalent iron for removal of various contaminants from aqueous solutions. Bioresource technology 152, 538–42. doi:10.1016/j.biortech.2013.11.021

Zhu, N., Yan, T., Qiao, J., Cao, H., 2016. Adsorption of arsenic, phosphorus and chromium by bismuth impregnated biochar: Adsorption mechanism and depleted adsorbent utilization. Chemosphere 164, 32–40.

Zhu, Z., Huang, C.P., Zhu, Y., Wei, W., Qin, H., 2018. A hierarchical porous adsorbent of nano-α-Fe2O3/Fe3O4 on bamboo biochar (HPA-Fe/C-B) for the removal of phosphate from water. Journal of Water Process Engineering 25, 96–104.